C 51.17/12:988/11

Tech Notes

November 1988

PB88-925911

PENNSYLVANIA STATE UNIVERSITY
NOV 11 1988
DOCUMENTS COLLECTION

NTIS

U.S. DEPARTMENT OF COMMERCE
National Technical Information Service
Center for the Utilization of Federal Technology

The Complete Guide to U.S. and State Government Business Help

For New and Growing Businesses

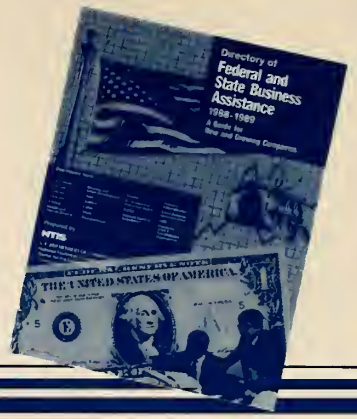

SECOND BIG EDITION!

Directory of Federal & State Business Assistance– A Guide for New and Growing Companies.

Your guide to sources of financing, technical information, planning and management know-how, procurement, and marketing assistance. Order this book today!

Describes 180 Federal and more than 500 State Programs

You get the information you need to directly contact hundreds of Federal and State sources of business assistance:

- Full summary of services offered
- Telephone number
- Mailing address
- Eligibility requirements (if any)

Take advantage of these programs designed to help U.S. businesses compete effectively in domestic and international markets.

Some of the programs listed:

Dept. of Commerce Export Licensing

Bureau of Labor Statistics Prices and Living Conditions Office

Federal Grant Data Center

Small Business Answer Desk

Florida Product Innovation Center

Iowa Small Business Loan Program

Michigan Biotechnology Institute

New York Direct Loan Program

You'll learn:

- How to get funding for your company's R&D
- Which states provide venture money
- How to take advantage of free export assistance
- What Federal and State contacts offer free management and procurement consulting
- Where to get mail lists of potential overseas business buyers
- Where to find evaluation of energy-related inventions or engineering help
- How to get help in selecting a site for your manufacturing plant
- Where to find customized economic impact statistics

and much more.

Federal Offices Want to Work with You

The 180 Federal entries selected for inclusion are arranged by agency. Discover sources of help in exporting, patent licensing, procurement, locating wage information, obtaining loan guarantees, finding marketing information, plus much more. A handy index lets you quickly locate just the Federal resources you need.

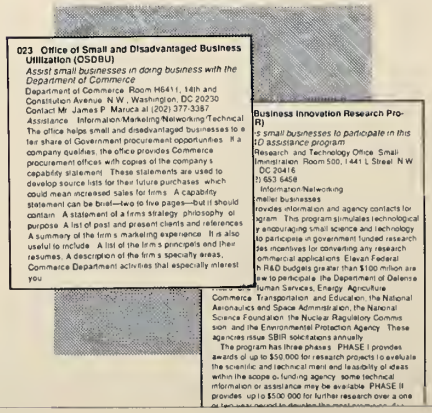
023 Office of Small and Disadvantaged Business Utilization (OSDBU)
Assist small businesses in doing business with the Department of Commerce
Department of Commerce Room H6411, 14th and Constitution Avenue, N.W., Washington, DC 20230
Contact Mr. James P. Maruca at (202) 377-3387
Assistance: Information/Marketing/Networking/Technical
The office helps small and disadvantaged businesses to get their share of Government procurement opportunities. If a company qualifies, the office provides Commerce procurement offices with copies of the company's capability statement. These statements are used to develop source lists for their future purchases, which could mean increased sales for firms. A capability statement can be brief—two to five pages—but it should contain: A statement of a firm's strategy, philosophy, or purpose. A list of past and present clients and references. A summary of the firm's marketing experience. It is also useful to include: A list of the firm's principals and their resumes. A description of the firm's specialty areas. Commerce Department activities that especially interest you.

Business Innovation Research Pro-
(R)
s small businesses to participate in this
ID assistance program
Research and Technology Office, Small
Innistration, Room 500, 1441 L Street, N.W.
DC 20416
) 653-6458
Information/Networking
maller businesses
rovides information and agency contacts for
gram. This program stimulates technological
y encouraging small science and technology
to participate in government-funded research
des incentives for converting any research
ommercial applications. Eleven Federal
h R&D budgets greater than $100 million are
w to participate: the Department of Defense,
Human Services, Energy, Agriculture,
Commerce, Transportation, and Education; the National Aeronautics and Space Administration; the National Science Foundation; the Nuclear Regulatory Commission; and the Environmental Protection Agency. These agencies issue SBIR solicitations annually.
The program has three phases. PHASE I provides awards of up to $50,000 for research projects to evaluate the scientific and technical merit and feasibility of ideas within the scope of a funding agency. Some technical information or assistance may be available. PHASE II provides up to $500,000 for further research over a one

Pennsylvania Capital Loan Fund
Department of Commerce, Bureau of Business Financing
494 Forum Building, Harrisburg, PA 17120
Contact Mr. James N. Graham at (717) 783-1768
Assistance: Financial
Eligibility: Smaller businesses
The fund receives funding from the Federal Appalachian Regional Commission, the Federal Economic Development Administration, and state appropriations. Eligibility criteria, terms and rates differ depending on the funding source.
Loans are made to small businesses with less than 100 employees which are engaged in manufacturing, industrial and/or advanced technology operations. Also included are those small businesses which are engaged in international export-related services, including commercial and computer-related services. Non-profit organizations are not eligible.
for working capital and for land
and equipment which is acquired
ed or used by a small business
n be used to finance up to 50% of the
,000, whichever is less. At least one
or each $15,000 loaned. The interest
e loans are fixed. Loan money is
al area loan organization, which in turn
sinesses. Applications and loan
ved first on the local level.

Pennsylvania Technical Assistance Program (PENNTAP)
The Pennsylvania State University, 501 J. Orvis Keller Building, University Park, PA 16802
Contact Dr. Roy Marrow at (814) 865-0427
Assistance: Information/Technical
The program is a service organization which promotes technology transfer; assists firms solving technological problems by gathering information and then tailors it to a particular program so that a business or other institution can make a decision. It helps Pennsylvania firms solve their technical problems in a way that will enhance the firm's ability to assume a stronger competitive position. As part of its mission, the program provides services that help small companies to start and grow, products to be developed or improved, jobs to be created or saved, and productivity to be expanded. Technical specialists are full time experienced professionals who personally handle each request for assistance.

States Want to Assist Your Business

States know that strong businesses mean a strong economy. Services described include venture financing, planning help, product marketing, employee training, exporting assistance, site location, technology development, and technical and management information.

Every effort has been taken to make this Directory a valuable working resource to assist the growth of your company.

TO ORDER:

ASK FOR the ***Directory of Federal & State Business Assistance – A Guide for New and Growing Companies.*** (180 pp. ISBN 0-934213-10-0). Reference order number PB88-101977/ABH. The price is $29 plus $3 for handling.

CALL (703) 487-4650 and use your American Express, VISA, MasterCard, or NTIS deposit account.

Or send a check payable to the

National Technical Information Service
U.S. DEPARTMENT OF COMMERCE
Springfield, VA 22161.

Tech Notes

Highlighting Selected U.S. Government Technology & Resources

November 1988

Contents

Agriculture & Food 927

Computers 929

Electrotechnology 935

Energy 948

Engineering 953

Environmental Science & Technology 965

Manufacturing, Machinery & Tools 969

Materials 976

Medicine & Biology 989

Natural Resources Technology & Engineering 995

Physical Sciences 996

Transportation & Components 1003

Published monthly by the National Technical Information Service (NTIS), Tech Notes bring together individual one- to two-page fact sheets prepared by Federal agencies, their laboratories, or contractors. These fact sheets highlight current Federal technology determined to have commercial or practical application. Topics cover new processes, materials, techniques, software, instrumentation, and resources.

Some of the current sources are the Department of the Navy, Department of the Army, NASA, Department of Energy, Environmental Protection Agency, Department of the Interior, and the Department of Agriculture.

Special assistance is provided by the Federal Laboratory Consortium.

Change of address or questions concerning subscriptions should be sent to:
Subscriptions Department
National Technical Information Service
Springfield, VA 22161
(703) 487-4630

Suggestions, comments, or questions concerning Tech Notes should be directed to:
Tech Notes Editor
Room 300B F
National Technical Information Service
Springfield, VA 22161
(703) 487-4805

U.S. Depository Co

How to Use Tech Notes

Every Tech Notes fact sheet lists a source for additional information. The source of this information may be a special support package from the originating agency, a personal contact, a licensing opportunity, or a backup report available from NTIS.

Each fact sheet also is perforated to allow for easy removal for those subscribers who may wish to keep a special fact sheet file or route to others in their organization

Sources of Further Backup Information

Below are two representative examples of how each Tech Note fact sheet provides you with a source of further information. In most cases, this information is provided directly by the agency or its laboratory.

However, there are cases where NTIS is the source for backup documentation. In these cases, use the order form at the end.

Examples:

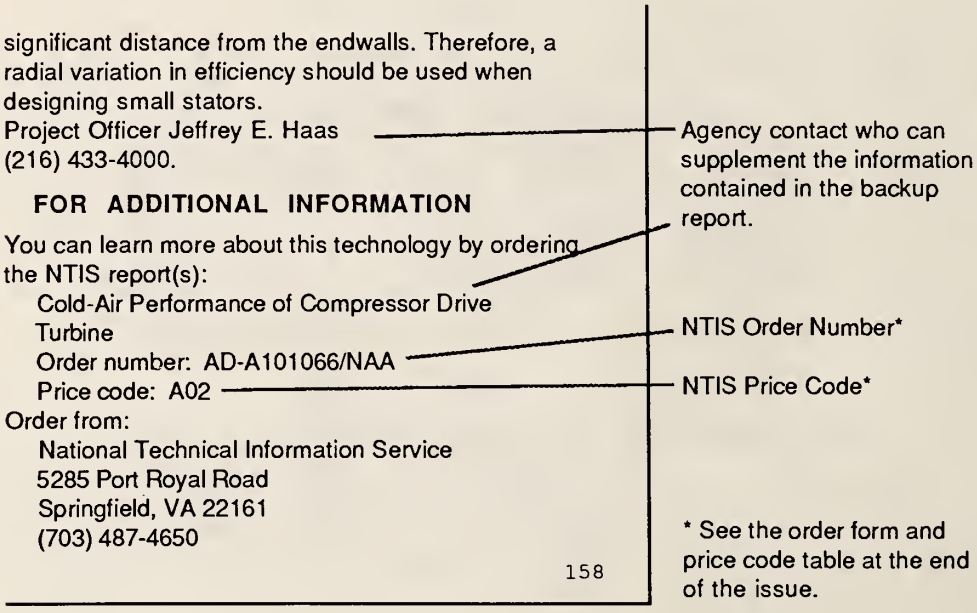
significant distance from the endwalls. Therefore, a radial variation in efficiency should be used when designing small stators.
Project Officer Jeffrey E. Haas
(216) 433-4000.
FOR ADDITIONAL INFORMATION
You can learn more about this technology by ordering the NTIS report(s):
Cold-Air Performance of Compressor Drive Turbine
Order number: AD-A101066/NAA
Price code: A02
Order from:
National Technical Information Service
5285 Port Royal Road
Springfield, VA 22161
(703) 487-4650
158
Agency contact who can supplement the information contained in the backup report.
NTIS Order Number*
NTIS Price Code*
* See the order form and price code table at the end of the issue.

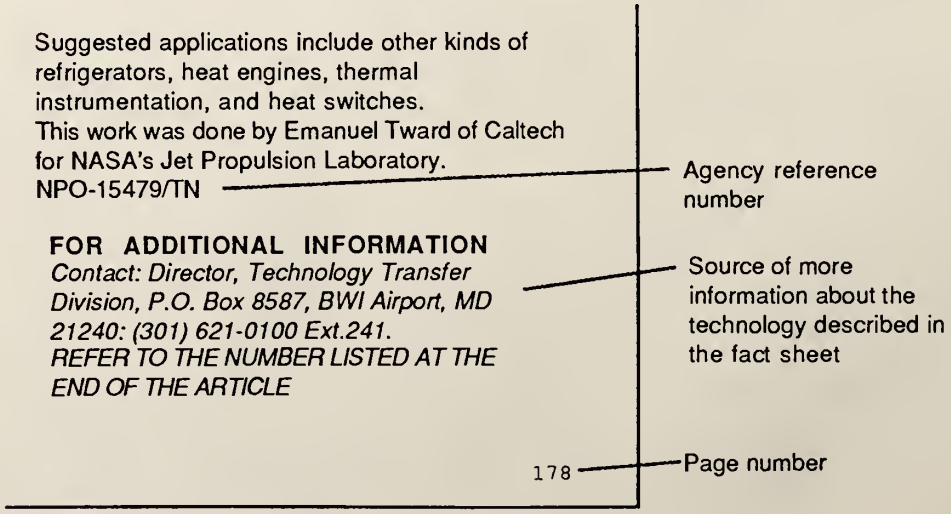
Suggested applications include other kinds of refrigerators, heat engines, thermal instrumentation, and heat switches.
This work was done by Emanuel Tward of Caltech for NASA's Jet Propulsion Laboratory.
NPO-15479/TN
FOR ADDITIONAL INFORMATION
Contact: Director, Technology Transfer Division, P.O. Box 8587, BWI Airport, MD 21240: (301) 621-0100 Ext.241.
REFER TO THE NUMBER LISTED AT THE END OF THE ARTICLE
178
Agency reference number
Source of more information about the technology described in the fact sheet
Page number

Tech Notes Title List for November 1988

Agriculture & Food

927 Super Slurper Saves the Day for Good Nematodes

928 Wetting Agent Unbungles Fungals (Licensing Opportunity)

Other Items of Interest

989 Dental Liquid Diets

Computers

929 Implementing and Managing Change: A Guide for Assessing Information Technology

930 New Guideline for Verifying, Validating Software

931 SQL Test Package Available from NBS

932 Single-Chip VLSI Reed-Solomon Decoder — Efficient utilization of computing elements reduces size while preserving throughput. (Licensing Opportunity)

Software

933 NASKERN Program Tests Computers — A "benchmark" program exercises computers on a set of standardized problems.

934 Subroutines for Image Processing — Dozens of functions and test programs are included.

Other Items of Interest

970 Research in Advanced Real-Time Computer Vision

Electrotechnology

935 Device Limits Fault Current Level

936 Fast Synchronization with Burst-Mode Digital Signals — An oscillator is quickly synchronized with the data clock.

937 Adaptive Receiver for Codes Communications — Acquisition and tracking of the signal are controlled automatically

938 Flexible Ceramic-Insulated Cable — The cable withstands heat, radiation, and oxidation.

939 GPS Satellite Multipath Range Errors — Measurements are proposed to resolve uncertainties.

940 Formula Gives Better Contact-Resistance Values — Lateral currents in the contact strips are taken into account.

941 Image-Method Gain Measurement with Mismatch — A new formula accounts for multiple reflections.

942 Least-Squares Frequency-Acquisition Algorithm — Performance rivals that of the FFT algorithm.

943 Maser Oscillator with Dielectric Resonators — A two-resonator design should yield low phase noise. (Licensing Opportunity)

944 Single-Layer, Multicolor Electroluminescent Phosphors — Etching is eliminated in producing phosphor layers for displays. (Licensing Opportunity)

945 Small, Optically-Driven Power Source — Power would be transmitted along fiber-optic cables.

Testing & Instrumentation

946 RF Testing of Microwave Integrated Circuits — Fixtures and techniques are undergoing development.

947 Tiny Sensor may Help Robots Handle Materials Accurately

Other Items of Interest

998 Thermoplastic Removes Hydrogen without Producing Water

Energy

948 Assessment of the Energy Savings Potential of Building Foundations Research

949 Efficient Alternatives for Electric Motors

950 Energy Measurements of Single-Family Houses

951 Passive Solar Designs Investigated

952 Corrosion in Amorphous-Silicon Solar Cells and Modules — Moisture severely affects amorphous-silicon units, bur encapsulation helps.

Engineering

953 Bulk Transfer of Chemical Materials

954 Spin Coating of Decon Agent Containers

955 Dust Control Handbook for Minerals Processing

956 Inspecting, Testing Fire Safety of HVAC Systems

957 NBS Model to Simulate Smoke Movement Through HVAC Systems

958 Liquid-Seeding Atomizer — Particles are sprayed in drops of evaporating liquid. (Licensing Opportunity)

959 Designing Shafts for Long Life — Fatigue lives are affected by many factors.

960 Hydrogen/Air-Ignition Torch — The torch is simple, reliable, and economical.

961 Measuring Fan-Blade-Tip Displacements — Magnets and Hall-effect transducers are used to monitor tip-to-shroud clearances. (Licensing Opportunity)

962 Short-Cycle Adsorption Refrigerator — Each adsorption unit includes a long-lived nonmechanical heat switch.

Software

963 Computing Flows Over Wavy Surfaces — Wind/wave interactions, drags, and related phenomena can be predicted.

964 Unsteady Flow in a Supersonic Cascade with Shocks — The operating range of turbomachinery for which stability can be calculated is extended.

Other Items of Interest

948 Assessment of the Energy Savings Potential of Building Foundations Research

951 Passive Solar Designs Investigated

965 Reverse Osmosis Treatment to Remove Inorganic Contaminants from Drinking Water

Engineering (Cont.)

966 A Study of Possible Economical Ways of Removing Radium from Drinking Water

976 An Overview of Technology on Bituminous Surfacing Materials for Low-Volume Roads

Environmental Science & Technology

965 Reverse Osmosis Treatment to Remove Inorganic Contaminants from Drinking Water

966 A Study of Possible Economical Ways of Removing Radium from Drinking Water

967 Ecological Research Needs at Hazardous Waste Disposal Sites

968 Update of Acute and Chronic Aquatic Toxicity Data for Heavy Metals and Organic Chemicals Found at Hazardous Waste Sites

Manufacturing, Machinery & Tools

969 Automated Ply Laminating System (APLS)

970 Research in Advanced Real-Time Computer Vision

971 Automated Paper Molding-Based Manufacturing System for 60mm M204 Increment Container Halves

972 Automated Production of Stick Propellant

973 Low Contraction (LC) Chromium Plating

974 Argon Welding Inside a Workpiece — Canopies convert a large, hollow workpiece into an inert-gas welding chamber.

Testing & Instrumentation

975 Test Apparatus for Oversize Ball-Bearing Models — A see-through machine enables direct observation and indirect measurements at moderate speeds. (Licensing Opportunity)

Materials

976 An Overview of Technology on Bituminous Surfacing Materials for Low-Volume Roads

977 Dyeing Flame-Retardant Fabrics (Licensing Opportunity)

978 Beta Processing Versus Crack Growth Rate

979 Laser Cladding of Magnesium with Zirconium

980 Studies of the Fracture Behavior of Ti-10V-2Fe-3A1

981 Weldability of 2219-T851 and 2519-T87 Aluminum Armor Alloys for Use in Army Vehicle Systems

982 Electrochromic Variable-Emissivity Surfaces — Temperature could be controlled by altering infrared radiative properties. (Licensing Opportunity)

983 Extending Fatigue Lives of Selected Alloys — Rejuvenating treatments have been demonstrated.

984 High-Emissivity Coatings for High-Temperature Surfaces — Plasma-sprayed coatings increase cooling by thermal radiation. (Licensing Opportunity)

985 PMR Composites of Increased Toughness — Toughness is increased without sacrificing processability or hot strength.

986 Readily Processable Polyimide — A polymer exhibits resistance to hydraulic fluid, excellent processability, and extremely high adhesive strength. (Licensing Opportunity)

Testing & Instrumentation

987 Reliability of Inspection by SLAM — Scanning laser acoustic microscopy finds flaws in ceramic specimen.

988 An Accurate Laboratory Test System Using Commercial Equipment for Eddy-Current Measurements

Other Items of Interest

998 Thermoplastic Removes Hydrogen without Producing Water

952 Corrosion in Amorphous-Silicon Solar Cells and Modules — Moisture severely affects amorphous-silicon units, bur encapsulation helps.

954 Spin Coating of Decon Agent Containers

999 Standard to Measure Carbon in Natural Materials

Medicine & Biology

989 Dental Liquid Diets

990 New Technique to Automate Sequencing of DNA

991 Dual Purpose Soft-Tissue Equivalent and Dosimetric Phantom Material

992 Sickle Cell Anemia New Study Technique

993 Technique for Imaging Blocked Coronary Arteries

994 Pressurized Sleeve — A garment part sustains a pressure differential without unduly restricting the user.

Other Items of Interest

967 Ecological Research Needs at Hazardous Waste Disposal Sites

968 Update of Acute and Chronic Aquatic Toxicity Data for Heavy Metals and Organic Chemicals Found at Hazardous Waste Sites

Natural Resources Technology & Engineering

995 Igneous Petrological Database: A Unique Global Geochemical Data Bank

Physical Sciences

996 JANAF Thermochemical Tables now Available Online Worldwide

997 New Technique for X-Ray Fluorescence Spectroscopy

998 Thermoplastic Removes Hydrogen without Producing Water

Testing & Instrumentation

999 Standard to Measure Carbon in Natural Materials

1000 Fast Data Acquisition for Mass Spectrometer — New equipment has the speed and capacity to process time-of-flight data. (Licensing Opportunity)

1001 Device Maintains Water at the Triple Point — A modified commercial freezer keeps water at 0.01 °C for over 10 weeks.

1002 Simultaneous Sampling of Two Spectral Sources — A fiber-optic bundle is used to sample a dye laser and a spectral lamp.

Other Items of Interest

982 Electrochromic Variable-Emissivity Surfaces — Temperature could be controlled by altering infrared radiative properties. (Licensing Opportunity)

Transportation & Components

1003 Acoustical Tests of a Scale-Model Helicopter Rotor — Data are obtained in simulated hovering flight in an open environment. (Licensing Opportunity)

1004 Fault-Tolerant Software for Flight Control — A redundant system performed well in flight tests. (Licensing Opportunity)

Agriculture & Food

927 Super Slurper Saves the Day for Good Nematodes

928 Wetting Agent Unbungles Fungals (Licensing Opportunity)

Other Items of Interest

989 Dental Liquid Diets

United States Department of Agriculture

Research Technology
Agricultural Research Service

Super Slurper Saves the Day for Good Nematodes

Body powder, batteries, and cold packs for injured bodies and picnic coolers have it; now soil in citrus groves could also receive a helping of a super thirsty, ARS-invented absorbent called super slurper. It seems that the absorbent keeps soil moist so tiny worms survive and kill weevils that chew up citrus tree roots.

In tests, the absorbent helped the soil worms—actually beneficial nematodes—kill 60 percent of citrus root weevils, compared to 25 percent without its help, says Agricultural Research Service entomologist William J. Schroeder.

Schroeder, based in Orlando, Florida, says that if unchecked, weevils can kill 20 to 30 percent of the trees in a grove and make others unable to produce fruit.

The nematodes, with the tongue-twisting names *Heterorhabditis heliothidis* and *Steinernema feltiae*, penetrate weevils' guts and release lethal bacteria. They don't harm plants or other organisms.

These nematodes haven't been used previously as natural weevil control because they die quickly if soil dries out.

Schroeder says, "I realized that to use this biological control, we would have to keep the soil moist." With its ability to hold up to 2,000 times its own weight in water, he figured super slurper would give him a way.

Other ARS scientists working at ARS' Northern Regional Research Center in Peoria, Illinois, invented the cornstarch-based super slurper in 1974. Schroeder is seeking a patent on his new use for the absorbent.

Commercial companies could mass-rear nematodes and package billions of them alive, he says. Growers could mix them with super slurper to put on citrus tree roots before planting. "What they would have then is a grove of trees with weevil control built-in around the roots—right where they need it."

For mature groves already inhabited by beneficial nematodes, Schroeder is looking into injecting super slurper into soil with a nozzle to make conditions more favorable for them.

Other ARS laboratories are testing the absorbent and nematodes to see how well the mix works to control pests of corn and vegetables.

William J. Schroeder is at the USDA-ARS Horticultural Research Laboratory, 2120 Camden Road, Orlando, FL 32803 (305) 897-7300. ♦

United States Department of Agriculture

Research Technology
Agricultural Research Service

Wetting Agent Unbungles Fungals

Scientists have recently noted that several species of fungi produce natural weed killers. But before these natural controls can be effectively exploited, ways must be found to improve their convenience and reliability.

Until now, the need to keep fungal herbicides in contact with dew or else to mist them with droplets of water has limited fungal herbicide's practicality. For if the fungal agent isn't kept wet for several hours after application, it won't grow and produce week-killing toxins.

Now there's a spray that can be applied to undesirable vegetation that enables fungi to germinate and grow without dependence on unpredictable dew or laborious misting.

The spray is made of a water/oil emulsion containing special additives to help get the herbicidal fungi started--a combination of lecithin with wax and/or a calcium salt. Weeds may get the patent-applied-for formula either in mixture with the fungus or immediately after they are inoculated with the fungal pathogen.

For technical information, contact Charles Quimby, Jr., USDA-ARS Delta States Research Center, PO Box 350, Stoneville, MS 38776. Patent Application Serial No. 07/114,952, "Control of Undesirable Vegetation."

FOR ADDITIONAL INFORMATION: Inquiries concerning rights for commercial use of this invention should be addressed to: Office of Federal Patent Licensing, Center for the Utilization of Federal Technology, Room 304, NTIS, Springfield, VA 22161; (703) 487-4738. Refer to Patent Application 7-114,952/TN.

Computers

929 Implementing and Managing Change: A Guide for Assessing Information Technology

930 New Guideline for Verifying, Validating Software

931 SQL Test Package Available from NBS

932 Single-Chip VLSI Reed-Solomon Decoder — Efficient utilization of computing elements reduces size while preserving throughput. (Licensing Opportunity)

Software

933 NASKERN Program Tests Computers — A "benchmark" program exercises computers on a set of standardized problems.

934 Subroutines for Image Processing — Dozens of functions and test programs are included.

Other Items of Interest

970 Research in Advanced Real-Time Computer Vision

Department of Energy

Technology Application

Oak Ridge National Laboratories

INFORMATION SCIENCE

IMPLEMENTING AND MANAGING CHANGE: A GUIDE FOR ASSESSING INFORMATION TECHNOLOGY

Key words: Information technology; information systems; office automation; management information systems; computers; evaluation

Office automation (OA) is rapidly transforming organizational life for workers on all levels. Driving this transformation is a considerable expenditure of money, effort, and time. Also attendant with OA are difficult changes in work patterns, both for employees who use OA and for those who interact with end-users. Because of these costs, it is important to minimize implementation of difficulties and to document the benefits of OA.

Extensive literature exists on evaluation, innovation adoption, and the impact of OA. However, until now there has been no single integration of this knowledge designed to help people implement OA or to assess its impact in specific settings. The ORNL report, *Implementing and Managing Change: A Guide for Assessing Information Technology,* presents this integration. This report addresses both stand-alone and networked systems and allows the user to choose whatever level of comprehensiveness or rigor is appropriate for his or her needs. Originally carried out for the U.S. Navy, this research can assist all implementors of OA in two ways: (1) it shows them how to monitor their implementation efforts, thus providing continual feedback to facilitate adoption of OA technology, and (2) it provides guidance for measuring the impact of OA on their employees and organizations.

The report presents a two-level framework for accomplishing these assessments. The first level is a conceptual overview of important issues. The second level contains numerous examples of how relevant factors were actually measured in a variety of studies.

The following issues are addressed in this report:

- review of previous measurement efforts,
- sources of data,
- methods of asking questions,
- determining the magnitude of impact (both positive and negative),
- value judgments about change,
- measuring productivity,
- the data collection process,
- sampling strategies,
- special requirements for assessing networking, and
- numerous specific examples of measurement.

Additional information:

Office of Technology Applications
Martin Marietta Energy Systems, Inc.
P.O. Box 2008
Oak Ridge, TN 37831-6257

Telephone (615) 574-4192; FTS 624-4192

J. A. Morell, R. Gryder, and M. Fleischer, *Implementing and Managing Change: A Guide for Assessing Information Technology*, ORNL/TM-10520, Oak Ridge National Laboratory (August 1987).

NBS technology update

National Bureau of Standards
U.S. Department of Commerce
Gaithersburg, MD 20899

New Guideline for Verifying, Validating Software

In today's world, many functions are controlled by computers--financial transactions, factory robots, even automobile operations. For any application it is important to have software that is correct and error-free; for software whose failure could have an impact on life safety and health or could cause large financial losses, it is absolutely vital. A new guideline, issued by NBS for use by the federal government, will help organizations improve the accuracy and quality of software during development and maintenance. The guideline adopts a document that was developed by the Institute of Electrical and Electronic Engineers (IEEE) with NBS assistance. It also has been approved by the American National Standards Institute as a voluntary industry standard.

FOR ADDITIONAL INFORMATION: A copy of this report is available from NTIS, Springfield, VA 22161; (703) 487-4600.

NTIS order number: FIPSPUB132
Price code: E07

NBS technology update

National Bureau of Standards
U.S. Department of Commerce
Gaithersburg, MD 20899

SQL Test Package Available From NBS

A package of tests to help users and vendors determine compliance with a new Federal Information Processing Standard Publication (FIPSPUB) 127 for the Database Language SQL will be available for purchase Aug. 3 from NBS. SQL is a voluntary industry standard language used to develop database management system applications. FIPSPUB 127 requires federal agencies to implement SQL in relational database managment system applications acquired or developed after Aug. 3, 1988. The test suite will help both users and vendors meet the standard. Database management systems can save time and money by making data, application programs, and trained users "portable" from one system to another. The NBS test package includes six types of tests in three programming languages--C, FORTRAN, and COBOL.

FOR ADDITIONAL INFORMATION: contact Joan Sullivan (301/975-3258) or Joseph Collica (301/975-3267) or write to A266 Technology Bldg., National Bureau of Standards, Gaithersburd, MD 20899. FIPS PUB 127 is available from the National Technical Information Service; (703/487-4650).

NASA Tech Brief
National Aeronautics and Space Administration
NASA's Jet Propulsion Laboratory, Pasadena, California

Licensing Opportunity

Single-Chip VLSI Reed-Solomon Decoder

Efficient utilization of computing elements reduces size while preserving throughput.

A real-time Reed-Solomon (RS) decoder based on a new pipeline architecture is realized on a single very-large-scale integrated (VLSI) circuit chip. The decoder architecture not only provides for error correction but also handles erasures in a pipeline manner. The new design is more efficient than previous designs and can be applied to a variety of digital communications that involve error-correcting RS codes.

Let $N = 2^m - 1$ = the length of the (N, l) RS code over $GF(2^m)$ with design distance d. Suppose that t errors and s erasures occur, and $s + 2t \leqslant d-1$. Let X_i be an error location or an erasure location and $\Lambda = \{X_i | X_i$ is an erasure location$\}$, $\lambda = \{X_i | X_i$ is an error location$\}$. Let Y_i be the corresponding errata magnitude and $r = (r_0, r_1, \ldots, r_{N-1})$ be the received vector. The pipeline architecture of the decoder (see Figure 1) performs the following decoding procedure:

1. Computes the syndrome polynomial

$$S(Z) = \sum_{k=1}^{\infty} S_k Z^{-k}$$

where

$$S_k = \sum_{n=0}^{N-1} r_n \alpha^{nk} = \sum_{i=1}^{S+t} Y_i X_i^k$$

for $1 \leqslant k \leqslant d-1$.

2. Computes the erasure-locator polynomial

$$\Lambda(Z) = \prod_{X_i \in \Lambda} (Z - X_i)$$

from Λ.

3. Multiplies $S(Z)$ and $\Lambda(Z)$ to obtain the Forney syndrome polynomial

$$T(Z) = S(Z)\Lambda(Z)$$

4. Computes the errata-evaluator polynomial $A(Z)$ and the error-locator polynomial $\lambda(Z)$ from $T(Z) = [A(Z)/\lambda(Z)]$ by the modified Euclid's algorithm.
5. Multiplies $\Lambda(Z)$ and $\lambda(Z)$ to get the errata-locator polynomial

$$P(Z) = \Lambda(Z)\lambda(Z)$$

6. Performs a Chien search on $\lambda(Z)$ to find the error-location set λ.

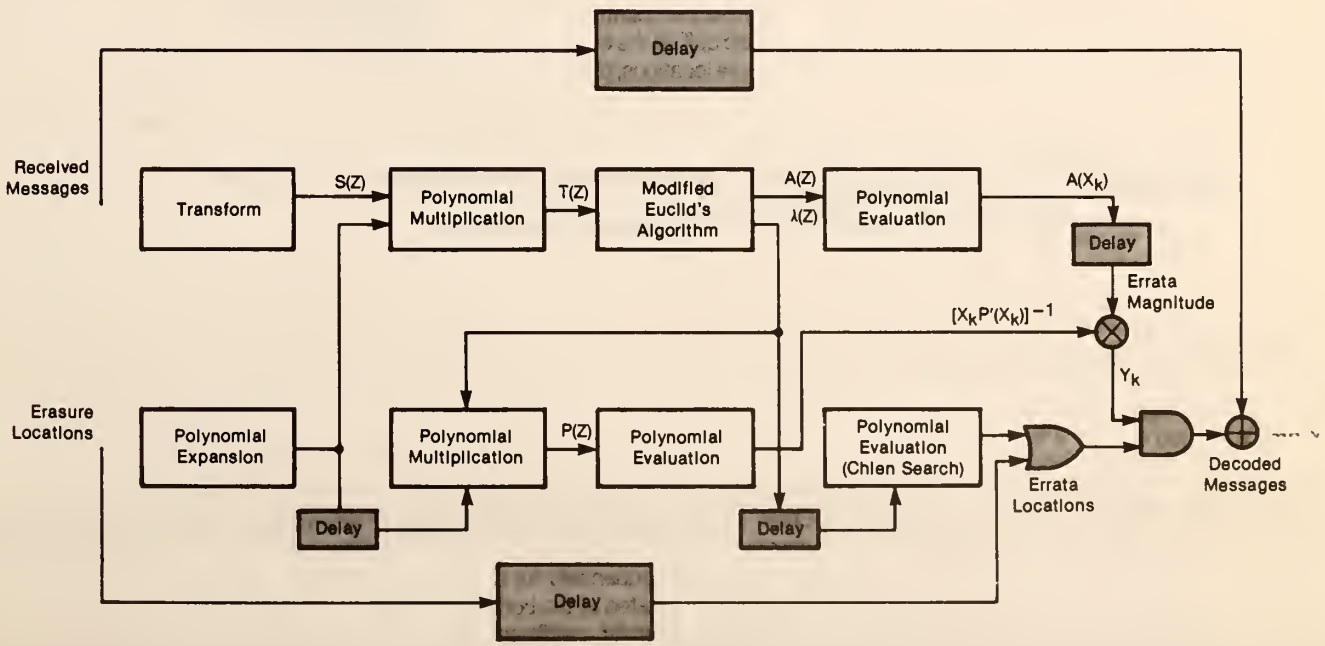

Figure 1. This **VLSI Architecture** represents a pipeline Reed-Solomon decoder for the correction of errors and erasures. The decoder uses a transform circuit to compute the syndrome polynomial $S(Z)$. The erasure information Λ enters the decoder as a binary sequence.

7. Computes the errata magnitudes

$$Y_k = \frac{A(X_k)}{X_k P'(X_k)}$$

for $1 \leq k \leq s + t$ by evaluating $A(Z)$ and $P'(Z)$. Uses sets λ and Λ to direct the additions of Y_k to the received vector r.

A new architecture implements the modified Euclid's algorithm by operating on the product of $S(Z)$ and $\Lambda(Z)$. The resulting error-locator polynomial $\lambda(Z)$ is then multiplied by $\Lambda(Z)$, thereby obtaining the errata-locator polynomial $P(Z)$. The derivative $P'(Z)$ of $P(Z)$ is obtained by dropping the even terms of $P(Z)$. The errata magnitudes Y_k are calculated then by a field inversion and a number of multiplications. Next the error locations are obtained in the form of a binary sequence by the use of another polynomial-evaluation circuit, which performs the Chien search on $\lambda(Z)$. This sequence of error locations, together with the input erasure-location binary sequence, directs the addition of Y_k to the received message.

The multiplications of $(Z - \alpha^k)$ can be implemented by the systolic array shown in Figure 2. Since it contains zeros as well as α^k's (where $\alpha^k \in \Lambda$), the input stream is used to control the updating of the latches in each basic cell. At the end of the arrivals of the erasure locations, the coefficients of $\Lambda(Z)$ are loaded from the latches into registers and shifted out serially.

Figure 2 also shows the new architecture to perform the modified Euclid's algorithm. The input multiplexer directs the syndrome polynomials to different cells. Each processor cell is used to process data recursively. Compared with the previous design of the systolic array, the present scheme for multiplexing the recursive cell computations significantly reduces the number of cells and, as a consequence, the number of circuits. The cell reduction is greater for high-rate codes.

Polynomials are evaluated not only in the Chien search process but also when the errata magnitudes are computed. $A_i(\alpha^j)^k$ is evaluated sequentially for each k at cell i. This is illustrated at the bottom of Figure 2. The polynomial coefficient A_i is multiplied by α^i at the initialization of cell i. From then on, a feedback loop computes the quantities $A_i(\alpha^j)^k$ for $k = 1, 2, 3, \ldots, N - 1$. The summation shown at the right in Figure 2 is implemented quite simply since all quantities are binary.

It is estimated that a (15,9) RS decoder chip would require about 29,000 transistors. A (31,15) RS decoder would require about 88,000 transistors. Considering the present VLSI technology, a high-throughput 5-bit (31,15) RS decoder could be implemented readily on a single VLSI chip.

This work was done by Howard M. Shao, Trieu-Kie Truong, In-Shek Hsu, and Leslie J. Deutsch of Caltech for **NASA's Jet Propulsion Laboratory**.

In accordance with Public Law 96-517, the contractor has elected to retain title to this invention. Inquiries concerning rights for its commercial use should be addressed to

Edward Ansell,
Director of Patents and Licensing
Mail Stop 301-6
California Institute of Technology
1207 East California Boulevard
Pasadena, CA 91125

Refer to NPO-16854, /TN

Jet Propulsion Lab.
NASA Resident Office
Technology Utilization Officer. Gordon S. Chapman
Mail Stop 180-801
4800 Oak Grove Drive
Pasadena, CA 91109
(818) 354-4849
Patent Counsel: Paul F. McCaul
Mail Code 180-801
4800 Oak Grove Drive
Pasadena, CA 91109
(818) 354-2734
Technology Utilization Mgr. for JPL: Norman L. Challin
Mail Stop 156-211
4800 Oak Grove Drive
Pasadena, CA 91109
(818) 354-2240

FOR ADDITIONAL INFORMATION: *Contact: Director, Technology Transfer Division, P.O. Box 8757, BWI Airport, MD 21240; (301) 621-0100 Ext. 241*

REFER TO THE NUMBER LISTED AT THE END OF THIS ARTICLE

NASA Tech Brief
National Aeronautics and Space Administration

NASKERN Program Tests Computers

A "benchmark" program exercises computers on a set of standardized problems.

A test computer program, NASKERN, has been developed for use by the Numerical Aerodynamic Simulation (NAS) project to aid in the evaluation of the performances of supercomputers. NASKERN consists of seven test-kernel programs that perform computations typical of supercomputer calculations at NASA Ames Research Center. It is expected that the performances of supercomputers when running this program will provide accurate projections of the performances of these computers on the actual computer codes of the NAS program.

The seven programs all emphasize the vectorized performance of a modern computer system. Each program is independent and consists of various looped floating-point operations. The programs include the following:

1. A matrix product;
2. An in-place, complex, radix-two, fast Fourier transform;
3. Parallel Cholesky decomposition;
4. Block tridiagonal matrix solution;
5. Gaussian elimination;
6. Creation of vortexes from boundary conditions; and
7. Simultaneous inversion of three matrix pentadiagonals.

NASKERN calculates performance statistics based on checks of accuracy, the number of operations performed, running times on the central processing units, and the resulting rates of calculation in terms of the number of floating-point operations per unit time.

NASKERN is written in FORTRAN 77 for batch execution and can be implemented on any machine with 64-bit precision. It has been run on a CRAY supercomputer under COS with a central-memory requirement of approximately 500 K of 64-bit words. NASKERN requires a machine-dependent clock-timing subroutine. The program was developed in 1986.

This program was written by David H. Bailey of Sterling Software for **Ames Research Center**. *ARC-11726 /TN*

FOR ADDITIONAL INFORMATION *CONTACT:*

COSMIC®
112 Barrow Hall
University of Georgia
Athens, GA 30602
(404) 542-3265

Subroutines for Image Processing

Dozens of functions and test programs are included.

The Image Processing Library computer program, IPLIB, is a collection of subroutines that facilitate the use of a COMTAL image-processing system driven by an HP 1000 computer. IPLIB uses an HP driver to direct all communications between the HP and a COMTAL Vision One/20 system. Dozens of functions are supplied, along with a test program for each function. Each IPLIB function takes the form of a FORTRAN subroutine invocation with appropriate parameters.

The functions include the addition or subtraction of two images with or without scaling, display of color or monochrome images, digitization of the image from a television camera, display of a test pattern, manipulation of bits, and clearing of the screen. IPLIB also provides the capability to read or write points, lines, and pixels from an image; read or write at the location of a cursor; and read or write an array of integers into COMTAL memory. The documentation catalogs the subroutines alphabetically and hierarchically for use as a cross-reference guide.

IPLIB is written in FORTRAN 77 for interactive execution and has been implemented on an HP 1000 computer operating under RTE VI with a central-memory requirement of approximately 64K. IPLIB is intended for use by those familiar with the COMTAL Vision One/20 image-processing system. The program was developed in 1985.

This program was written by Nettie D. Faulcon and James H. Monteith of **Langley Research Center** *and Keith W. Miller of the College of William and Mary.*
LAR-13620 /TN

FOR ADDITIONAL INFORMATION *CONTACT:*

COSMIC®
112 Barrow Hall
University of Georgia
Athens, GA 30602
(404) 542-3265

Electrotechnology

935 Device Limits Fault Current Level

936 Fast Synchronization with Burst-Mode Digital Signals — An oscillator is quickly synchronized with the data clock.

937 Adaptive Receiver for Codes Communications — Acquisition and tracking of the signal are controlled automatically

938 Flexible Ceramic-Insulated Cable — The cable withstands heat, radiation, and oxidation.

939 GPS Satellite Multipath Range Errors — Measurements are proposed to resolve uncertainties.

940 Formula Gives Better Contact-Resistance Values — Lateral currents in the contact strips are taken into account.

941 Image-Method Gain Measurement with Mismatch — A new formula accounts for multiple reflections.

942 Least-Squares Frequency-Acquisition Algorithm — Performance rivals that of the FFT algorithm.

943 Maser Oscillator with Dielectric Resonators — A two-resonator design should yield low phase noise. (Licensing Opportunity)

944 Single-Layer, Multicolor Electroluminescent Phosphors — Etching is eliminated in producing phosphor layers for displays. (Licensing Opportunity)

945 Small, Optically-Driven Power Source — Power would be transmitted along fiber-optic cables.

Testing & Instrumentation

946 RF Testing of Microwave Integrated Circuits — Fixtures and techniques are undergoing development.

947 Tiny Sensor may Help Robots Handle Materials Accurately

Other Items of Interest

998 Thermoplastic Removes Hydrogen without Producing Water

Device Limits Fault Current Level

A solid-state impedance fault current limiter (IFCL) designed and constructed at the David Taylor Research Center (DTRC) recently performed successfully during shipboard evaluation. DTRC personnel evaluated the device aboard USS JOHN HANCOCK (DD 981).

Developed in support of the 400-Hertz Power Continuity Program, the IFCL limits fault current levels on individual shipboard distribution lines; it permits solid-state frequency changer output bus voltage to remain within a specified voltage tolerance. As a result, other critical load equipment, such as computers, continue to receive quality power, even though a fault has occurred on a distribution line coming off the same solid-state frequency changer. The IFCL is rated for 400-hertz, 3-phase, 450-volt high current operation.

When the current exceeds a preset trip level, the IFCL power semiconductors, which carry the normal system load current, turn off immediately. Current flow to the fault is then limited by high impedance components connected in parallel with power semiconductors. If circuit breakers do not coordinate or trip out after a specified period of time, the IFCL shunt-trips the source AQB-A101 breaker.

Current limiters like this can improve power continuity of shipboard solid-state power conversion equipment.

For Additional Information:

Backup material on this effort is available from:

Navy Domestic Technology Fact Sheet
Reader Reply Service
Code E211
Naval Surface Weapons Center
Dahlgren, VA 22448-5000
(703) 663-8921

Refer to 121202/TN

NASA Tech Brief
National Aeronautics and Space Administration
NASA's Jet Propulsion Laboratory, Pasadena, California

Fast Synchronization With Burst-Mode Digital Signals

An oscillator is quickly synchronized with the data clock.

A clock-signal-extracting system reduces the time required by a receiver in a burst-mode digital communication system to synchronize its data-sampling oscillator with the digital signal to be sampled. By reducing the number of bit periods required for synchronization, the system reduces the required length of the preamble at the beginning of each burst of transmission, thereby increasing the amount of time available for the transmission of information during the burst. The system is compatible with most modulation techniques used for digital transmissions, and because it consists mostly of digital components, it reduces the complexity of the receiver.

The receiver includes circuits that sample the modulation of the received signal. For correct sampling and to minimize the bit-error rate, the sampling clock must be brought quickly into synchronism with the beginnings of the symbol periods; in effect, the system must extract the data-clock signal from the data signal.

The digital sequence "0101..." is contained in the preamble of each burst. The input signal is passed through a channel filter to remove noise; this filter has such a narrow passband that it strongly attenuates the harmonics of the 0101... square-wave modulation, so that its output is almost a pure sinusoid with a frequency equal to half the symbol rate.

The sampling clock causes the sinusoid to be sampled at intervals of approximately one-fourth the sinusoidal period (see figure). If the time of the sampling signal differs from the zero crossing of the sinusoid by a phase angle θ with respect to the sinusoid, then the samples have the values $\sin\theta$, $\cos\theta$, $-\sin\theta$, and $-\cos\theta$, respectively. In principle, θ can be calculated by taking the arc tangent of the sine and cosine samples and the result used to generate a control signal to adjust the oscillator to the correct timing.

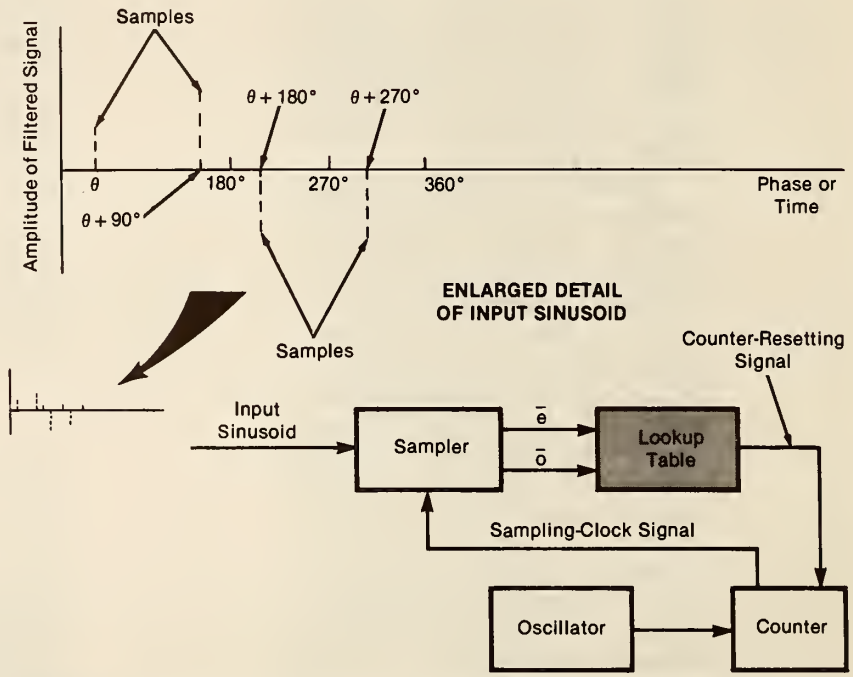

The Sampling Clock Is Synchronized with a sinusoid by a feedback technique. The feedback signal is a measure of the phase-error angle θ and is generated digitally by a technique related to the calculation of θ from periodic samples of the sinusoid.

The system functions according to a variation of this principle. To make the phase of the sampling clock digitally controllable, the clock includes an analog voltage-controlled oscillator that runs at a higher frequency, and the sampling signal is obtained by dividing the frequency in a resettable digital counter. Initially, the clock runs freely at its nominal frequency. The even-numbered samples e_i are collected in one group, and the odd-numbered samples o_i are collected in another group.

When n samples in each group have been accumulated, the system computes the averages

$$\bar{e} = \frac{1}{n}\sum_{j=1}^{n} |e_i| \text{ and } \bar{o} = \frac{1}{n}\sum_{j=1}^{n} |o_i|$$

The values of $\bar{e}$ and $\bar{o}$ are quantized, then fed as address inputs to a read-only memory "lookup" table that contains digital oscillator-phase-correction values for every possible combination of $\bar{e}$ and $\bar{o}$. The correction value is sent to the frequency-dividing counter, causing it to reset to the proper phase. Once synchronization is acquired, the digital decision feedback loop of the receiver takes over the responsibility of maintaining the correct sample timing.

This work was done by Lin-nan Lee, Ajit Shenoy, and Michael Kitming Eng of Comsat Laboratories for **NASA's Jet Propulsion Laboratory**. *NPO-16925 /TN*

FOR ADDITIONAL INFORMATION: *Contact: Director, Technology Transfer Division, P.O. Box 8757, BWI Airport, MD 21240; (301) 621-0100 Ext. 241*
REFER TO THE NUMBER LISTED AT THE END OF THIS ARTICLE

NASA Tech Brief
National Aeronautics and Space Administration
Ames Research Center, Moffett Field, California

Adaptive Receiver for Coded Communications

Acquisition and tracking of the signal are controlled automatically.

A radio receiver operating under automatic control processes Manchester-coded binary-phase-shift-keying signals under difficult reception conditions. The receiver locks onto the timing of the modulation, the frequency, and the phase of a signal, starting from a condition of considerable uncertainty about the amplitude and frequency.

The principal feature of the receiver is an adaptive control algorithm that guides the acquisition, tracking and demodulation of the signal, providing for the orderly transition through the following sequence of operating modes:

1. Estimation of out-of-band noise;
2. Acquisition of the coarse frequency and timing of the data signal employing a sequential probability-ratio test and a handover process;
3. Synchronization with the symbols and frequency of the data signal;
4. Synchronization with symbols and phase of the data signal; and
5. Confirmation of lock in the feedback loop.

After loss of lock, the mode control transfers the receiver operation back to the appropriate restart mode.

The acquisition of the signal begins with a sequential probability-ratio-test (SPRT) search of the frequency-uncertainty band. This is done by sweeping the band with a 4-point discrete-Fourier-transform (DFT) filter bank. Each filter is matched to the 512-Hz Manchester symbol rate, which is twice the coded-symbol rate $1/T = 256$ Hz, so that the bandwidth covered by the filter bank is 1,536 Hz.

Two filter sets separated in time by an offset of T/2 are formed at the Manchester symbol rate. At each dwell, the DFT filter outputs are accumulated and compared with SPRT thresholds until it is decided that the signal is or is not present. After the signal is detected, the residual 1536-Hz frequency uncertainty is too large to permit the frequency-lock loop (FLL) to start. Consequently, a handover procedure is initiated to narrow the uncertainty band to 512 Hz.

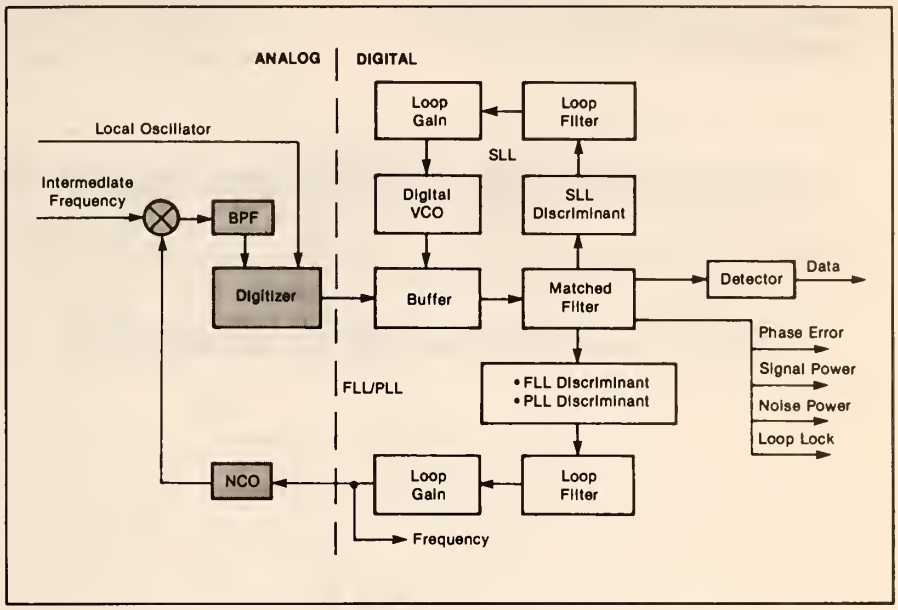

The **Receiver Is Constructed In Analog and Digital Portions** so that signal-processing functions that would otherwise be unwieldy can be performed economically by digital microprocessors.

In handover, multiple DFT filters are formed to cover the uncertainty regions of frequency and time. Outputs are accumulated, and the filter with the largest sum is chosen. The chosen filter center frequency and time offset are accepted as estimates of the signal frequency and timing if, in addition, the sum passes a Neyman-Pearson false-alarm-threshold test.

Following handover, the FLL and symbol-lock loop (SLL) are initiated. The FLL tracks the frequency and enables the performance of a least-squares estimate of the frequency and the rate of change of frequency. These estimates are calculated at the end of the FLL operation and are used to start the phase-lock loop (PLL).

The SLL tracks the symbol timing. When the PLL is turned on, its bandwidth is opened wide to improve acquisition and gradually narrowed to its operating value under the control of the PLL lock-detector statistic. After lock is confirmed by the other lock detectors, the demodulator output data are considered to be valid, and telemetry data are measured.

Preferably, the receiver is constructed as a hybrid analog/digital system (see figure). This partitioning enables the computation-intensive operations to be performed by programmable digital microprocessors. After being heterodyned to the intermediate frequency, the input signal is mixed with the output of the numerically controlled oscillator (NCO), limited in bandwith by a bandpass filter (BPF), and synchronously translated to baseband where it is digitized with 8-bit resolution. The resulting in-phase and quadrature digital data streams are processed to form the set of 4-point (DFT) filters at the Manchester symbol rate. DFT outputs are used to form the tracking-loop discriminants, the lock detectors, and the symbol-detection filter that provides the soft-decision demodulator output.

The FLL, PLL, and SLL operate at the symbol rate. FLL and PLL outputs drive the NCO, and the SLL output drives the digital voltage-controlled oscillator (VCO). This VCO is a digital integrator, the output of which is a pointer that selects the starting time for the DFT matched filters. Since the SLL resides in the processor, the digitizer operates at 4 times the Nyquist rate of

2 kHz for the DFT filters. This enables the SLL to select the DFT timing at time increments of T/32. Every T/2 seconds, the DFT filters are formed, and at T-second intervals, the receiver state is updated. To improve the performance, the loop bandwidths for the FLL, SLL, and PLL are opened wider at turn-on and then reduced with time.

This work was done by U. A. von der Embse of Hughes Aircraft Co. for **Ames Research Center**. *ARC-11815 /TN*

FOR ADDITIONAL INFORMATION: *Contact: Director, Technology Transfer Division, P.O. Box 8757, BWI Airport, MD 21240; (301) 621-0100 Ext. 241*

REFER TO THE NUMBER LISTED AT THE END OF THIS ARTICLE

NASA Tech Brief
National Aeronautics and Space Administration
NASA's Jet Propulsion Laboratory, Pasadena, California

Flexible Ceramic-Insulated Cable

The cable withstands heat, radiation, and oxidation.

A proposed ceramic-insulated cable would be flexible, would protect its metal conductor from ionizing radiation, and would resist high temperatures. Developed for use in outer space, the cable is also suitable for furnaces, nuclear reactors, and robots operating in hot, radioactive environments — in dismantling aging nuclear power plants, for example.

The cable would include a central conductor of copper surrounded by ceramic beads shaped so that their ends slide on each other, thus allowing the cable to flex (see figure). Two layers of copper tapes would be wrapped diagonally around the beads to absorb or deflect ions, electrons, protons, and electromagnetic radiation. An indium tin oxide coating on the surface of the outer tape would protect against oxidants.

To ensure reliable service at temperatures up to 800 °C, copper was selected as the conductor rather than aluminum because the former has a higher melting point. The insulating beads would be made of a porcelain that offers high dielectric strength, high electrical volume resistivity, and low dielectric loss factor.

The beads would be fabricated by casting. The central hole for the copper conductor could be drilled by a laser beam. The ends of the beads would be finished by grinding and polishing to provide smooth sliding surfaces for adjacent beads. The ends of the central holes would be rounded so that the conductor could flex easily in the beads. Lubricants, which would deteriorate in a hot, radiation-filled environment, would not be used. All the beads along a cable would be identical except for those at the ends of the cable, which would be slotted to hold the ends of the tapes.

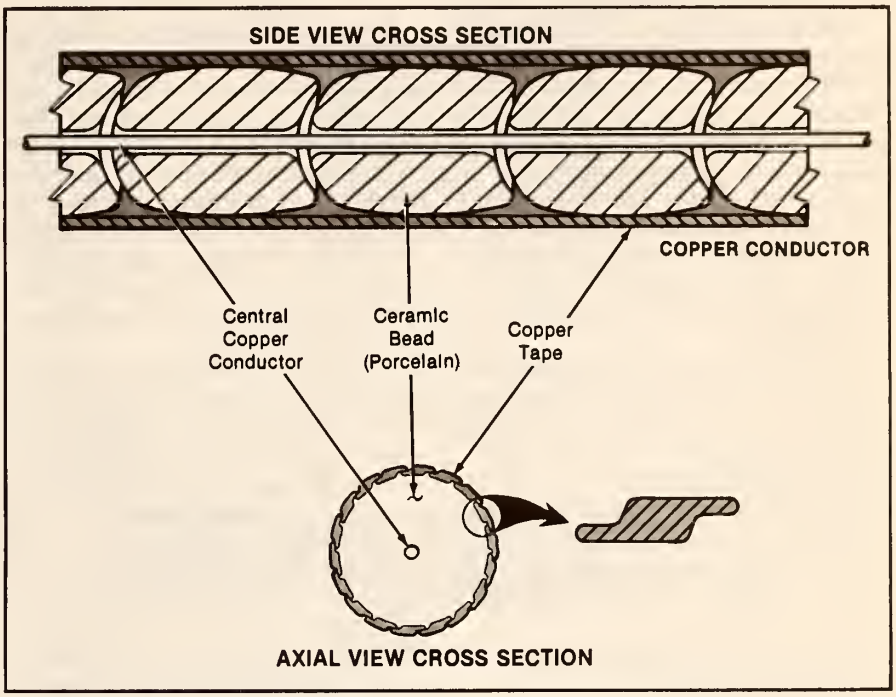

Ceramic Beads would electrically insulate a copper conductor from a sheath of copper tape.

Each tape would be wrapped at an angle of 30° to 45° with a small amount of slack to prevent binding. To prevent the formation of gaps during flexing, each tape would overlap each adjacent tape by about one-eighth inch (3 mm).

For service at higher temperatures, the tapes could be made of tantalum instead of copper. In addition, for added tensile strength, a wire of metal that does not soften as much as copper does in the range of operating temperatures could be twined around the copper core or around the ceramic beads.

This work was done by Frank L. Bouquet of Caltech for **NASA's Jet Propulsion Laboratory**. *NPO-16917 /TN*

FOR ADDITIONAL INFORMATION: *Contact: Director, Technology Transfer Division, P.O. Box 8757, BWI Airport, MD 21240; (301) 621-0100 Ext. 241*
REFER TO THE NUMBER LISTED AT THE END OF THIS ARTICLE

NASA Tech Brief
National Aeronautics and
Space Administration

GPS Satellite Multipath Range Errors

Measurements are proposed to resolve uncertainties.

A report discusses errors in range measurements in the Global Positioning Satellite (GPS) system due to multipath transmissions originating at the satellites. At present, large uncertainties in the sizes of multipath errors limit the precision of GPS measurements. Experiments are proposed to determine the systematic multipath errors under various operating conditions, with a view toward applying corrections to increase the precision of future GPS measurements.

The use of properly-designed GPS receivers is expected to enable the accurate measurements of baselines up to thousands of kilometers in length. A key to these accurate measurements is the common-mode rejection of instrumental errors originating at the satellites through differencing of the measured pseudoranges to a pair of ground receivers from a single satellite.

This measurement technique fails in the presence of effects that originate at a satellite but that are not the same for different ground receivers observing the same satellite. Multipath caused by some of the signal power from a satellite antenna bouncing off other parts of the satellite is an example of this: The additional signal delay caused by multipath transmission is dependent on the angle between the centerline of the antenna and the line of sight to the receiver on the ground, also called the "angle off boresight" or "boresight angle."

It has been estimated that a multipath effect with a magnitude of a few centimeters may remain after differencing and cannot be calculated with confidence. It is, therefore, necessary to conduct experiments to quantify the effect, to determine whether it can be ignored, must be modeled, or presents a fundamental obstacle to the use of P-code (a pseudorandom-noise code used in the GPS system) measurements to resolve carrier-cycle ambiguities.

At an antenna-testing range, a GPS antenna was mounted on a ground plane and used to transmit P-code ranging signals toward a GPS receiver 800 ft (240 m) away. The P-code delay was measured as a function of the boresight angle from 0° to 14° and found to have variations of as much as 67 times the 0.03-ns accuracy required for the use of P-code pseudorange measurements to reliably resolve carrier-cycle ambiguities. However, the measurements may have been strongly affected by multipath effects of the test range itself, and experiments are being conducted with a satellite in orbit to determine whether the variations due to the satellite and its antenna are either less than, or can be calculated to, within 0.03 ns.

The experiments exploit the fact that the changes in delay due to multipath are expected to be much larger in the P-code than in the carrier signals in most instances. The differential change in range between the carrier and P-code is monitored as a function of the satellite elevation. The remaining sources of experimental error include system noise, multipath at the ground antenna, errors in ionospheric calibration, noncoherence of carrier and P-code circuits at the satellite or ground receiver, and errors in the orientations of satellites. Possible variations of effects among satellites, or dependence of delay on the azimuth angles of the satellite antennas will be investigated.

This work was done by Lawrence E. Young of Caltech for **NASA's Jet Propulsion Laboratory**. *"An Experimental Technique To Monitor the In-Orbit Multipath Performance of Satellite Antennas," NPO-17020 /TN*

FOR ADDITIONAL INFORMATION: *Contact: Director, Technology Transfer Division, P.O. Box 8757, BWI Airport, MD 21240; (301) 621-0100 Ext. 241*

REFER TO THE NUMBER LISTED AT THE END OF THIS ARTICLE

NASA Tech Brief
National Aeronautics and Space Administration
NASA's Jet Propulsion Laboratory, Pasadena, California

Formula Gives Better Contact-Resistance Values

Lateral currents in the contact strips are taken into account.

A quasi-two-dimensional, mathematical model accounts for the effects of three-dimensional distributions of electrical currents in and around square ohmic contacts. The "Thin-Film" model will improve the extraction of the areal resistivities of contacts from current and voltage measurements of four-terminal test structures in integrated circuits.

In a four-terminal contact-test structure (see Figure 1), an electrical current I is applied through taps on the upper and lower conducting strips, while the voltage V_K across the contact is measured via side taps connected to the conducting strips. Because some of the current flows laterally in the strips around the narrower square contact, the measured contact resistance $R_K = V_K/I$ is larger than the true contact resistance $R_I = \varrho/L^2$ (where ϱ is the areal contact resistivity and L is the width of the square).

In the Thin-Film model, the upper conducting strip (e.g., metal) is treated as an equipotential surface. The lower conducting strip (e.g., doped semiconductor) is treated as two-dimensional. An equipotential core smaller than the contact is considered to be embedded in the lower conducting strip, connected to the upper strip through a lumped resistance of R_I (see Figure 2). The last two features model horizontal current flow under and vertical current flow in the actual contact; i.e., a thin but highly resistive layer between the conducting strips (Figure 1).*

The current is introduced to the lower conductor at the left, far from the contact (Figure 2). While the current through the back edge of the contact is neglected, the currents through the front and side edges are analyzed by dividing the structure into three regions. No current is allowed to flow between regions. Current is considered to be injected into those regions through long feeding strips and, therefore, to be distributed according to the width of each strip.

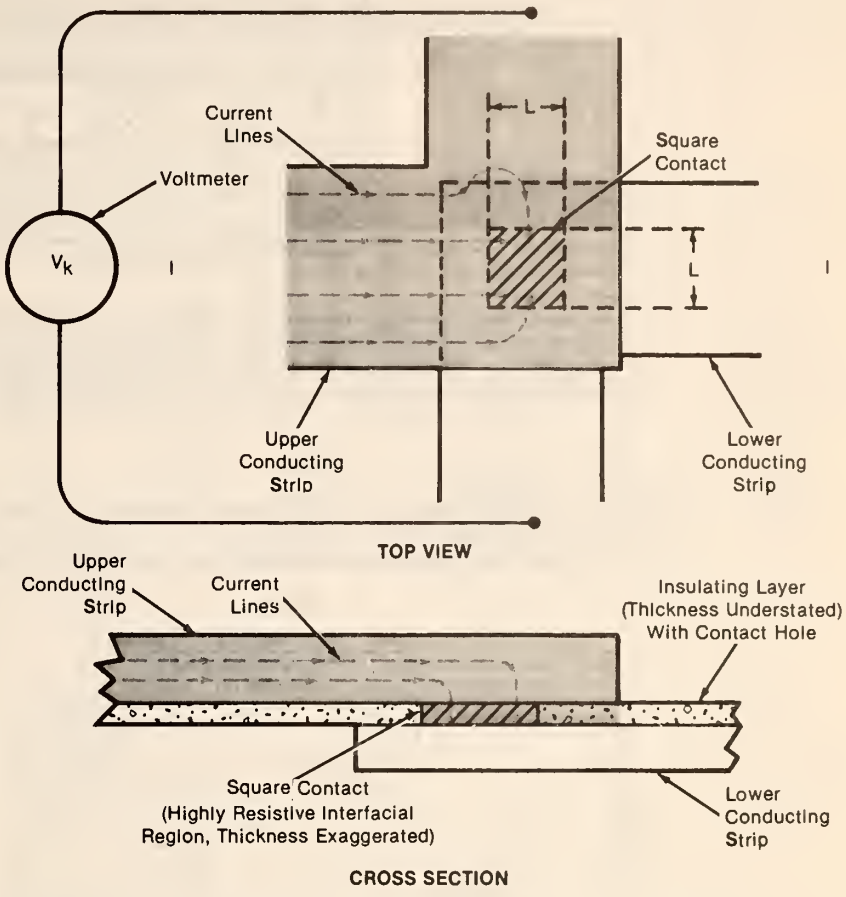

Figure 1. **Four-Terminal Test Structures** like this one are added to integrated circuits to enable the measurement of interfacial resistivities of contacts between thin conducting layers.

The resulting potential distribution in the side region with the voltage tap is found by conformal mapping. The potential at the end of this tap, referred to the core zone, is $V_S = R_S I$, where R_S is given as a function of contact size L, width and sheet resistance of the lower strip, and the areal resistivity ϱ itself.* From Figure 2 follows

$$R_K = R_S + R_I$$

and, hence,

$$\varrho = L^2 (R_K - R_S)$$

This equation must be solved iteratively. However, the solution converges rapidly: a FORTRAN program on a VAX (or equivalent) computer requires only about 0.3 s of central-processor time.

The model has been used to analyze square contacts of AuGeNi/GaAs. The areal resistivities of the contacts were found to be 2 to 8 times lower than extracted previously (without subtraction of R_S) and independent of contact size in the range of 1.5 to 10 μm.

*U. Lieneweg and D. J. Hannaman, "New Flange Correction Formula Applied to Interfacial Resistance Measurements of Ohmic Contacts to GaAs," IEEE Electron Device Letters, in print.

This work was done by Udo Lieneweg and David J. Hannaman of Caltech for **NASA's Jet Propulsion Laboratory**.
NPO-17096 /TN

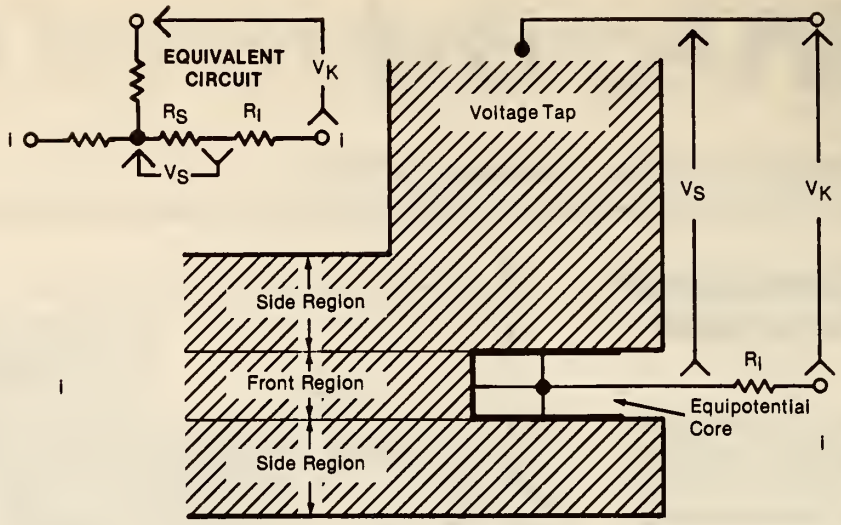

Figure 2. The **Thin-Film Model** is a simplified quasi-two-dimensional potential model that accounts adequately for the complicated three-dimensional, nonuniform current densities in the test structure of Figure 1. The effects of nonuniformity caused by lateral current flow in the strips are summarized in the equivalent resistance R_S and voltage V_S.

FOR ADDITIONAL INFORMATION: *Contact: Director, Technology Transfer Division, P.O. Box 8757, BWI Airport, MD 21240; (301) 621-0100 Ext. 241*

REFER TO THE NUMBER LISTED AT THE END OF THIS ARTICLE

NASA Tech Brief
National Aeronautics and Space Administration
Lewis Research Center, Cleveland, Ohio

Image-Method Gain Measurement With Mismatch

A new formula accounts for multiple reflections.

An equation has been derived for measurement of the absolute gain of a microwave antenna by the image method where the antenna is mismatched with its waveguide. While the image method (see figure) is simple to use, up to now its accuracy has depended on the assumption of a perfect match.

The perfect-match formula for absolute-gain measurements is

$$|\Gamma|^{-1} = 8\pi R/G\lambda$$

where Γ^2 is the ratio of received power to transmitted power, R is the distance from the antenna to the reflecting plane as shown in the figure, λ is the wavelength, and G is the gain. To obtain G, it is first necessary to measure the received and transmitted powers at various distances R to obtain a plot of $1/|\Gamma|$ versus R. The slope of the mean straight line interpolated through this plot is $8\pi/G\lambda$, from which G is then easily calculated.

If the antenna and waveguide are mismatched, then some of the received power is reflected from the waveguide/antenna junction and sent out again along with the transmitted power. A portion of this reflected power is returned to the antenna in a series of reflections of ever-decreasing power. When the effects of the multiple reflections are included, the gain-measurement formula becomes

$$|\Gamma - \Gamma_o|^{-1} = 8\pi R/G\lambda(1 - |\Gamma_o|^2)$$

where Γ_o is the reflection coefficient of the waveguide/antenna junction and it is assumed that the imaging plane is a perfect reflector.

The formula was tested by applying the image method to two antennas having previously known gains of 15.0 dB at 22 GHz and 23.9 dB at 20 GHz, respectively. Using the formula, the image-method gains were 14.65 dB and 23.98 dB, respectively.

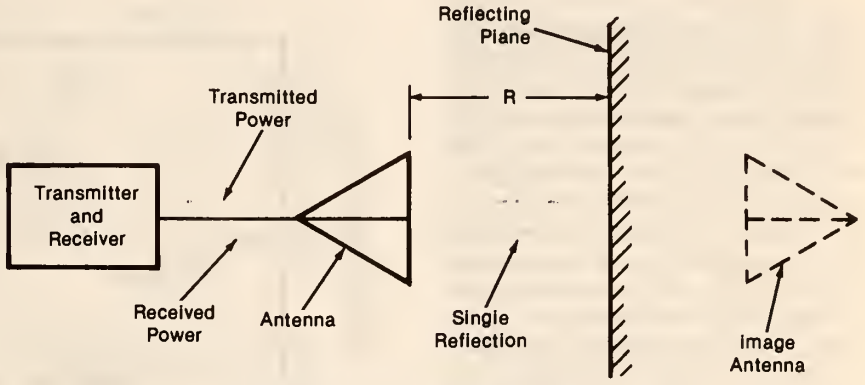

ANTENNA AND WAVEGUIDE MATCHED

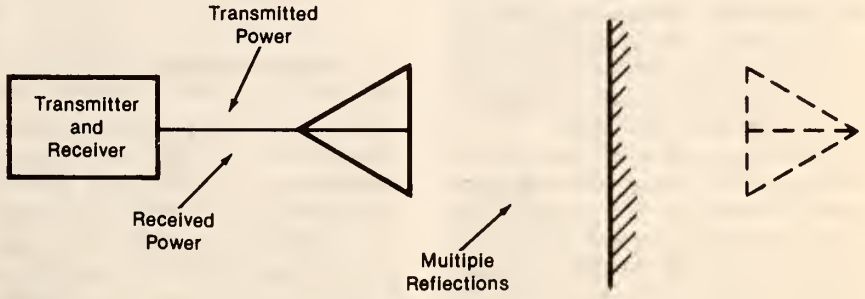

ANTENNA AND WAVEGUIDE MISMATCHED

In the **Image Method** an antenna is placed facing its image in a reflecting plane. The power transmitted by the antenna and the portion of the transmitted power received by the antenna after reflection from the plane are measured at various distances R.

This work was done by Richard Q. Lee and Maurice F. Baddour of **Lewis Research Center**. *Further information may be found in NASA TM-88924 [87-16968/NSP], "Absolute Gain Measurement by the Image Method Under Mismatched Condition." [A02]*

Copies may be purchased from the National Technical Information Service, Springfield, Virginia 22161, Telephone No. (703) 487-4650.

Rush orders may be placed for an extra fee by calling (800) 336-4700.

LEW-14555 /TN

FOR ADDITIONAL INFORMATION: *Contact: Director, Technology Transfer Division, P.O. Box 8757, BWI Airport, MD 21240; (301) 621-0100 Ext. 241*

REFER TO THE NUMBER LISTED AT THE END OF THIS ARTICLE

NASA Tech Brief
National Aeronautics and Space Administration
NASA's Jet Propulsion Laboratory, Pasadena, California

Least-Squares Frequency-Acquisition Algorithm

Performance rivals that of the FFT algorithm.

A least-squares algorithm finds the frequency and phase of a sinusoidal signal in the presence of noise (see figure). The algorithm is a special case of more-general, adaptive-parameter-estimation techniques. The computational requirements of the new algorithm are comparable to those of the corresponding fast-Fourier-transform (FFT) algorithm. The new algorithm works directly in the time domain, whereas the FFT algorithm transforms the data into the frequency domain for estimation and detection and requires a secondary algorithm to interpolate between frequencies.

The received signal is assumed to be demodulated by a carrier reference signal of known frequency and phase and by its 90°-phase-shifted version. The problem is to determine the frequency and phase of the received signal from the noise-corrupted in-phase and quadrature samples of the demodulated signal plus noise.

The basic equations for the measurements express the noisy samples as a truncated (nth-order) series involving the unknown frequency and phase, the sampling times, and the noise samples. The equations can be put in linear form involving a matrix of parameters that depend on the frequency and phase and from which, in principle, the frequency and phase can be extracted.

The algorithm obtains the matrix of parameters from a sequence of N pairs of measurements. It involves the inverse of an $n \times n$ matrix (the "state-vector" matrix)

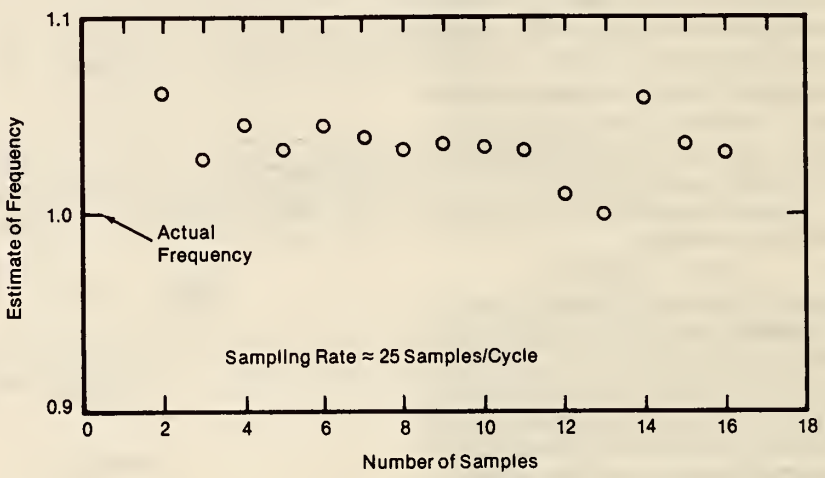

In a **Numerical Simulation** without noise, the algorithm gave an estimate close to the actual frequency in a fraction of the signal period.

that contains terms dependent on the sampling times and that can be precomputed, multiplied by a matrix formed from the measurements. The state-vector matrix has a special structure that makes it possible to use a rapid inversion algorithm: as a result, the desired matrix of parameters can be obtained in about $6n\log_2(n)$ operations, much fewer than the number of operations required for the "brute-force" calculation of a general matrix equation of similar form.

Initially, the estimation error of the least-squares algorithm approaches zero as the reciprocal of the factorial of the number of measurements. As the number of observations increases, the algorithm converges even faster — at an exponential rate. The computational requirements of the least-squares algorithm are determined predominantly by the product of the signal frequency and the observation period, whereas those of the FFT algorithm depend predominantly on the number of samples.

This work was done by Rajendra Kumar of Caltech for **NASA's Jet Propulsion Laboratory**. *NPO-17104 /TN*

FOR ADDITIONAL INFORMATION: *Contact: Director, Technology Transfer Division, P.O. Box 8757, BWI Airport, MD 21240; (301) 621-0100 Ext. 241*
REFER TO THE NUMBER LISTED AT THE END OF THIS ARTICLE

NASA Tech Brief
National Aeronautics and Space Administration
NASA's Jet Propulsion Laboratory, Pasadena, California

Licensing Opportunity

Maser Oscillator With Dielectric Resonators

A two-resonator design should yield low phase noise.

A proposed sapphire-maser oscillator would exhibit phase noise intermediate between the phase noises of unstabilized microwave oscillators and those of stabilized ruby-maser oscillators with superconducting cavities. Instead of the conventional single resonator, the oscillator would contain two total-internal-reflection (TIR) dielectric resonators in a normally-conductive (that is, nonsuperconductive) copper cavity. Because the TIR resonators would not require superconductivity to achieve a relative bandwidth of 10^{-7} to 10^{-8}, the oscillator could be operated at a relatively high temperature — typically at 10 to 80 K — for which inexpensive commercial coolers are available. The oscillator would also not include the magnets that are required in ruby masers.

The two resonators would have a wheel-like ring-and-disk configuration (see figure). The upper resonator, made of sapphire doped with iron, would be sized and shaped to operate at the 31-GHz pump frequency appropriate for iron/sapphire masing at zero applied magnetic field. The pump signal would be coupled in through a coaxial cable. This resonator would be made with only as much dielectric as is necessary to contain the resonant electromagnetic mode, so that its entire volume could be pumped for effective regeneration of whatever signal fields are coupled to it from the lower resonator.

The lower resonator would be made of sapphire in a size and shape to resonate at the 12-GHz output-signal frequency of iron/sapphire masing. Like the upper resonator, this one is also designed to suppress the plethora of resonant modes (other than the desired one) that is ordinarily characteristic of older disk-and-cylinder resonators.

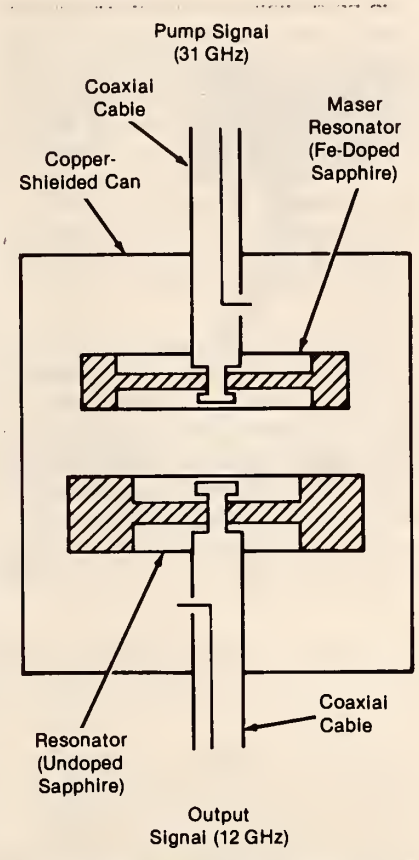

The **Two-Resonator Maser Design** would provide phase stability, isolation between the pump and output channels, and variable maser coupling.

The output signal would be coupled through a second coaxial cable.

Because the iron-atom maser spins are coupled to both the pump and signal frequencies via the radio-frequency magnetic field and because the fields are confined to the TIR resonators primarily by dielectric effects, the fringing magnetic fields would be used to couple the spins in the lower and upper resonators. The distance between the resonators would be adjusted by a conventional mechanical tuning mechanism to vary the degree of coupling.

This work was done by G. John Dick and Donald M. Strayer of Caltech for **NASA's Jet Propulsion Laboratory**.

This invention is owned by NASA, and a patent application has been filed. Inquiries concerning nonexclusive or exclusive license for its commercial development should be addressed to the Patent Counsel, NASA Resident Office-JPL. Refer to NPO-17157. /TN

Jet Propulsion Lab.
NASA Resident Office
Technology Utilization Officer: Gordon S. Chapman
Mail Stop 180-801
4800 Oak Grove Drive
Pasadena, CA 91109
(818) 354-4849
Patent Counsel: Paul F. McCaul
Mail Code 180-801
4800 Oak Grove Drive
Pasadena, CA 91109
(818) 354-2734
Technology Utilization Mgr. for JPL: Norman L. Chalfin
Mail Stop 156-211
4800 Oak Grove Drive
Pasadena, CA 91109
(818) 354-2240

FOR ADDITIONAL INFORMATION: *Contact: Director, Technology Transfer Division, P.O. Box 8757, BWI Airport, MD 21240; (301) 621-0100 Ext. 241*
REFER TO THE NUMBER LISTED AT THE END OF THIS ARTICLE

NASA Tech Brief
National Aeronautics and Space Administration
Langley Research Center, Hampton, Virginia

Licensing Opportunity

Single-Layer, Multicolor Electroluminescent Phosphors

Etching is eliminated in producing phosphor layers for displays.

A new method has been conceived for the construction of a single phosphor layer composed of two or more different color phosphors for use in thin-film electroluminescent (TFEL) displays. In order to display the full color spectrum, including white, electronic displays must have the three primary colors red, green, and blue. Full-color TFEL displays, therefore, require red, green, and blue phosphors placed close together side-by-side in the same layer or in separate superimposed layers or in some combination of the two. The phosphor layers in a TFEL display device are formed by vacuum deposition of the phosphors, in thicknesses of 2,000 to 5,000 Å, onto a glass substrate that already has on one surface a pattern of transparent electrodes covered with a transparent insulating layer.

Prior methods for producing the single-layer, two-color phosphor layers for TFEL displays involve deposition, masking, and etching of both the red and green phosphors. The etching steps are very difficult to control and result in low yield and high cost for display production. Also, the etching leaves, on the phosphor layer, an uneven surface that promotes dielectric breakdown in the insulating layer that covers the phosphor in a TFEL display device.

The new process enables the production of the single-layer, two-color phosphor layer without etching. The method of construction, beginning with the glass substrate with electrode and insulator layers, involves the deposition of the green phosphor, ZnS:TbF_3; masking with a metal mask or photoresist; diffusion or ion implantation of manganese through the mask to produce the red phosphor, ZnS:Mn:TbF_3; and removal of the mask.

This technique can also be used to produce both single-layer, two-color phosphors of other colors and single-layer, three-color phosphors. The phosphors must be of the same host material, but with different impurities. A two-color example is SrS:Ce_2S_3 (red) and SrS:CeF_3 (blue). A three-color example is ZnS:Mg (blue), ZnS:Mn:TbF_3 (red), and ZnS:TbF_3 (green).

This work was done by James B. Robertson of **Langley Research Center.**

This invention is owned by NASA, and a patent application has been filed. Inquiries concerning nonexclusive or exclusive license for its commercial development should be addressed to the Patent Counsel, Langley Research Center. Refer to LAR-13616/TN

Langley Research Ctr.
Technology Utilization Officer: John Samos
Mail Stop 139A
Hampton, VA 23665
(804) 865-3281
Patent Counsel:
George F. Helfrich
Mail Code 279
Hampton, VA 23665
(804) 865-3725

FOR ADDITIONAL INFORMATION: *Contact: Director, Technology Transfer Division, P.O. Box 8757, BWI Airport, MD 21240; (301) 621-0100 Ext. 241*
REFER TO THE NUMBER LISTED AT THE END OF THIS ARTICLE

NASA Tech Brief
National Aeronautics and Space Administration
NASA's Jet Propulsion Laboratory, Pasadena, California

Small, Optically-Driven Power Source

Power would be transmitted along fiber-optic cables.

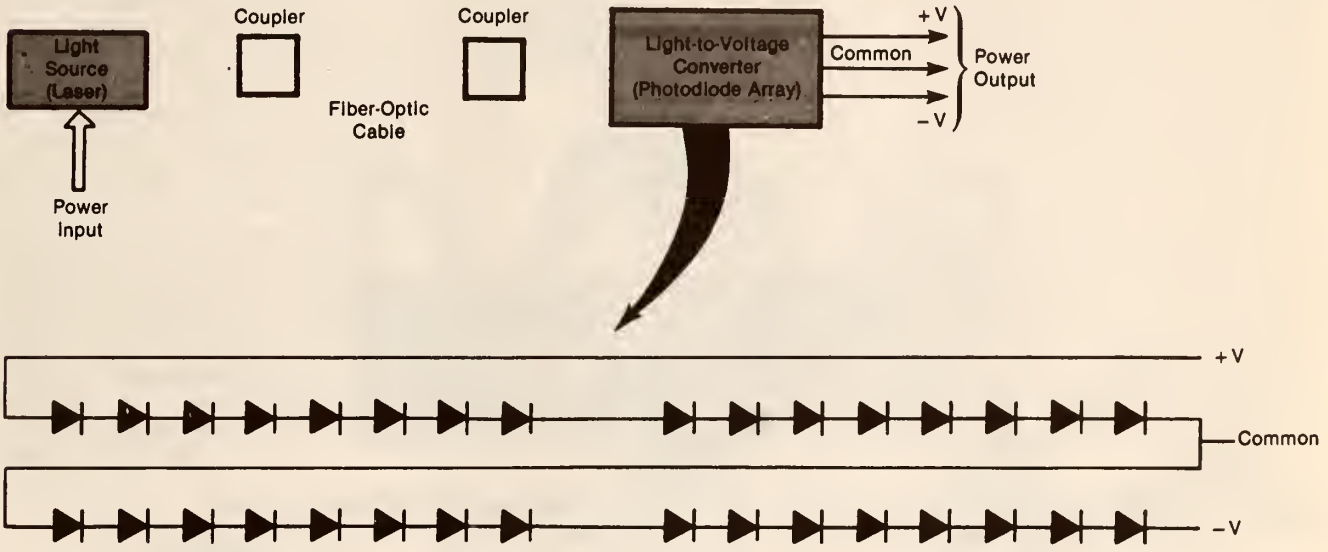

Figure 1. **Power Would Be Transmitted** as infrared light along a fiber-optic cable, then converted to electricity to supply a small electronic circuit. The power source and the circuit could thus remain electrically isolated from each other for safety or to reduce electromagnetic interference.

Arrays of AlGaAs/GaAs photodiodes undergoing development are expected to deliver 4 to 12 V at currents up to 1 mA under infrared illumination at a wavelength of 850 nm. The conversion efficiency of optical to electrical energy may be as high as 40 percent. In the intended application, the infrared light would be transmitted along optical fibers to the diode array (see Figure 1) to supply power to a small electronic circuit that has to be electrically isolated; for example, to an electric-field sensor in or near a source of high voltage.

An experimental version of the power-conversion device includes 32 AlGaAs/GaAs diodes connected in four strings of eight diodes each (see Figure 2). Even though it is more difficult to fabricate, GaAs is used because its higher energy-conversion efficiency at 850 nm enables the fabrication of a thin diode array that fits into a small package. The array was made according to standard integrated-circuit design rules, using standard glass photomasks for the photolithographic process.

The diode layers are grown by metal/organic chemical-vapor deposition. A semi-insulating GaAs wafer serves as the substrate and electrically isolates the diodes from each other. A thick layer of n-type GaAs is deposited on the substrate, followed by a thinner layer of p-type GaAs; these two layers form the p/n diode junction that converts the light to electricity. A thin layer of p-type AlGaAs is then deposited as a surface-passivation layer.

The layers are etched into individual mesas, each of which will become a diode. A layer of SiO_2 is deposited by radio-frequency sputtering, then etched to remove all oxide except that on one side of the mesas. This oxide prevents the shorting of the diodes when the interconnecting metal (Ag) is evaporated onto the device. The metal is etched to form the interconnections. Finally, the device is mounted in a standard TO-5 package.

This work was done by Richard H. Cockrum and Ke-Li J. Wang of Caltech for **NASA's Jet Propulsion Laboratory**.
NPO-16827 /TN

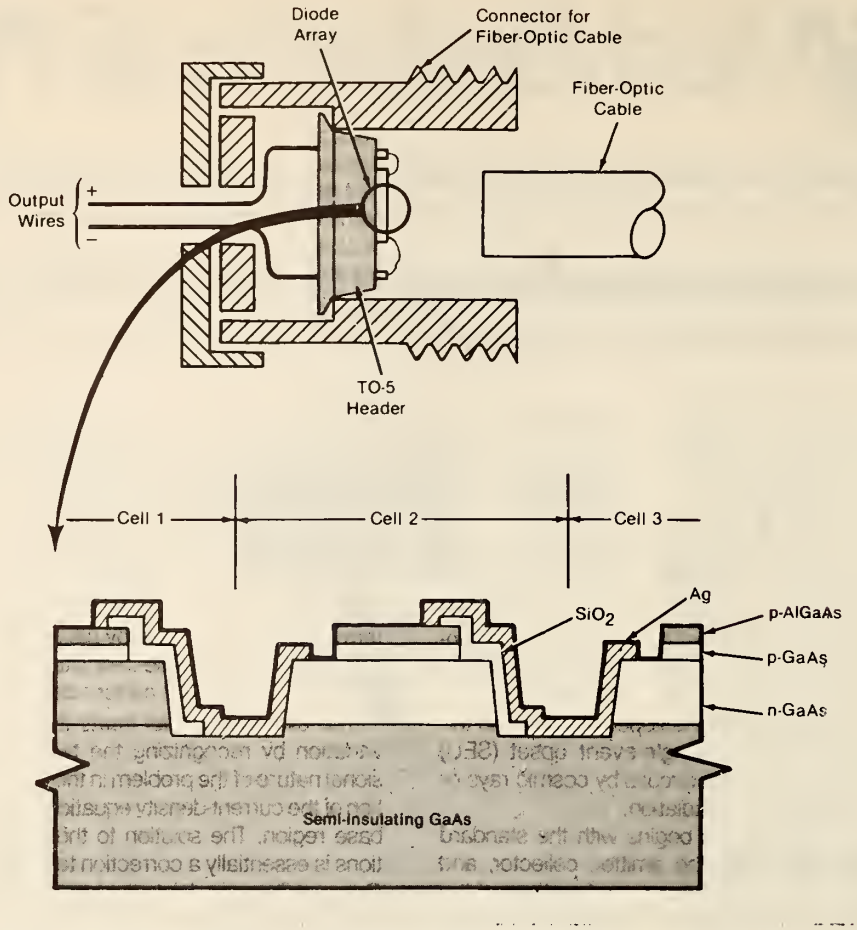

Figure 2. The **Array of Diodes** is made by standard integrated-circuit techniques and packaged for mounting at the end of the fiber-optic cable.

FOR ADDITIONAL INFORMATION: *Contact: Director, Technology Transfer Division, P.O. Box 8757, BWI Airport, MD 21240; (301) 621-0100 Ext. 241*

REFER TO THE NUMBER LISTED AT THE END OF THIS ARTICLE

NASA Tech Brief
National Aeronautics and Space Administration
Lewis Research Center, Cleveland, Ohio

RF Testing of Microwave Integrated Circuits

Fixtures and techniques are undergoing development.

Four test fixtures and two advanced techniques have been developed in a continuing effort to improve the radio-frequency (RF) characterization of monolithic microwave integrated circuits (MMIC's) in the K and K_a bands (18 to 26.5 and 26.5 to 40 GHz, respectively). RF characterization requires small-signal input/output scattering-parameter measurements by automatic vector network analyzers; these measurements are difficult at and above the K band because the increased effects of parasitics at these frequencies introduce inaccuracy and nonrepeatability, the mounting of MMIC's in conventional fixtures is time consuming, and it is difficult or impossible to couple test equipment to MMIC's in a nondestructive manner.

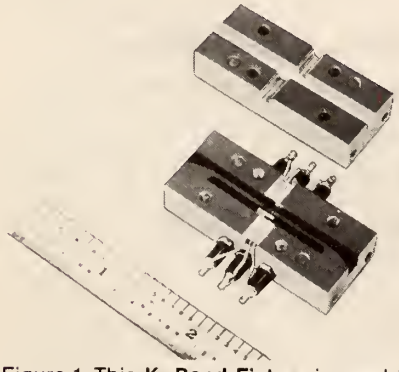

Figure 1. This **K_a-Band Fixture** is used to test MMIC submodules of a 30-GHz receiver. A 3-bit switched-line phase shifter is bonded to the fixture.

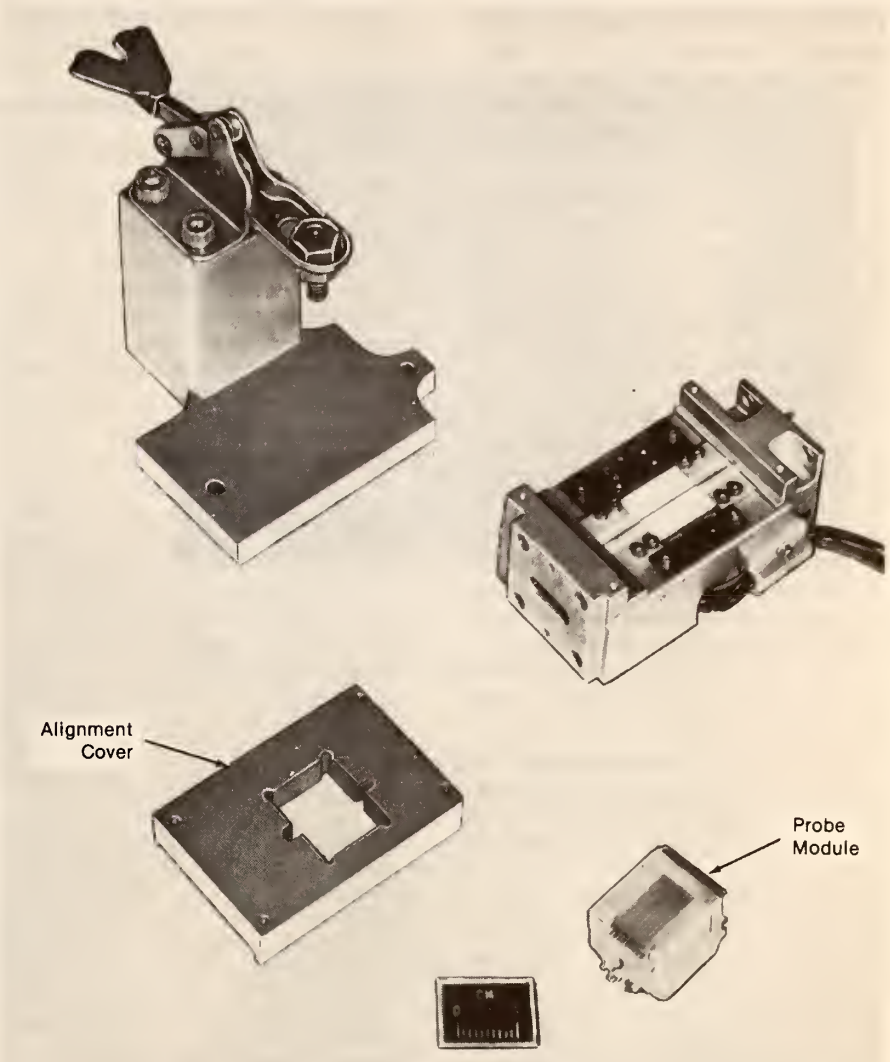

Figure 2. This **K-Band Fixture** is used to test packaged components of a 20-GHz MMIC transmitter. The alignment cover guides the probe module onto the MMIC.

The finline/waveguide test fixture shown in Figure 1 was developed to test submodules of a 30-GHz monolithic receiver. The fixture provides accurate and repeatable data. However, ribbon and wire bonds are needed to secure each MMIC, and skill is required to solder the MMIC to a carrier block in the fixture; consequently, testing is difficult, and it is almost impossible to reuse the MMIC after testing.

A "universal" commercially-manufactured coaxial test fixture was modified to enable the characterization of various microwave solid-state devices in the frequency range of 26.5 to 40 GHz. The coaxial-to-microstrip transition and its housing were replaced by a waveguide-to-microstrip transition and a suitable housing, which is compatible with the existing fixture while minimizing transition losses and eliminating resonant modes. Preliminary tests indicate problems with waveguide modes and nonreproducibility of characteristics.

The probe/waveguide fixture of Figure 2 is compact, simple, and designed for the nondestructive testing of a large number of MMIC's. All four scattering parameters have been measured on this fixture. Although the measurements were less repeatable than they were on other fixtures, they are expected to improve considerably with the addition of a precise probe-alignment cover.

Another nondestructive-testing fixture includes a cosine-tapered ridge, to match the impedance of the waveguide to that of

the microstrip. Although contact is achieved through a critical pressure fit between the ridge and the chip carrier, this fixture promises high repeatability due to the elimination of ribbon bonds and of the need for a spring mechanism.

One of the emerging techniques for characterization is microwave-wafer probing. A wafer probe is essentially an adapter from coaxial cable to bonding pads and performs about as well as a normal SMA connector. However, accuracy can be enhanced significantly through the use of chip-level impedance standards. A "de-embedding" procedure requires the use of short, open, and load standards for one-port characterization and an additional through connection and isolation standards for two-port characterization.

The second emerging technique is electro-optical sampling. Short-pulse lasers and ultra-high-speed photoconductors are used to generate wideband electronic pulses to provide direct electronic sampling on GaAs devices or integrated circuits. The technique provides characterization without bonding of the device or circuit under test and can yield measurements at frequencies from 2 to 100 GHz.

This work was done by R. R. Romanofsky, G. E. Ponchak, K. A. Shalkhauser, and K. B. Bhasin of **Lewis Research Center**. *Further information may be found in NASA TM-88948 [N87-22065/NSP], "RF Characterization of Monolithic Microwave and mm-Wave IC's." [A02]*

Copies may be purchased from the National Technical Information Service, Springfield, Virginia 22161, Telephone No. (703) 487-4650.

Rush orders may be placed for an extra fee by calling (800) 336-4700. LEW-14639 /TN

FOR ADDITIONAL INFORMATION: *Contact: Director, Technology Transfer Division, P.O. Box 8757, BWI Airport, MD 21240; (301) 621-0100 Ext. 241*

REFER TO THE NUMBER LISTED AT THE END OF THIS ARTICLE

Department of Energy

Technology Application

Sandia National Laboratory

Tiny Sensor May Help Robots Handle Materials Accurately

A tiny sensor to give robots a hetter sense of touch has been developed and demonstrated at Sandia National Laboratories. The successful demonstration shows that tactile (touch) sensors can he made small enough for use as sensitive fingertips on robotic hands, according to its primary developer. This could improve the ahility of rohots to handle materials with a greater degree of sensitivity and accuracy.

The sensing area of the digital tactile sensor (DTS) is only one-half inch square, roughly the size of a human fingertip. Its 256 sensing elements, arranged in a 16 hy 16 pattern, are special resistors whose resistance varies as a function of mechanical load. The array can sense forces ranging from an ounce to about a thousand pounds, which makes it potentially useful for a wide range of applications.

"Smart" robotic systems that use various kinds of visual, acoustic, and tactile sensors are heing developed and studied now by researchers around the world. The systems use computers to process information gathered by the sensors and make the decisions that direct a robot's actions.

Contained in small package

Sandia's new tactile sensor is contained inside a package that is eight-tenths of an inch square by one-quarter of an inch deep. The package includes the electronic circuitry on a microcircuit that is the same size as the sensor. The microcircuit scans the 256-element sensor array and provides digital output ready to be analyzed hy a microprocessor or other computer.

The new DTS system uses piezoresistive sensing elements called force-sensing resistors. The resistors are made from a commercially availahle thick-film piezoresistive polymer, and Sandia was the first organization to use this polymer in a tactile sensor. The polymer is made by Interlink Electronics, Inc., Santa Barbara, Calif. In piezoresistive materials, electrical resistance drops as mechanical load increases. Resistance changes rapidly for loads below 16 lb; at higher loads, the resistance change is smaller and approximately linear.

Sandia electrical engineer Bert Tise says tactile sensing is becoming more important as scientists and engineers are developing complex robots that can make intelligent decisions hased on the'r operating environments and the condition of the materials they are handling. Tise, primary developer of the new device, says rohotics specialists often want to design smart robots that have human-like senses and reactions.

"Humans use their basic senses of touch, sound, sight, smell, and taste to make many decisions—conscious and subconscious," he says. "For example, imagine that you want to pick up a delicate glass. Your senses of touch and sight (if you're looking at the glass) tell your brain when you make contact with the glass. Then your brain tells your muscles to contract to apply additional force on the glass—enough to prevent it from slipping, but not enough to break it.

Two digital tactile sensors illustrate the two sides of the device. The right one shows the force-sensing resistor side that would grasp an object. The left one shows results of electronics miniaturization, Sandia's primary contribution.

Allows robot to react similarly

"A tactile sensor working properly in a computerized robotic system should allow the robot to react in a similar way to objects that it is programmed to handle," he explains. "It should cause a robotic hand to apply the right amount of force in the right direction at the right time. Our sensor has that capahility."

Smart robotic systems are expected to be used increasingly hy industry, government, and the military for tasks that humans don't do efficiently, safely, or willingly. Sandia is researching a variety of smart robotic systems, including some that may automate mechanical assemhly; handle nuclear wastes; patrol interior and exterior areas to detect intruders and hazardous events; maintain mechanical equipment in hazardous environments; and destroy enemy vehicles during military hattle. The tactile sensor could be useful on some of these systems.

Tise emphasizes that the new DTS is still being studied and that further development is necessary before a production model can he designed. The working prototype is being used in continuing Sandia research in dexterous manipulation. The goal is to develop techniques that will allow a robot to manipulate a wide range of objects for various tasks. This requires that a robot be able to interact intelligently with its environment; tactile perception is one major requirement for this interaction.

Tests on commercial robotic hand

Sandia researchers will mount and test tactile sen-

sors on the fingers of a commercial robotic hand. The piezoresistive polymer, sandwiched between Mylar film, will be wrapped around the fingers in a similar manner to a plastic bandage around a human finger. A thin, protective elastomer will then cover the robotic fingers and sensors.

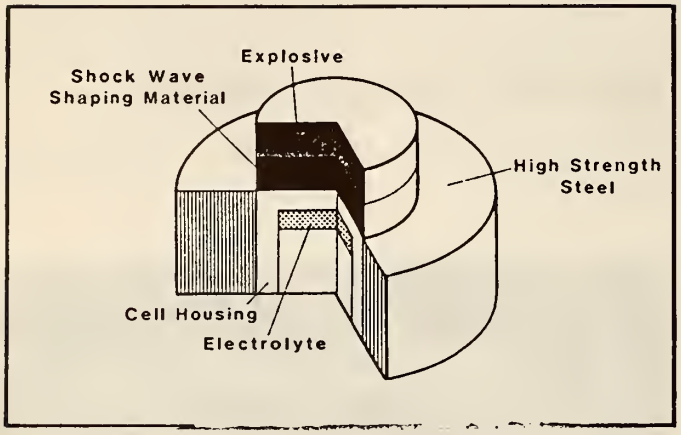

Until the shock activation concept was developed, a limitation of thermal batteries was the speed—measured in seconds—required to activate them with a chemical heat source. The new Sandia innovation means that similar batteries can be developed for use where extremely rapid startup times—measured in millionths of a second—are needed.

Promises a longer pulse

Other shock-activated power sources have been identified in prior research, hut have had the disadvantages of low energy density and very short pulse duration, explains Rohert A. Graham, a physicist in Sandia's Shock Wave and Explosive Physics Division.

The concept has been proven in the laboratory, but devices suitable for use in actual ordnance systems have yet to be engineered.

Experiments with the current design have produced electrical pulses lasting nearly one second. Researchers believe this time period could he greatly extended for the shock-activated batteries. "Lengthening the pulse is very useful because power has to be available at the time you need it," explains Graham. "If you have a surge of only microseconds, you have to put it to work under very restrictive conditions."

Graham and his supervisor Bruno Morosin began work on shock-initiated thermal hatteries nearly 2 years ago, and now are listed along with Sandian William B. Benedick as co-inventors on a patent application that has grown out of a 6-year project.

Shock wave deforms/melts electrolyte

In the laboratory, Graham and colleagues applied carefully controlled shock pulses to a specially configured electrochemical cell and measured the resulting current. In these experiments, a solid electrolyte was sandwiched between anode and cathode and subjected to a planar shock pulse initiated hy the detonation of a small charge of high explosive. In its solid state, the electrolyte is incapable of supporting the exchange of ions that typifies the chemical reaction of a storage hattery. In these experiments, however, the shock wave deforms and melts the electrolyte, permitting current to flow through.

A potassium chloride-lithium chloride solid eutectic electrolyte was used in the experiments. (A eutectic is an alloy of two substances that undergoes melting and freezing at a temperature that is lower than either of the two suhstances.) The electrochemical cell included a lithium-silicon alloy anode and a cathodic mixture of iron sulfide, the eutectic, and inert silicon dioxide. The cell remained inactive until shock pressure caused the electrolyte to melt.

Computer-predicted responses of shock pressure and temperature with different densities of electrolyte, carried out with David Wehb (recently retired from Sandia) and Lee Davison of the Labs' Solid Dynamics Department, helped the research team to determine the shock-wave conditions needed to generate power with the new source. This is the continuing direction of research, Graham said: "We need to understand electrochemistry under high pressure shock-wave loading."

Prototypes being designed now

This study will help engineers and scientists involved with battery and shock component technology determine the feasibility of huilding a thermal battery capahle of near-instant activation.

Applications, other than for ordnance, could include energizing measuring instruments or mechanical devices on a near-instantaneous basis. Impact events, with their resultant shocks, could actuate electrical current for a variety of uses, possibly without the need for additional pressure sensors.

The battery could also prove useful in emergency situations, say for aerospace programs, where long shelf life battery power may he required on a critical timing hasis. "It's so radically different, other potential uses are still being conceived," Graham says.

FOR ADDITIONAL INFORMATION

Public Information Division,
Code 3161,
Department of Energy,
Sandia National Laboratories,
Albuquerque, NM 87185-5800
(505) 844-4207
Refer to announcement 23, No. 3

Energy

948 Assessment of the Energy Savings Potential of Building Foundations Research

949 Efficient Alternatives for Electric Motors

950 Energy Measurements of Single-Family Houses

951 Passive Solar Designs Investigated

952 Corrosion in Amorphous-Silicon Solar Cells and Modules — Moisture severely affects amorphous-silicon units, bur encapsulation helps.

Department of Energy

Technology Application

Oak Ridge National Laboratories

ENERGY CONSERVATION

ASSESSMENT OF THE ENERGY SAVINGS POTENTIAL OF BUILDING FOUNDATIONS RESEARCH

Key words: Buildings; foundations; insulation; thermal protection; moisture barrier; radon mitigation

The foundation of a building is an important part of its thermal envelope, and foundation heat transfer is a significant component of the thermal interaction of a building with its environment. During the last 10 years, the aboveground envelopes of many buildings have been insulated and tightened. However, less than 5% of the existing building stock and only 30% of new residences have any foundation insulation. For that reason, uninsulated foundations may now account for 50% of the heat loss from otherwise heavily insulated homes. It has been estimated that a moderate level (R-10) of slab-perimeter or basement-wall insulation in all residences would result in an annual savings equivalent of 0.5 to 0.6% of the U.S. national energy consumption for 1984.

As part of the DOE/ORNL National Program for Building Thermal Envelope Systems and Materials, the University of Minnesota assessed the status of current foundation insulation research and evaluated the benefit of further study. This extensive inquiry is summarized in *Assessment of the Energy Savings Potential of Building Foundations Research: Summary Report,* which concludes that further research in foundation heat transfer is a necessary component of the drive to improve the energy efficiency of the nation's building stock.

This report contains information about different foundation designs (Fig. 1) and possible insulation

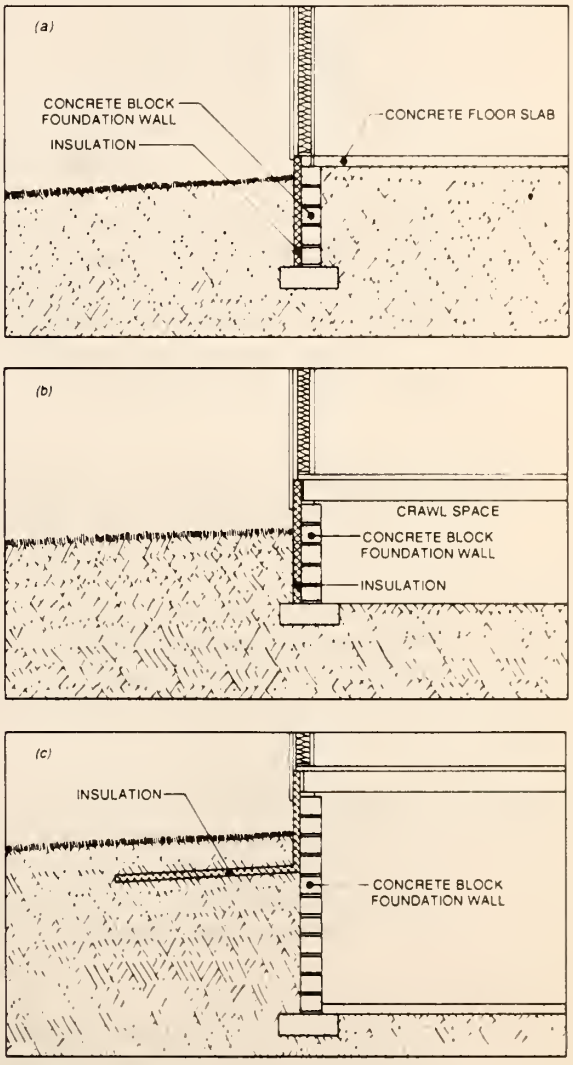

Fig. 1. Examples of possible configurations of foundation insulation, *(a)* slab-on-grade, *(b)* crawl space, and *(c)* full basement.

strategies for residential and commercial buildings in various geographical areas. It suggests that builders and designers need better information to allow them to incorporate thermally efficient foundation techniques into their buildings; the best way to deal with the hard image of high first cost for foundation insulation is to clearly document the total benefits from thermal protection, moisture protection, and radon mitigation and to convey these benefits to builders. A discussion of the direction of further research is included in this report.

For more information about the research, contact

Raymond Sterling
University of Minnesota
Underground Space Center
790 Civil and Mineral Engineering Building
500 Pillsbury Drive SE
Minneapolis, MN 55455

For a copy of the reports, contact

National Technical Information Service
U.S. Department of Commerce
5285 Port Royal Road
Springfield, VA 22161

R. Sterling, G. Miexel, and L. Shen, *Assessment of the Energy Savings Potential of Building Foundations Research,* ORNL/Sub-84-00240/1, Oak Ridge National Laboratory (January 1985).

R. Sterling et al., *Assessment of the Energy Savings Potential of Building Foundations Research: Summary Report,* ORNL/Sub/85-27497/1, Oak Ridge National Laboratory (November 1986).

Efficient Alternatives for Electric Motors

Research examined alternative technologies that improve the efficiency of electric drive systems. The goal was to evaluate each alternative's energy efficiency, economic efficiency, and possible effect on future electricity demand. Three technologies are examined: energy-efficient induction motors, new motor designs, and adjustable-speed drives (ASDs).

Although it is relatively easy to identify technologies that offer significant energy efficiency improvements to drive systems, the great diversity in the type, size, and use of electric motors, and the lack of comprehensive data to characterize the existing motor stock make it difficult to determine the economic efficiency of an "average" application. In all technologies evaluated, an effort is made to consider typical applications. However, common variations are also evaluated to show the sensitivity of the economics to these variations.

This analysis provides calculations characterizing the economic attractiveness of several existing and potential options. One attractive option given particular attention is the adjustable-speed drive which can replace throttles or valves for many pumping operations. A major conclusion is that, throughout industry, options that are both energy-saving and economically attractive appear to penetrate markets more slowly than would be socially optimal.

A report covers this effort. It has three more general sections that examine important engineering and economic conditions affecting motor energy consumption.

One section characterizes the current U.S. motor population, electricity consumption, and applications (end-uses). From the general patterns of motor use presented, particular users who have control over large amounts of motor capacity and who are sensitive to electric motor operating costs are identified.

Another section describes the environment in which electric motors are employed, the basic energy conversion principle of an electric motor, and the design of three different types of motors, with a focus on the alternating current (ac) induction motor. This section gives background for the technology options investigated and explains why ac induction motors dominate in industry.

A final section discusses four general factors that affect decisions concerning the purchase of electric motors--future product demand, capital availability, split incentives, and information availability and reliability. The section shows that factors not included in the economic

analyses can affect decisions concerning motors, and that these factors can lead to a sub-optimal choice for the industrial motor user.

FOR ADDITIONAL INFORMATION: A copy of this report is available from NTIS, Springfield, VA 22161; (703) 487-4600.

NTIS order number: DE88-003733/NAC

Price code: A04

Department of Energy

Technology Application

Oak Ridge National Laboratories

ENERGY CONSERVATION

ENERGY MEASUREMENTS OF SINGLE-FAMILY HOUSES

Key words: Radiant barriers; insulation; energy conservation; radiant heat transfer; heating; ventilation; air-conditioning

Testing was conducted by ORNL researchers to determine the energy savings attributable to radiant barriers installed in attics of unoccupied single-family houses. This research was carried out under joint sponsorship of DOE and the Tennessee Valley Authority. The subject houses are located in Karns, a community halfway between Oak Ridge and Knoxville, Tennessee. Tests were carried out over two cooling and two heating seasons.

The radiant barrier material used in these tests is a perforated, 1.3-mil-thick trilaminate (a film substrate sandwiched between two thin layers of aluminum foil). The objective of the testing was to quantify the energy-saving potential of horizontal (Fig. 1) and truss (Fig. 2) radiant barriers used in combination with R-11, R-19, and R-30 fiberglass insulation.

Radiant barriers save more space-conditioning energy with lower levels of attic insulation (R-11 and R-19). Specifically, radiant barriers work better in cooling than in heating, and work better in combination with R-11 and R-19 attic insulation than with R-30. Also, horizontally installed barriers are more effective than truss-mounted barriers in reducing heating and cooling loads.

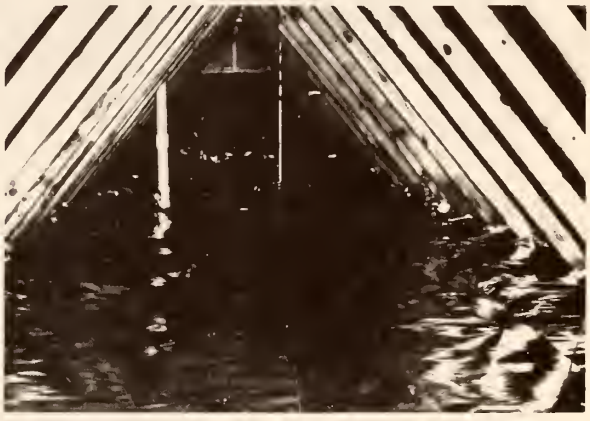

Fig. 1. Horizontal radiant barrier.

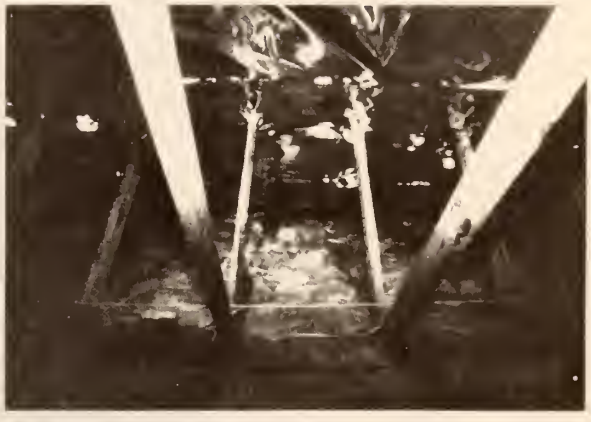

Fig.2. Truss radiant barrier.

Moisture can condense on the underside of a horizontal barrier in cold weather and is a potential problem. However, no deleterious effects were noted in the two heating-season

tests. The long-term effects of accumulated moisture or dust on the performance surface of the radiant barrier are unknown.

Additional information:

National Technical Information Service
U.S. Department of Commerce
5285 Port Royal Road
Springfield, VA 22161

W. P. Levins and M. A. Karnitz, *Heating Energy Measurements of Single-Family Houses with Attics Containing Radiant Barriers in Combination with R-11 and R-30 Ceiling Insulation,* ORNL/CON-239, Oak Ridge National Laboratory (March 1988).

W. P. Levins and M. A. Karnitz, "Energy Measurements of Single-Family Houses with Attics Containing Radiant Barriers," *ASHRAE Trans.* **93** Pt. 2, 182-99 (1987).

"Cooling-Energy Measurements of Unoccupied Single-Family Houses with Attics Containing Radiant Barriers," Bulletin No. 587, *Technology Applications Bulletins,* Oak Ridge National Laboratory.

NAVY
Domestic Technology Transfer Fact Sheet

Passive Solar Designs Investigated

Researchers at the Naval Civil Engineering Laboratory, Port Hueneme, California, and the Los Alamos National Laboratories, Los Alamos, New Mexico, have investigated the applicability of passive solar designs for increasing the energy efficiency of Navy buildings. The results of this program have been incorporated into a military handbook.

A passive solar building is one that derives a substantial part of its heat from the sun; the building, in effect, becomes a solar collector and heat storage system. These design procedures are applicable to new buildings, large or small, and to retrofit designs in older buildings.

The handbook provides three levels of help for building designers. First, to familiarize the reader, a general discussion of the basic concepts and principles of passive solar heating is presented. Then, a set of guidelines is presented for preliminary design or for initial screening of designs. These guidelines enable the user to quickly define a building with cost-effective performance. Finally, a quantitative design-analysis procedure is presented in the form of worksheets that give an accurate estimate of the auxiliary heating requirements of selected designs.

Some of the features of the handbook include:

- Data for 200 geographical locations
- Data on 179 passive solar designs
- Seven reference degree day bases (40° F to 70° F)
- Nine reference contour maps of the ratio of solar aperture area to floor area
- Estimates of the summer cooling penalty to determine if the passive solar design increases summer air conditioning costs
- Recommendations for defensive cooling strategies if a summer penalty exists

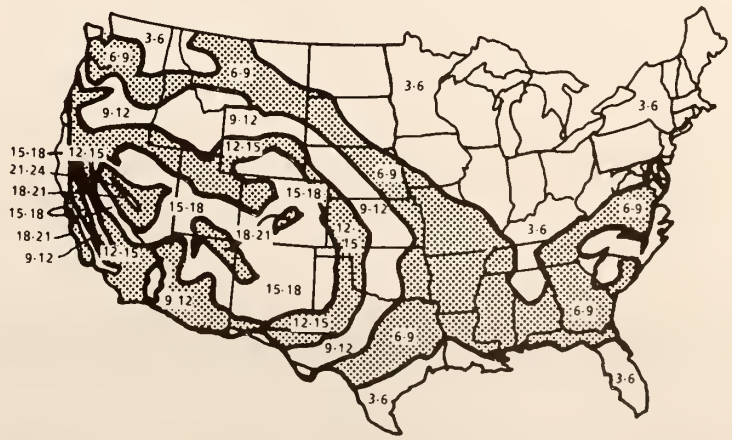

One of the nine contour maps for different passive designs to allow the user to select the percentage ratio of passive solar aperture area to floor area. For example, at Naval Air Station, Fallon, Nevada, a solar area of between 15 and 18 percent of the floor area is a good design starting point.

- Estimates of effective heat capacity of thermal storage walls
- Adjustments for off-south orientation
- Sizing of shading devices
- Calculations of monthly and annual performance
- Sizing of backup heating systems

The handbook has expanded the knowledge base for passive solar design in the following areas:

- The Los Alamos National Laboratories solar load ration method was modified so that yearly performance instead of monthly performance could be calculated with no loss in accuracy. This method saves time in calculation, and monthly performance can also be evaluated.
- New correlations (not previously available) were developed for 8-inch concrete block storage, thermosiphon air panels, and metal radiant panels.
- The handbook contains methods for using nighttime setback controls for HVAC equipment.

For Additional Information:

Backup material on this effort is available from:

Navy Domestic Technology Fact Sheet Reader Reply Service,
Code E211,
Naval Surface Weapons Center,
Dahlgren, VA 22448-5000
(703) 663-8921

Refer to 130601/TN

NASA Tech Brief
National Aeronautics and Space Administration

Corrosion in Amorphous- Silicon Solar Cells and Modules

Moisture severely affects amorphous-silicon units, but encapsulation helps.

A paper reports on corrosion in amorphous-silicon solar cells and modules. The paper, based on field and laboratory tests, discusses the causes of the corrosion, ways of mitigating the effects, and consequences for modules already in the field.

In general, modules exposed to a natural outdoor environment corroded more than modules exposed to uniform temperatures and humidities in the laboratory. The outdoor environment is apparently more severe, involving direct contact with water in the form of dew, rain, and snow. Moreover, natural cycles of temperature and humidity induce damaging stresses in cells and modules. To make matters worse, the concentration of moisture in a module tends to increase during long exposures outdoors because modules tend to retain sorbed moisture.

Laboratory tests at 85 °C and 85 and 100 percent relative humidity showed that encapsulation of a cell retards the gross loss of metalization in the active region of the cell. However, when the metal is resistant to corrosion, the encapsulation does not seem to retard the increase in the sheet resistivity of a cell.

The paper suggests the sealing of the edges as a way of reducing the entry of moisture. Cell-free perimeters or sacrificial electrodes are suggested to mitigate the effects of sorbed moisture. The development of a truly watertight module may prove to be more cost-effective than attempting to mitigate the effects of moisture.

This work was done by Gordon R. Mon, Liang-Chi Wen, and Ronald G. Ross, Jr., of Caltech for **NASA's Jet Propulsion Laboratory**. *"Corrosion of Amorphous Silicon Cells and Modules," NPO-17302/TN*

FOR ADDITIONAL INFORMATION: *Contact: Director, Technology Transfer Division, P.O. Box 8757, BWI Airport, MD 21240; (301) 621-0100 Ext. 241*

REFER TO THE NUMBER LISTED AT THE END OF THIS ARTICLE

Engineering

953 Bulk Transfer of Chemical Materials

954 Spin Coating of Decon Agent Containers

955 Dust Control Handbook for Minerals Processing

956 Inspecting, Testing Fire Safety of HVAC Systems

957 NBS Model to Simulate Smoke Movement Through HVAC Systems

958 Liquid-Seeding Atomizer — Particles are sprayed in drops of evaporating liquid. (Licensing Opportunity)

959 Designing Shafts for Long Life — Fatigue lives are affected by many factors.

960 Hydrogen/Air-Ignition Torch — The torch is simple, reliable, and economical.

961 Measuring Fan-Blade-Tip Displacements — Magnets and Hall-effect transducers are used to monitor tip-to-shroud clearances. (Licensing Opportunity)

962 Short-Cycle Adsorption Refrigerator — Each adsorption unit includes a long-lived nonmechanical heat switch.

Software

963 Computing Flows Over Wavy Surfaces — Wind/wave interactions, drags, and related phenomena can be predicted.

964 Unsteady Flow in a Supersonic Cascade with Shocks — The operating range of turbomachinery for which stability can be calculated is extended.

Other Items of Interest

948 Assessment of the Energy Savings Potential of Building Foundations Research

951 Passive Solar Designs Investigated

965 Reverse Osmosis Treatment to Remove Inorganic Contaminants from Drinking Water

966 A Study of Possible Economical Ways of Removing Radium from Drinking Water

976 An Overview of Technology on Bituminous Surfacing Materials for Low-Volume Roads

U.S. Army Fact Sheet

Bulk Transfer of Chemical Materials

Pine Bluff Arsenal's mission involves the manufacture of chemical munitions. Manufacture/transportation procedures represent the technology of the pre-WWII era. Retrieval, weighing, and transporting pyrotechnic chemical constituents are accomplished by labor intensive operations. Current methods of material handling include manually weighing, filling, and transporting mix smoke containers by push carts. Recent legislation and enforcement of laws pertaining to toxic and hazardous substances required new methods of material handling be developed to minimize operator exposure.

The objective of this effort was to provide new material handling systems for the bulk transfer of raw chemical materials. This involved the use of current technology which complied with production requirements and industrial hygiene/safety constraints.

Two options were studied applying the latest material handling concepts. They were to construct a new consolidated smoke facility or modify existing facilities. For the new facility, the building layout was designed to minimize interbuilding material transfer distances and conflicts in material/process flow paths. To modernize existing facilities, emphasis was on adapting the present buildings to the recommended equipment. For both options, the recommended material handling equipment included the use of aluminum bulk containers and aluminum transportainers for finished smoke mixes. The new facility allowed the consideration of automatic dumping and pneumatic conveying of smoke mix to fill/press lines.

Based on the study, the conclusions recommended the construction of the new smoke complex since capital cost would be lower and the operating costs would be reduced compared to the present operation. However, in the interim, pending approval of the new facility, some of the improvements proposed were adapted into the present facility.

As a result of this project, transportainers and mechanical dump stations have been procured for installation in the existing facility at Pine Bluff Arsenal. A proposed concept was developed for the layout and design of a new consolidated smoke complex.

FOR ADDITIONAL INFORMATION: Mr. Peter Martin, AMXIB-PG, Production Engineering Division, U.S. Army Industrial Base Engineering Activity, Rock Island, IL 61299-7260; (309) 782-5235.

US Army Fact Sheet

Spin Coating of Decon Agent Containers

Current metallic containers used to hold corrosive chemical decontamination agents corrode before the required shelf life of the agents is reached. These chemicals attack the chimes, seams, localized cavities, and sealant compounds in their containers. Corrosion of the container results in leaking and deterioration of chemicals by moisture and air.

This effort was performed to establish a process for coating containers to insure that the decontamination agent does not become contaminated and unuseable in the field. Leakfree containers would also eliminate a safety hazard.

Initially, several potential coating materials and container materials were subjected to Super Tropical Bleach (STB) and Decontamination Solution (DS2) at elevated temperatures to determine their resistance and/or rate of deterioration. Halar and Ryton were reported to be the most promising candidates for coatings inside the DS2 containers. Halar, High-Density Polyethylene (HDPE), phenolic and epoxy coatings were the most promising candidates for STB containers.

The final task consisted of testing the containers. The Halar coated DS2 containers passed all tests but impact. Each candidate material that was able to resist DS2 for an extended period of time was too brittle to pass the required impact tests. Halar, although the most promising candidate material, would require further optimization before possible adaption could be recommended. The unlined welded steel can provide appropriate protection if adequate quality control of the welding process is maintained.

HDPE containers and steel containers coated inside and out with phenolic and epoxy resins, respectively, were tested after filling with STB. These containers passed the required tests and are being considered as an alternate to the present container.

FOR ADDITIONAL INFORMATION: Peter Martin, AMXIB-PG, Production Engineering Division, U.S. Army Industrial Engineering Activity, Rock Island, IL 61299-7260; (309) 782-5235.

Technology News

From the Bureau of Mines, United States Department of the Interior

Dust Control Handbook for Minerals Processing

A special report was prepared overviewing dust control engineering techniques for metal and non-metal mineral processing. Dust prevention, formation, and control are examined, and wet and dry control systems, personal protection, testing methods, and costing methodologies are discussed. Prospective users of the handbook include maintenance foremen, plant engineers, mill supervisors, and safety directors. The contents include:

Chapter 1: Dust and Its Control
- What is Dust?
- How is Dust Generated?
- Types of Dust?
- Why is Dust Control Necessary?
- Health Hazard Factors
- How is Dust Controlled?

Chapter 2: Preventing Dust Formation
- Introduction
- Belt Conveyors
- Transfer Chutes
- Enclosures
- Crushers
- Screens
- Storage Bins and Hoppers
- Bucket Elevators
- Feeders
- Screw Conveyors
- Pneumatic Conveyors
- Grinding Mills
- Dryers
- Stockpiles
- Haul Roads
- Truck and Railroad Car Dumping
- Powder Handling and Packing

Chapter 3: Dust Control Systems
- Why Dust Control?
- Types of Dust Control Systems
- Selection of a Dust Control System
- Dust Collection Systems
- Wet Dust Suppression Systems
- Airborne Dust Capture Systems
- Design of a Water-Spray System

Chapter 4: Collecting and Disposing of Dust
- What Is a Dust Collector?
- Necessity for Dust Collectors
- Types of Dust Collectors
- Types of Inertial Separators

Fabric Collectors
Wet Scrubbers
Electrostatic Precipitators
Unit Collectors
Selecting a Dust Collector
Fan and Motor
Disposal of Collected Dust

Chapter 5: Specific Illustrations

Chapter 6: Estimating Costs of Dust Control Systems
Necessity for Cost Estimates
Cost Estimating Procedures
Cost Components
Cost Justification

Chapter 7: Controlling Surrounding Dust Sources
Introduction
Contributing Sources/Factors
Administrative Measures
Preventive Maintenance Program
Proper Operating Procedures
Managerial Measures
Outside Dust Source Control
Recirculation of Uncontrolled Emissions

Chapter 8: Sampling Dust in the Work Environment
Personal Dust Sampling
ABC's of Personal Dust Sampling
Personal Dust Sampling Equipment
Sampling Procedure
Errors in Respirable Dust Sampling

Chapter 9: Testing Dust Control Systems
Reason for Testing
Dust Collection System Testing
Wet Dust Suppression
Evaluating Dust Control Systems

Bibliography

FOR ADDITIONAL INFORMATION: A copy of this report is available from NTIS, Springfield, VA 22161; (703) 487-4600.
NTIS order number: PB88-159108/NAC
Price code: A10

NBS technology update

National Bureau of Standards
U.S. Department of Commerce
Gaithersburg, MD 20899

Inspecting, Testing Fire Safety of HVAC Systems

Heating, ventilating and air conditioning (HVAC) systems can contribute to the hazard of a fire in several ways. HVAC systems can spread smoke to parts of a building distant from the fire. In addition, the natural fire resistance of walls, floors, and ceilings can be reduced when they are penetrated to allow passage of HVAC air ducts. Over the past several decades, technology to control these problems has been evolving. But few guidelines have been written concerning inspecting and testing the fire safety of HVAC systems. Researchers in the NBS Center for Fire Research have developed detailed inspection and testing procedures to determine the fire safety of an air moving system with or without fire or smoke controls. The procedures are intended to be examples that can be modified to suit users' needs.

FOR ADDITIONAL INFORMATION: Fire Safety Inspection and Testing of Air Moving Systems (NBSIR 87-3660) is available from NTIS, Springfield, VA 22161; (703) 487-4600.

NTIS order number: PB88-155809/NAC
Price code: A03

NBS technology update

National Bureau of Standards
U.S. Department of Commerce
Gaithersburg, MD 20899

NBS Model To Simulate Smoke Movement Through HVAC Systems

During a fire, a heating, ventilating, and air conditioning (HVAC) system can distribute smoke to parts of a building remote from the fire. Statistics show that between 80 and 90 percent of the people who die during a fire succumb to smoke inhalation. Researchers in the NBS Center for Fire Research have developed a computer model to simulate smoke movement through an HVAC system and predict the quantity of smoke being transported. The model, called SMACS (Smoke Movement by Air Conditioning Systems), will help evaluate the hazards due to smoke that is distributed by these systems and the impact an HVAC system has on fire growth and development. Experiments are being conducted at NBS to validate the model's predictions. A users guide and program manual will be developed. A Computer Model of Smoke Movement by Air Conditioning Systems (SMACS) (NBSIR 87-3657) is available which describes calculation methods and program logic.

FOR ADDITIONAL INFORMATION: A copy of this report is available from NTIS, Springfield, VA 22161; (703) 487-4600.

NTIS order number: PB88-159462/NAC
Price code: A03

NASA Tech Brief
National Aeronautics and Space Administration
Ames Research Center, Moffett Field, California

Licensing Opportunity

Liquid-Seeding Atomizer

Particles are sprayed in drops of evaporating liquid.

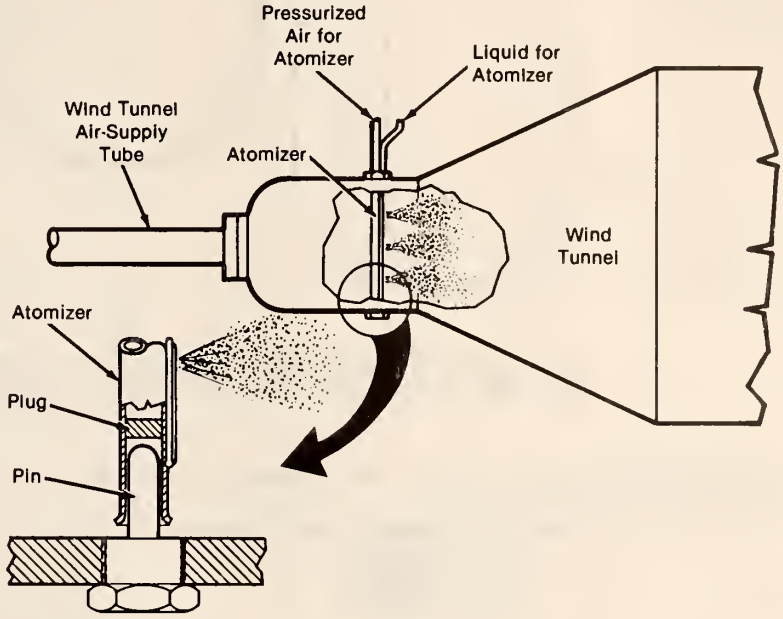

Figure 1. **Placed Near the Wind-Tunnel Inlet,** the atomizer sprays evaporating liquid containing solid particles into the wind-tunnel airflow. The particles are entrained in the flow and scatter light, thus enabling the flow to be observed optically. One end of the atomizer slides on a stationary pin to accommodate thermal expansion and contraction.

An improved atomizer for use in a wind tunnel (see Figure 1) generates a well-defined spray of uniformly sized liquid drops and solid particles for use in laser Doppler velocimetry or visualization of the airflow about a model. The atomizer does not disturb the airflow measurably at the model. In contrast with conventional atomizers, the new one is less bulky and can therefore be inserted through a small access hole in the wind-tunnel wall.

The major structural component of the atomizer is an air-supply tube that spans the wind tunnel (see Figure 2). Orifices for air are placed at evenly spaced locations along the downstream side of the tube, wherever a spray is required. A liquid-feed tube is silver soldered or otherwise fastened along its entire length to the air-supply tube on each side of the line of orifices for air. Orifices for liquid are drilled in the sides of the liquid-feed tubes facing each other, adjacent to the orifices for air.

The distance between the liquid-feed tubes is about 70 percent of the diameter of the orifices for air, so that the air flowing out of the orifices creates a venturi effect. Because the liquid-feed tubes are restrained from vibrating away from the air-supply tube, the fluid jets do not become distorted and form large droplets, as they can in some conventional atomizers.

The liquid-feed tubes are joined at one end; they could be made by suitably bending one piece of stainless-steel tubing. With this shape, the tubes can be cleaned by circulating a cleaning fluid through them, without having to remove the atomizer from the wind tunnel.

For proper seeding of the wind-tunnel airflow, the sprayed mixture should consist of uniformly sized microscopic particles in a liquid that evaporates quickly before the spray reaches the wind-tunnel test section. One such mixture is 0.2 weight percent of ½-μm-diameter polystyrene-latex spheres in alcohol or an alcohol/water solution. A typical air-supply pressure, air-orifice diameter, and liquid-orifice diameter are 400 psi (2.8 MPa), 0.180 in. (4.57 mm), and 0.015 in. (0.38 mm), respectively.

The atomizer can be used in supersonic and transonic wind tunnels. With suitable spacing of the orifice groups, the sprays

from the separate groups consolidate into one large fan-shaped spray. The width of the spray can be chosen via the number and spacing of orifice groups. The thickness of the spray can be altered by changing the distance between tubes, the air pressure, and/or the orifice size. Thus, the spray can be configured so that it does not deposit obscuring particles on the observation parts and does not clog the porous boundary-layer suction plates of the wind tunnel.

This work was done by Henry L. B. Seegmiller of **Ames Research Center.**

Inquiries concerning rights for the commercial use of this invention should be addressed to the Patent Counsel, Ames Research Center. Refer to ARC-11631/TN

Ames Research Ctr.
Technology Utilization Officer: Laurance Milov
Mail Code 223-3
Moffett Field, CA 94035
(415) 694-6471
Patent Counsel:
Darrell G Brekke
Mail Code 200-11
Moffett Field, CA 94035
(415) 694-5104

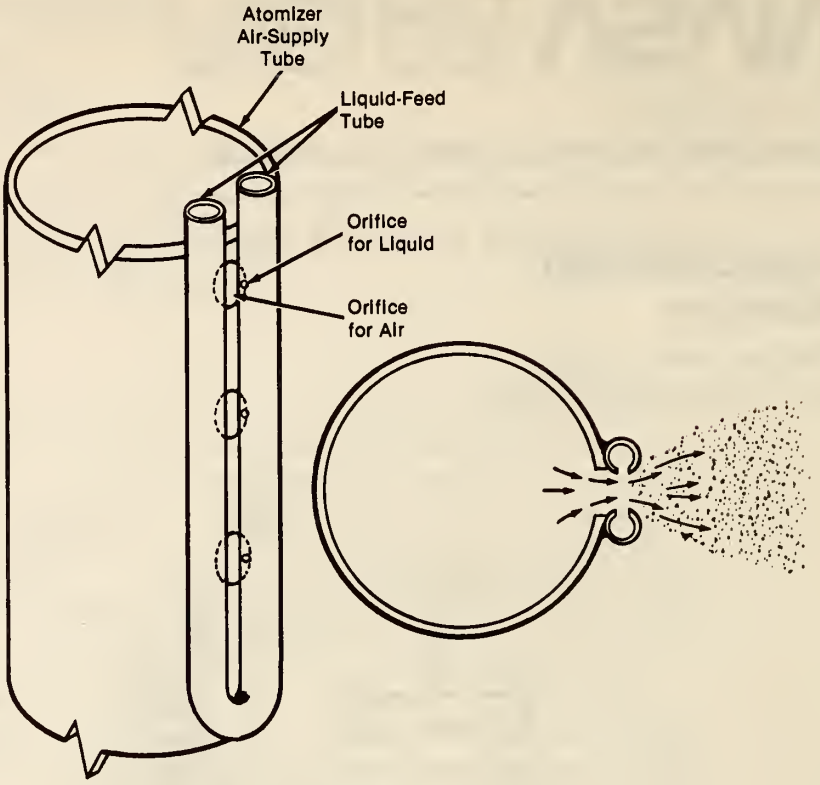

Figure 2. **Air Flows Through a Narrow Space** between two liquid-feed tubes. A liquid/particle mixture from the tubes enters the spray, forming uniform droplets.

FOR ADDITIONAL INFORMATION: *Contact: Director, Technology Transfer Division, P.O. Box 8757, BWI Airport, MD 21240; (301) 621-0100 Ext. 241*

REFER TO THE NUMBER LISTED AT THE END OF THIS ARTICLE

NASA Tech Brief
National Aeronautics and Space Administration
Lewis Research Center, Cleveland, Ohio

Designing Shafts for Long Life

Fatigue lives are affected by many factors.

An improved method has been developed for choosing the sizes of power-transmitting shafts for limited or unlimited service lives under a variety of operating conditions. In essence, the method replaces some traditional simplifying approximations and guesswork by more-refined design equations based on considerations of metal fatigue. The method will be especially beneficial where critical compromises have to be made between shaft weights and reliabilities or where the penalties of shaft failure are severe.

The basic problem is to estimate the diameter required for a shaft to survive a specified number of cycles under an expected sequence of steady or variable-amplitude loads. Preferably, the analysis for a given shaft would begin with the experimental determination of its curve of stress amplitude versus number of stress cycles to failure under the appropriate mean loading condition (see figure). However, in the absence of full fatigue-life data, the analysis is based on a nominal-stress-life approximation, in which a straight line on a log-log plot connects the true fracture strength at 1 cycle to the fatigue limit of the shaft at 10^6 or 10^7 cycles.

A number of factors are introduced to modify the stress levels and slopes on the log-log fatigue-life plot for the effects of environmental, geometrical, and loading conditions likely to be encountered in service. These factors are based on previous experimental and theoretical determinations of the effects of surface finishes, temperatures, the inclusion of more inherent defects with increases in size, stress concentrations at splines and keyways, press-fitted collars, residual manufacturing stresses, and corrosion.

The effects of variable-amplitude loading are treated by expressing a complicated, irregular loading history as a series of constant-amplitude events and by invoking the Palmgren-Miner linear-damage rule. This rule assumes the accumulation of damage at a linear rate without regard to the sequence of loading and in some cases may have to be replaced by more-complicated cumulative-damage theories that express the effects of different load sequences.

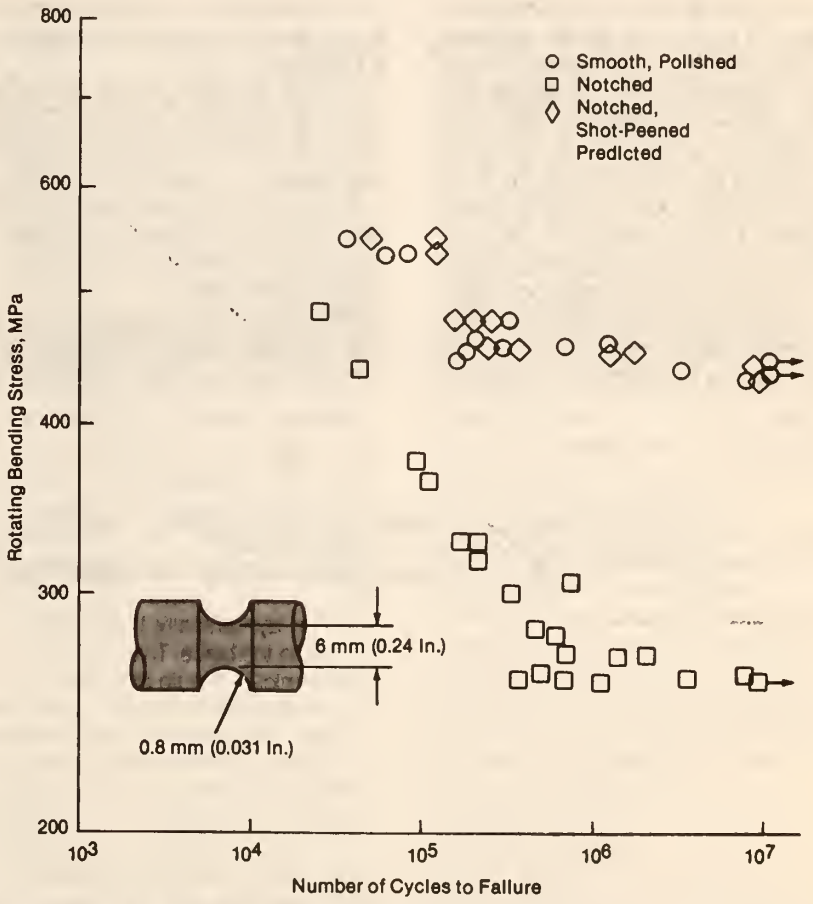

The Stress Versus Fatigue Life of a proposed shaft design is plotted, then modified to account for expected operating conditions and used to calculate a shaft diameter required for a given fatigue life. If the diameter of the shaft represented by the plot equals or exceeds the required diameter, the shaft is considered adequate.

In some applications of the new design method, it was shown that occasional cyclic overloads reduce the fatigue strength considerably or else require the use of a much larger shaft diameter. The sensitivity of shaft fatigue life to bending stress was found to depend primarily on the tensile strength and the overall fatigue-life-modifying factor: the life might vary with stress to the −14th power for a small, smooth, high-strength-steel shaft or to the −5th power for a large, rough, heavily notched, low-strength-steel shaft.

This work was done by Stuart H. Loewenthal of **Lewis Research Center**. *Further information may be found in NASA TM-87354 [N86-27661/NSP], "New Methodology for Shaft Design Based on Life Expectancy."*

Copies may be purchased [prepayment required] from the National Technical Information Service, Springfield, Virginia 22161, Telephone No. (703) 487-4650. Rush orders may be placed for an extra fee by calling (800) 336-4700. [A02]
LEW-14517

FOR ADDITIONAL INFORMATION: *Contact: Director, Technology Transfer Division, P.O. Box 8757, BWI Airport, MD 21240; (301) 621-0100 Ext. 241*
REFER TO THE NUMBER LISTED AT THE END OF THIS ARTICLE

NASA Tech Brief
National Aeronautics and Space Administration
Lewis Research Center, Cleveland, Ohio

Hydrogen/Air-Ignition Torch

The torch is simple, reliable, and economical.

A hydrogen/air-ignition torch has been devised for burning off excess hydrogen that accumulates in scrubber exhaust ducts. The torch consists of a welded concentric double-tube assembly with gaseous hydrogen flowing through the inner tube and the air flowing through the outer tube. The airflow cools the inner tube prior to flowing through openings in the inner tube and mixing with the gaseous hydrogen. A spark plug connected to a constant-duty simple ignition transformer is threaded into the side of the torch and into the inner tube. The transformer is used to excite the spark plug for a period long enough to ignite the gas. After that, the transformer is turned off.

To give constant assurance that the torch is lit, two type-K, open-ball, Chromel/Alumel (or equivalent) thermocouples are spot welded to the exit end of the torch to monitor the air temperature near the flame. The torch operates at a mixture ratio of 6:1, and the flame leaves the torch at subsonic velocities.

This torch is simple to operate, inexpensive, and very reliable. The burning of excess hydrogen by means of this torch has proven to be more economical than the previous carbon dioxide insertion technique.

This work was done by George A. Repas of **Lewis Research Center**. *Further information may be found in NASA TM-88882 [N87-13470/NSP] "Hydrogen Air-Ignition Torch." [A02]*

Copies may be purchased [prepayment required] from the National Technical Information Service, Springfield, Virginia 22161, Telephone No. (703) 487-4650. Rush orders may be placed for an extra fee by calling (800) 336-4700. LEW-14552

/TN

FOR ADDITIONAL INFORMATION: *Contact: Director, Technology Transfer Division, P.O. Box 8757, BWI Airport, MD 21240; (301) 621-0100 Ext. 241*

REFER TO THE NUMBER LISTED AT THE END OF THIS ARTICLE

NASA Tech Brief

National Aeronautics and Space Administration

Langley Research Center, Hampton, Virginia

Licensing Opportunity

Measuring Fan-Blade-Tip Displacements

Magnets and Hall-effect transducers are used to monitor tip-to-shroud clearances.

The fan blades in a wind tunnel are subjected to a myriad of forces during service. The material, construction, and age of the blades and the temperature, humidity, and density of the tunnel fluid combine with the turning speed and the resultant centrifugal loads to influence the size of the space between the fan blades and the wind-tunnel shroud. If this space becomes critically small, scuffing between the tip of the fan blade and the surface of the shroud could result in catastrophic failure of the fan set and consequential damage to the fan-driving system.

A technique has been developed for dynamically measuring the clearance between the fan-blade tip and the shroud. This technique entails mounting a permanent magnet in the end of the fan blade and monitoring the tip-to-shroud distance by use of the output of Hall-effect transducers affixed to the surface of the shroud. The Hall-effect transducers provide real-time information. By placing magnets in each fan-blade tip, a complete set can be monitored sequentially as each blade rotates past the sensor. Further, the placement of multiple magnets in each blade at leading and trailing edges and the monitoring of the times of relative peak outputs at corresponding sensors afford an opportunity to ascertain dynamically the presence of twist within the blade. This ability to measure dynamically the tip displacement and the blade twist would significantly enhance the analysis of such blade-performance parameters as the mounting scheme, materials, construction, service performance, and life expectancy.

The permanent magnet affixed to the radial-tip surface of the fan blade should have a low mass and positive means of attachment because the magnet and capture assembly are subjected to centrifugal forces commensurate with the mass and the rotary speed. Also, the field of the magnet must be sufficient to traverse the tip (magnet)-to-shroud distance and excite the transducer. These criteria are satisfied by a small, commercially-available rare-earth magnet that has a mass of only 2.59 g and produces a magnetic-flux density of 350 G at a distance of 0.200 in. (5.08 mm).

The Hall-effect displacement transducer should have a stable, accurate, and linear output at relatively high levels. It should be small and easily configured, both electrically and mechanically. Again, a commercially available model was found to satisfy the requirements. This sensor has a linearity of ± 1.5 percent and a sensitivity of 7.5 ± 0.2 mV/G.

The displacement-measurement technique is based on a transducer output proportional to the sensed magnetic-flux density and to the corresponding separation. This information can be used in two basic ways. First, the level of the output is monitored to ascertain the displacement, and this signal is usable as a real-time alarm parameter to prevent scuffing of the blade tip and resultant catastrophic failure. Second, the time of peak sensor excitation can be compared between multiple blade-magnet/sensor sets to ascertain dynamically changes in the aerodynamic shape.

This technique has already been successfully demonstrated on a laboratory prototype. Although the technique was developed for wind tunnels, it should have potential application in many rotating machines, provided that the surrounding materials are nonmagnetic and that the temperatures are not severe.

This work was done by Robert F. Berry, Jr., of **Langley Research Center**. *No further documentation is available.*

This invention is owned by NASA, and a patent application has been filed. Inquiries concerning nonexclusive or exclusive license for its commercial development should be addressed to the Patent Counsel, Langley Research Center
Refer to LAR-13722/TN

Langley Research Ctr.
Technology Utilization Officer: John Samos
Mail Stop 139A
Hampton, VA 23665
(804) 865-3281
Patent Counsel
George F. Helfrich
Mail Code 279
Hampton, VA 23665
(804) 865-3725

FOR ADDITIONAL INFORMATION: *Contact: Director, Technology Transfer Division, P.O. Box 8757, BWI Airport, MD 21240; (301) 621-0100 Ext. 241*
REFER TO THE NUMBER LISTED AT THE END OF THIS ARTICLE

NASA Tech Brief
National Aeronautics and Space Administration
NASA's Jet Propulsion Laboratory, Pasadena, California

Short-Cycle Adsorption Refrigerator

Each adsorption unit includes a long-lived nonmechanical heat switch.

A modular adsorption/Joule-Thomson-effect refrigerator offers fast regeneration; when fully developed, its adsorption/desorption cycle time is expected to be only 1 minute, as compared with 15 minutes in previous versions. The refrigerator is smaller and lighter than the previous units of equivalent capacity. A modular configuration makes it relatively easy to build refrigerators that have capacities from milliwatts to watts, according to cooling needs.

The refrigerator is intended for the long-term cooling (up to 10 years) of infrared sensors and other equipment in space to temperatures ranging from 4 to 80 K. The only moving parts are small check valves. The refrigerator is designed to be powered mostly by waste heat. A prototype containing 12 compressor modules connected in banks of 4 provides one-quarter watt of cooling at 25 K. Operating under the control of a computer, the four banks of compressor modules are operated in a phased heating/cooling sequence so that nearly steady cooling is provided for the external heat load.

In the refrigerator, pressurized hydrogen generated by a bank of compressor modules during its heating phase passes through a system of check valves and expands in a Joule-Thomson junction as it enters a refrigeration chamber. There, the hydrogen absorbs heat from the load before it is sucked out by another bank of compressor modules in its cooling phase.

In each compressor module, adsorbing charcoal is contained in an inner pressure vessel of stainless steel (see figure). An open-foam copper matrix holds the charcoal and enhances the transfer of heat. A brass outer vessel surrounds the stainless-steel cylinder, and the gap between inner and outer vessels constitutes the heat switch. When the gap is filled with hydrogen, the heat switch exhibits high heat conductance (is on). When the gap is empty, the switch exhibits low heat conductance (is off). A miniature charcoal adsorption pump supplies the gas for the switches in each bank of four compressor modules.

To demonstrate the refrigerator, an electric heater was used to supply heat to each module to cause the desorption of hydrogen from the charcoal in its core. (In a practical model, the heat for desorption would come from waste heat such as that from electronic equipment.) With the heat switch turned off, the adsorber was heated. The adsorber gave off hydrogen as it heated up. When the pressure reached about 80 atm (8.1 MPa), the heater was turned off, and the heat switch was turned on. The adsorber transferred its heat to a liquid-nitrogen bath surrounding the module, readsorbing hydrogen as it cooled and eventually becoming saturated with the gas, ready for another heating cycle. Cooling from 165 K to 85 K took only 50 seconds.

This work was done by C. K. Chan of Caltech for **NASA's Jet Propulsion Laboratory**. *NPO-16571 /TN*

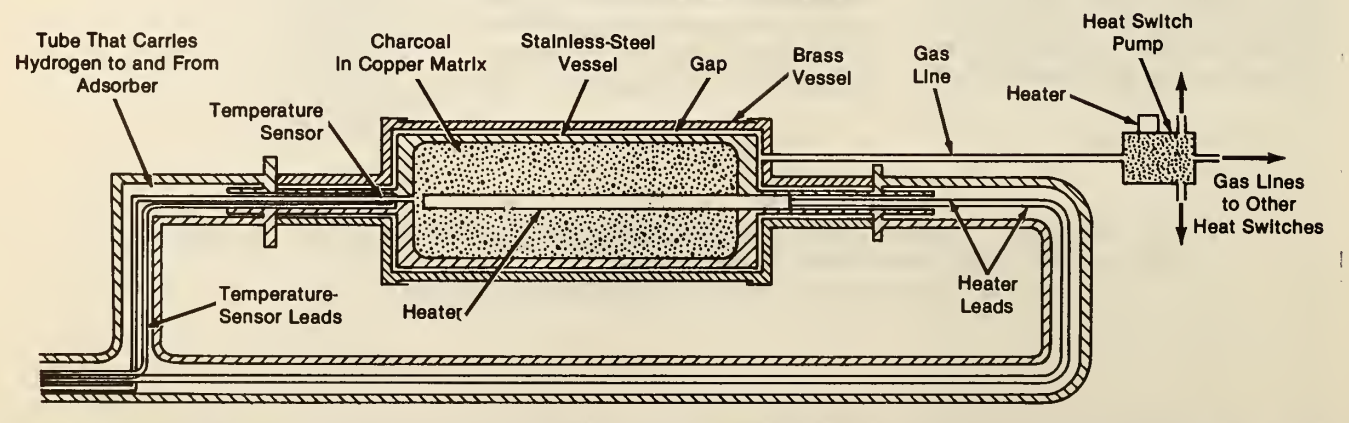

The **Heat Switch Is a Gap** between concentric cylindrical vessels. For rapid heating and cooling of the core, the gap must be less than about 50 μm.

FOR ADDITIONAL INFORMATION: *Contact: Director, Technology Transfer Division, P.O. Box 8757, BWI Airport, MD 21240; (301) 621-0100 Ext. 241*
REFER TO THE NUMBER LISTED AT THE END OF THIS ARTICLE

Computing Flows Over Wavy Surfaces

Wind/wave interactions, drags, and related phenomena can be predicted.

WAVEGEM is a package of algorithms developed to study two-dimensional turbulent flow past wavy surfaces. The component programs include (1) PROFILE — a program that creates initial equilibrium turbulent flat-plate profiles for a given flow condition, (2) CONMAP — a conformal-mapping program, and (3) WAVY — the two-dimensional Navier-Stokes equation solver, which simulates flow over a wavy surface. The WAVEGEM package can be used to estimate the effects of waviness introduced through fabrication and to study interactions between wind and waves. It can also be applied to the examination of the reduction of drag on wavy walls.

The typical problems studied with WAVEGEM are flows over stationary wave trains, the amplitudes of which are much smaller than the wave number. The geometrical coordinates of a wavy surface over 1 wavelength are fed to CONMAP. CONMAP uses fast and efficient conformal-mapping techniques to develop an orthogonal grid system. The mapping coefficients and physical grid coordinates are held in mass storage. CONMAP also performs a linear interpolation of the input velocity field using measured data or values calculated from PROFILE to create a velocity field in the computational domain at time zero.

The evolution of flow at subsequent times is determined by WAVY, which solves the Reynolds-averaged Navier-Stokes equations with higher-order Fourier/Chebyshev spectral techniques. The primary input to the programs includes the free-stream velocity, viscosity, skin-friction coefficients, thickness of the boundary layer, and the geometrical specification of the wave. The output of WAVY consists of short-cycle printed tables containing pressure at the wall, velocity at a point above the wall, friction drag, pressure drag, and Reynolds number.

WAVEGEM is written in FORTRAN 66 for batch execution and has been implemented on the CDC CYBER 170-series computers operating under NOS with a central-memory requirement of approximately 200K (octal) of 60-bit words. The program was developed in 1986.

This program was written by John C. Lin and Barbara H. Pitts of **NASA's Langley Research Center** *and R. Balasubramanian of Cambridge Hydrodynamics, Inc.*
LAR-13659 /TN

FOR ADDITIONAL INFORMATION *CONTACT:*

COSMIC®
112 Barrow Hall
University of Georgia
Athens, GA 30602
(404) 542-3265

NASA Tech Brief
National Aeronautics and Space Administration

Unsteady Flow in a Supersonic Cascade With Shocks

The operating range of turbomachinery for which stability can be calculated is extended.

The computer program TIPS (Two In-Passage Shocks) calculates unsteady lifts and moments on a compressor blade if the relative mach number is supersonic and if there are two shock waves in the blade passage. It accounts for three-dimensional effects in observed flows by using a hypothetical blade shape in a two-dimensional cascade. There is enough flexibility in the choice of blade shape to accommodate a desired entrance angle, exit angle, boundary-layer thickness, and stage pressure ratio at a given entrance mach number.

The model divides the mean flow into regions of uniform or one-dimensional flow in which the solutions for the superimposed unsteady flow can be found successively. The analysis makes use of previous solutions for unsteady flow in cascades and over an oscillating wedge.

Six flow conditions are chosen in the range of parameters for which the two-shock model is valid for studies of flutter in torsion and bending. It is found, in keeping with previous results from a single-shock model, that in each case the instability increases with decreasing frequency.

The analysis of unsteady flows in blade rows has been facilitated by the use of models for the underlying steady flow that permit the governing differential equations to be written with constant coefficients. This has been true for both supersonic flows and mixed flows with single shock waves in which the mean flows were assumed to be uniform. Numerous experiments, using both pressure sensors and laser anemometers, have shown that multiple shock waves are common in the tip regions of the blades, especially near the operating point of the compressor. One of the frequent patterns observed in the experiments includes an oblique shock wave at the leading edge of each blade and a nearly-normal shock wave at the trailing edge. It is that flow this program addresses.

A model for the mean flow incorporates the two shock waves and modifies the actual blade surfaces to account for the effects of three-dimensional flows. Three mean-flow domains are modeled as either uniform or one-dimensional flow so that the greatest use can be made of previous solutions for unsteady flow in a duct and flow around an oscillating wedge. Considerable use is made of the analysis previously developed for the flow in a blade passage in the presence of a single normal shock wave. The range of validity of the model is estimated, and six numerical examples are calculated, covering the intervals of inlet mach number and stage pressure ratio for which the model is valid.

This model for a supersonic blade row with shock waves has extended the operating range of turbomachinery for which calculations related to stability can be made. Based on the single configuration explored here, the model is appropriate at an entrance mach number ≤ 1.3 at the lowest applicable stage pressure ratio and, for any pressure ratio, at entrance mach numbers higher than those of the single-shock model. The calculations for specific cases show that in this operating region the presence of shock waves has a strong influence on the unsteady flow and that the tendency for instability at low frequencies observed in the single-shock model persists in the two-shock model. The thickness ratio appears to have significant influence on the stability of the flow at high frequencies.

The program is written in FORTRAN IV and run on an IBM 3033 with 370TSS operating system.

This program was written by Frank B. Molls of **Lewis Research Center** *and Willis H. Braun. LEW-14339 /TN*

FOR ADDITIONAL INFORMATION
CONTACT:

COSMIC®
112 Barrow Hall
University of Georgia
Athens, GA 30602
(404) 542-3265

Environmental Science & Technology

965 Reverse Osmosis Treatment to Remove Inorganic Contaminants from Drinking Water

966 A Study of Possible Economical Ways of Removing Radium from Drinking Water

967 Ecological Research Needs at Hazardous Waste Disposal Sites

968 Update of Acute and Chronic Aquatic Toxicity Data for Heavy Metals and Organic Chemicals Found at Hazardous Waste Sites

United States
Environmental Protection
Agency

Water Engineering
Research Laboratory
Cincinnati OH 45268

Research and Development

EPA

Project Summary

Reverse Osmosis Treatment to Remove Inorganic Contaminants from Drinking Water

A pilot study by the Charlotte Harbor Water Association determined the removal of a number of inorganic contaminants from drinking water using five state-of-the-art reverse osmosis membrane elements. The test system consisted of a small, 19 m^3/day (5,000 gal/day) capacity, reverse osmosis system that was modified to accept the five different membranes.

A Florida ground water was spiked with the contaminants and test runs of 1 to 13 days were made with each membrane. Removal data were collected for each membrane for all spiked contaminants and for several naturally occurring substances.

The five state-of-the art membranes in the study were Toray SC 3100*, Filmtec BW 30-4021, Dow 5K, Dupont B-9, and Hydranautics P/N 4040 LSY-IFCI. The spiked contaminants consisted of fluoride, cadmium, mercury, chromium, arsenic, selenium, nitrate, and lead. Limited tests were also conducted on nitrite, molybdenum, copper, and two naturally occurring radionuclides – uranium and radium. During each test run, removal data was collected on several naturally occurring substances, hardness, chloride, sulfate, total dissolved solids (TDS), and, on a limited basis, on calcium and sodium.

Although the membranes operated under different conditions (pressure, recovery) according to manufacturer's specifications, rejection of the spiked and natural substances was generally in agreement for all membranes. Highest removals (above 95%) were achieved on arsenic V, calcium, cadmium, chromium III and VI, copper, lead, molybdenum, sodium, radium, selenium IV and VI, uranium, hardness, and total dissolved solids. Moderate removals (85% to 94%) were obtained on fluoride, chloride, nitrate, and nitrite and lowest removals (below 85%) on arsenic III and inorganic mercury.

Wide variations in removal occurred with four contaminants: arsenic III, mercury, fluoride, and nitrate. Because nitrite tests were so limited, no conclusion could be made on variability. Variability in removal of these contaminants was attributed to the chemistry of the contaminants and the test waters, membrane material, and test conditions.

This Project Summary was developed by EPA's Water Engineering Research Laboratory, Cincinnati, OH, to announce key findings of the research project that is fully documented in a separate report of the same title (see Project Report ordering information at back).

Introduction

Reverse osmosis (RO) is a relatively new water treatment process, having been applied successfully in desalting brackish water for domestic use for less than two decades. RO systems typically operate at 5,520 kPa (800 psig) for seawater applications (35,000 mg/L total dissolved solids [TDS]) and at 2,760 kPa (400 psig) for brackish water applications with TDS ranging from 1,000 to 15,000 mg/L. In the late 1970's, tremendous progress was made in membrane technology during which advancements not only occurred with the traditional 2,760 kPa (400 psig), 90% TDS rejecting membranes, but even more significantly with the reduced pressure membranes that require approximately 1,380 kPa (200 psig) to achieve TDS rejection in excess of 90%. These membranes also operate in a wider range of feedwater pH and thus are capable of increasing applications. The major advantage, however, is the reduced energy requirement and therefore lower operating cost.

RO is effective for the removal of most dissolved solids. Extensive studies have been conducted to ascertain the efficacy of RO to reject common water constituents such as sodium, chloride, sulfate, TDS, calcium, etc., however, very

brackish water for domestic use for less than two decades. RO systems typically operate at 5,520 kPa (800 psig) for seawater applications (35,000 mg/L total dissolved solids [TDS]) and at 2,760 kPa (400 psig) for brackish water applications with TDS ranging from 1,000 to 15,000 mg/L. In the late 1970's, tremendous progress was made in membrane technology during which advancements not only occurred with the traditional 2,760 kPa (400 psig), 90% TDS rejecting membranes, but even more significantly with the reduced pressure membranes that require approximately 1,380 kPa (200 psig) to achieve TDS rejection in excess of 90%. These membranes also operate in a wider range of feedwater pH and thus are capable of increasing applications. The major advantage, however, is the reduced energy requirement and therefore lower operating cost.

RO is effective for the removal of most dissolved solids. Extensive studies have been conducted to ascertain the efficacy of RO to reject common water constituents such as sodium, chloride, sulfate, TDS, calcium, etc., however, very limited experimentation has been performed to evaluate the effectiveness of RO to remove many of the heavy metals and other inorganic contaminants listed in the National Interim Primary Drinking Water Regulations (NIPDWR). The investigations have generally consisted of laboratory studies, and most results have not been verified on either a pilot plant or full-scale level.

The primary objective of this research project was to determine the rejection of most of the inorganic contaminants listed in the NIPDWR using several state-of-the-art RO membrane elements. Several other contaminants being considered for future regulations were also studied. Because of various problems associated with the specific chemistry of the raw water, some contaminants were not investigated. This project was a continuation of a similar project reported by Huxstep in 1981.

Procedures

The basic test procedure consisted of spiking the test water with contaminant and operating the system according to manufacturer's operating specifications. Initially, the test water was spiked with one contaminant and the system was operated continuously for 6 to 8 hrs per day during a regular, 5-day work week. Because this schedule required an inordinate amount of time to complete a full series of tests with all the inorganic contaminants, the program was shortened by combining 2 or 3 contaminants. Each contaminant of a contaminant group was generally tested over a time period sufficient to permit the collection of 12 or more samples per test run. Occasionally a test was repeated to verify unrealistic or inconsistent data, particularly in the case of mercury, where analytical results were quite varied. During the last study with the Hydranautics membrane, several short term tests were added for copper, nitrite, and molybdenum. These tests provided limited data of only 2 to 8 samples.

Summary

Considering the test data from all five membranes as a whole, Table 6 shows the contaminants (natural and spiked) grouped into three categories according to removal capability:

(1) Highly removed (above 95%);
(2) Moderately removed (85% to 94%); and
(3) Poorly removed (below 85%).

Wide variation in removals occurred with four contaminants: As + 3, Hg, F, and NO_3. Because nitrite tests were limited to a 2-day test with one membrane, no general conclusion on variability for nitrite removal can be made. The variation in removals of these contaminants occurred among membranes and with each membrane test. The reason for the variation is concluded to be the chemistry of the contaminants and water matrix, membrane material, and test conditions. In the case of mercury, analytical procedures may also have contributed to the variation in results.

The full report was submitted in fulfillment of Cooperative Agreement No. CR-808358 by the Charlotte Harbor Water Association, Inc., under the sponsorship of the U.S. Environmental Protection Agency.

Table 6 *Removal of Specific Contaminants by Reverse Osmosis*

Highly Removed (above 95%)	*Moderately Removed (85% to 94%)*	*Poorly Removed (below 85%)*
Arsenic V	*Fluoride*	*Arsenic III*
Calcium	*Chloride*	*Mercury (Inorganics)*
Cadmium	*Nitrate*	
Chromium III	*Nitrite*	
Copper		
Lead		
Molybdenum		
Sodium		
Radium		
Selenium IV		
Selenium VI		
Uranium		
Total Hardness		
Total Dissolved Solids		

Martin R. Huxstep is with Charlotte Harbor Water Association, Inc., Harbour Heights, FL 33950. Thomas J. Sorg (also the EPA Project Officer, see below) is with the Water Engineering Research Laboratory, Cincinnati, OH 45268.

The complete report, entitled "Reverse Osmosis Treatment to Remove Inorganic Contaminants from Drinking Water," (Order No. PB88-147 780 AS; Cost: $14.95, subject to change) will be available only from:
National Technical Information Service
5285 Port Royal Road
Springfield, VA 22161
Telephone: 703-487-4650

The EPA Project Officer can be contacted at:
Water Engineering Research Laboratory
U.S. Environmental Protection Agency
Cincinnati, OH 45268

United States
Environmental Protection
Agency

Water Engineering
Research Laboratory
Cincinnati OH 45268

Research and Development

EPA

Project Summary

A Study of Possible Economical Ways of Removing Radium from Drinking Water

A study was undertaken to determine variables that control the incidental removal of radium observed to occur as a consequence of treatment to remove iron by oxidation-sand filtration. This study also evaluated the possibility of exploiting these factors to provide an inexpensive means of removing radium using existing or modified iron removal facilities. Emphasis was placed on the use of aeration to oxidize soluble iron. The initial objective was to determine how water chemistry influences ^{226}Ra sorption to iron oxides produced by aeration. Studies were also conducted to evaluate radium sorption to hydrous manganese oxides produced by permanganate oxidation. A latter objective was to evaluate the potential of exploiting sorption to filter sand as a novel removal technology. Batch and pilot plant studies were conducted in the laboratory and in the field at a city whose supply contains excessive radium.

Sorption of iron and manganese oxides and filter sand appears to be controlled primarily by the presence of calcium and magnesium, which are believed to compete for sorption sites. Excessive pH values would need to be used to obtain significant sorption to iron oxides at concentrations typical of natural waters. Removals obtained by freshly precipitated hydrous manganese oxides in batch studies were much greater than those obtained in systems containing only iron oxides or mixtures of iron and manganese oxides produced by the oxidation of ferrous iron by potassium permanganate. This suggests that sorption to manganese oxides could possibly be exploited to remove radium if iron did not interfere. The presence of iron may limit the utility of permanganate oxidation of iron as a means to reduce radium.

Filter sand has a potential capacity to sorb significant concentrations of radium at typical hardness concentrations if the capacity is maintained by periodically rinsing the sand with a dilute acid. Removal efficiencies of approximately 80% to 90% could be achieved in laboratory and field studies using a 61-cm (2-ft) deep sand bed at conventional loading rates when daily rinsing with a dilute acid was practiced.

This Project Summary was developed by EPA's Water Engineering Research Laboratory, Cincinnati, OH, to announce key findings of the research project that is fully documented in a separate report of the same title (see Project Report ordering information at back).

Introduction

Radium in drinking water is a concern because of suspected detrimental health effects, primarily the formation of cancers. Concentrations exceeding the current EPA-mandated maximum contaminant level (MCL) of 5 pCi/L total radium (^{226}Ra + ^{228}Ra) have been observed in several areas, the most notable occurrences in the United States being in Florida, North Carolina, Virginia, the New England states, the uranium mining areas of the mountain states, and in the midwestern states of Iowa, Illinois, Wisconsin, Missouri, and Minnesota.

It has been estimated that 500 municipal supplies may contain excessive radium. Lucas reported in 1985 approximately 1.4 million people in a total of 177 cities in the midwest alone are delivered a water containing ^{226}Ra in excess of 3 pCi/L (the 1962 U.S. Public Health Service drinking water standard and the value above which mandatory analysis for ^{228}Ra is required). Radium concentrations in the range of 5 to 20 pCi/L are typical of the majority of these supplies although higher levels (up to nearly 50 pCi/L) have been reported. In many cases removal efficiencies in the range of 50% to 75% would be adequate to put these waters into compliance.

Several conventional water treatment practices bring about the removal of radium. Sorg and Logsdon have pointed out that the two most efficient methods are sodium ion exchange and lime-soda softening, each generally removing about 85% to 95% of the influent radium. In those processes radium removal is only incidental to other changes in water quality that may not be needed or even

desired. For example, sodium ion exchange causes an increase in sodium concentration, which has been associated with an increased risk of heart disease. In particular, conventional processes are not suited to the many small communities that have excessive radium. Other removal technologies have also been investigated but to date no processes to remove radium alone are in widespread use.

Many supplies having high radium also have unacceptably high concentrations of iron and sometimes manganese that must be removed, commonly through processes involving oxidation and sand filtration. It has been observed that some radium removal occurs during iron removal treatment, presumably by sorption/coprecipitation with the hydrous metal oxides. Radium, like other alkaline earth metals, probably exists in water as a divalent cation and has been shown to sorb to many types of materials. For example, sorption to glass is a common sampling problem that is overcome by acidification. An understanding of the factors that control radium removal in iron removal processes could possibly aid in the development of inexpensive radium removal methods based largely on the use of existing facilities.

The primary objective of this study was to determine what factors control the incidental removal of radium occurring in iron removal plants typical of those operating in the midwest utilizing aeration and sand filtration. The study also evaluated the possibility of exploiting these factors as an inexpensive means of removing radium from drinking water using existing iron removal facilities. The initial focus was on modification of the water chemistry expected to affect sorption to iron oxides produced by aeration. Studies were also conducted to evaluate radium sorption to hydrous manganese oxides produced by permanganate oxidation. A latter objective was to evaluate the potential of exploiting sorption to filter sand as a novel removal technology.

Conclusions

Increasing sand filter influent pH to increase sorption to hydrous iron oxides produced by aeration does not appear to be a realistic strategy to increase radium removals. Differences in radium removals occurring as a result of iron removal processes involving aeration-sand filtration are probably due to differences in pH, iron concentration, and hardness. Regardless of these differences, little removal is expected.

The favorable results obtained using hydrous manganese oxide suggests that they could potentially be used to effectively remove radium if iron did not interfere. If a significant interference is caused by precipitation of iron oxides onto manganese oxides, then a two-stage oxidation process may be warranted when both iron and manganese are present. Iron could be oxidized by aeration in the first stage, followed by permanganate addition in the second to oxidize manganese. Filtration of the iron oxides prior to hydrous manganese oxide formation may also be desirable. Addition of manganous ion to waters containing low concentrations of naturally occurring soluble manganese might be useful to increase concentrations of hydrous manganese oxides. Direct addition of preformed hydrous manganese oxides may also be technically feasible and a relatively easily controlled approach to radium removal. In either strategy, filter runs are expected to decrease when a single filter is used to remove both iron and manganese precipitates. Length of filter run might, therefore, limit the utility of adding hydrous manganese oxides or manganous ion.

Radium removal using a regenerable sand filter has been demonstrated. While sorption to filter sand is believed an important mechanism, another is possibly involved. Significantly increased capacities are probably needed before use of a regenerable sand filter process could be generally recommended unless frequent rinsing with a dilute acid was acceptable. Further work is needed to better characterize the removal mechanisms, and to determine maximum possible removals and sorptive capacities. Studies should be conducted in a variety of waters and, in particular, its performance evaluated when operated to simultaneously remove both radium and iron flocs. Studies should also be conducted over much longer time periods than those used in this study. A trade-off between dilute acid strength and volume is expected to lead to a least-cost regeneration scheme. However, even with a 4 bed volume pH 1 daily regeneration scheme, acid costs to treat Oxford water are estimated to be $0.12/1,000 gal (based on a cost of $7/100 lb of sulfuric acid). Neutralization of the spent regenerant will probably be required before discharge but since pH control is probably not critical, an inexpensive system utilitzing crushed limestone may be adequate. However, sludges may be produced that must be disposed of. Other anticipated costs are associated with possible modifications to make the sand filter resistant to damage by dilute acid.

Richard L. Valentine, Roger C. Splinter, Timothy S. Mulholland, Jeffrey M. Baker, Thomas M. Nogaj, and Jae-Jie Horng are with the University of Iowa, Iowa City, IA 52242
Richard P. Lauch is the EPA Project Officer (see below).
The complete report, entitled "A Study of Possible Economical Ways of Removing Radium from Drinking Water," (Order No. PB 88-158 464/AS; Cost: $19.95, subject to change) will be available only from
National Technical Information Service
5285 Port Royal Road
Springfield, VA 22161
Telephone: 703-487-4650
The EPA Officer can be contacted at
Water Engineering Research Laboratory
U.S. Environmental Protection Agency
Cincinnati, OH 45268

Department of Energy

Technology Application

Oak Ridge National Laboratories

ENVIRONMENTAL TECHNOLOGY

ECOLOGICAL RESEARCH NEEDS AT HAZARDOUS WASTE DISPOSAL SITES

Key words: Hazardous waste; ecosystems; risk analysis; food webs; toxicity

The release of toxic substances from contaminated sites or waste disposal facilities can pose a threat both to human health and to the integrity of the ecosystem. The Superfund Amendments and Reauthorization Act of 1986 includes sections calling for basic research to detect toxic substances in the environment and to assess and quantify the risks to human health and the environment resulting from exposure to such substances. Protection of the environment and its various ecosystems is an explicit component of the legislation. The research programs outlined in the ORNL report, *Ecological Research Needs at Hazardous Waste Disposal Sites,* provides information critical to the assessment of hazards associated with chemically contaminated sites, to various cleanup approaches and their potential consequences, and to biological monitoring programs set up for surveillance after remedial actions have been taken.

Exposure to environmental insults cannot be quantified readily by measuring body burdens of contaminants. Many deleterious chemicals are rapidly metabolized, are excreted, or are toxic at concentrations below analytical detection limits. Furthermore, the relationship between body burden and toxic response is complex and highly variable. Assessing the significance of exposure to complex mixtures of chemicals, the most realistic scenario, is even more problematic. Constructing inventories of chemical contaminants is often prohibitively difficult, time-consuming, and expensive. Such inventories may ignore possible synergistic or antagonistic interactions of chemicals, which can invalidate predictions based on the toxicity of individual chemicals.

Evaluating the potential for exposure to contaminants in the environment is a challenging task because of the diversity and multiplicity of the routes of exposure (air, water, food, soil particles); the large differences in the biological availability of contaminants in these media; and the complexity of molecular, biochemical, and toxicological interactions within exposed organisms, populations, and ecosystems. This complexity limits the capability to either quantify exposure to chemical or physical agents in the environment or to assess the ecological significance of such exposure.

The ORNL report contains six essays that discuss the following related topics:

- biological monitoring,
- chemical-soil-biological interactions,
- microbial ecology,
- ecological risk analysis,
- interaction between food webs and toxic substances, and
- ecosystem stability and risk analysis.

Additional information:

Office of Technology Applications
Martin Marietta Energy Systems, Inc.
P.O. Box 2008
Oak Ridge, TN 37831-6257

Telephone (615) 574-4192; FTS 624-4192

S. I. Auerbach, ed., *Ecological Research Needs at Hazardous Waste Disposal Sites,* ORNL/TM-10368, Oak Ridge National Laboratory (August 1987).

Department of Energy

Technology Application

Oak Ridge National Laboratories

CHEMICAL AND WASTE MANAGEMENT

UPDATE OF ACUTE AND CHRONIC AQUATIC TOXICITY DATA FOR HEAVY METALS AND ORGANIC CHEMICALS FOUND AT HAZARDOUS WASTE SITES

Key words: Organic chemicals; heavy metals; aquatic toxicity; LC_{50}; EC_{50}; bioconcentration factors

The ORNL report, *Update of Acute and Chronic Aquatic Toxicity Data for Heavy Metals and Organic Chemicals Found at Hazardous Waste Sites,* provides updated information about chemicals commonly found at hazardous waste disposal sites. Although 50,000 different organic chemicals exist, fewer than 100 have been detected at 5 or more hazardous waste sites. The information in this report is based on a recent survey of the organic chemicals and heavy metals detected at sites on the National Priorities List (NPL).

The ORNL researchers selected the chemicals and metals found in surface water and groundwater at 40 or more NPL sites for inclusion in this review. Also considered were ten other chemicals that were found less frequently but were considered to be particularly toxic (Table 1).

The scientific literature was searched from the late 1970s to June 1987 to collect information on the acute and chronic toxicity to aquatic fauna by the selected toxicants. The document contains 156 pages of tables listing the following data:

- chemical name,
- Chemical Abstracts Service (CAS) number,
- bioconcentration factors,
- effective concentration for a specified response in 50% of a given population (EC_{50}),

Table 1. Chemicals and metals surveyed

Acenaphthene	Mercury
Acetone	Methylene chloride
Acetonitrile	Naphthalene
Arsenic	Nickel
Benzene	Pentachlorophenol
Benzo[*a*]pyrene	Phenanthrene
Cadmium	Phenols
Chloroform	Phthalates
Chromium	Polychlorinated biphenyls
Copper	Selenium
Cyanide	Tetrachloroethane
1,2-Dichlorethane	1,1,2,2-Tetrachloroethylene
Dichloroethylene	1,1,1-Trichloroethane
2,6-Dimethylnaphthalene	1,1,2-Trichloroethane
Hexachlorobenzene	Trichloroethylene
Hexachlorobutadiene	Toluene
Hexachloropentadiene	Zinc
Lead	

- lethal concentration for 50% of a given population (LC_{50}),
- test species, and
- references.

Additional information:

National Technical Information Service
U.S. Department of Commerce
5285 Port Royal Road
Springfield, VA 22161

E. L. Etnier et al., *Update of Acute and Chronic Aquatic Toxicity Data for Heavy Metals and Organic Chemicals Found at Hazardous Waste Sites,* ORNL-6392, Oak Ridge National Laboratory (June 1987).

Manufacturing, Machinery, & Tools

969 Automated Ply Laminating System (APLS)

970 Research in Advanced Real-Time Computer Vision

971 Automated Paper Molding-Based Manufacturing System for 60mm M204 Increment Container Halves

972 Automated Production of Stick Propellant

973 Low Contraction (LC) Chromium Plating

974 Argon Welding Inside a Workpiece — Canopies convert a large, hollow workpiece into an inert-gas welding chamber.

Testing & Instrumentation

975 Test Apparatus for Oversize Ball-Bearing Models — A see-through machine enables direct observation and indirect measurements at moderate speeds. (Licensing Opportunity)

Automated Ply Laminating System (APLS)

A major factor influencing the acquisition of modern aircraft is the manufacturing cost of composite parts. As advanced aircraft designs continually turn to the use of increasing amounts of composite materials for weight savings and high-temperature applications, the cost to manufacture those aircraft continues to rise. Traditional composite manufacturing requires hand layup processes which are extremely time consuming and expensive. A composite part consists of many individual plies which, when placed together on a tool and cured through elevated temperature and pressure, produce the desired part. This is a tedious process with limited quality control. Individual ply location is often out of tolerance, and foreign object detection (FOD) is dependent upon the operator. These factors result in long lead times and excessive amounts of rework and scrap.

To address these excessive manufacturing costs, the Naval Air Systems Command (NAVAIR) Manufacturing Technology Office (AIR-5143) has teamed up with the McDonnell Aircraft Company (MCAIR) to design, build and implement a first-of-its-kind composite parts production line. The program is being conducted under NAVAIR MT project number A1941, "Automated Ply Laminating System (APLS)".

APLS is a modular production line incorporating automated equipment from material laydown and cutting through ply build-up, or lamination. It will produce completed laminates for flat and slightly contoured parts and will also produce kits containing all plys for more severe contours, which will still require manual laydown of individual plies onto the tool.

APLS consists of various stations or modules integrated into a continuous line operation. The cell has two identical lines operating independently of one another. The main components of APLS are the Ply Cutter, Ply Pick-Up or Ply Plucker, the Sort/Storage Magazines, and the Ply Laminator. The

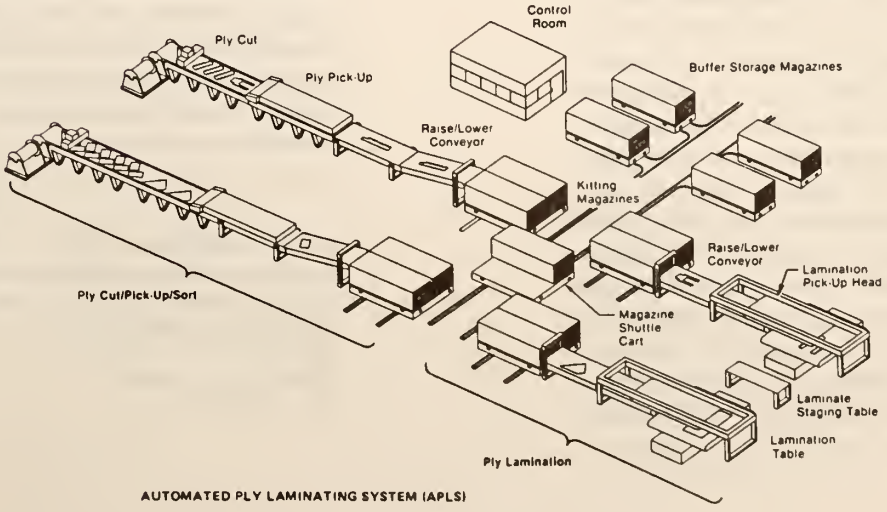

AUTOMATED PLY LAMINATING SYSTEM (APLS)

process begins with composite material spools manually loaded onto an automatic material dispenser. When needed, the material is pulled from the spool onto the cutting table. As the material leaves the spool, the vendor backing paper is removed and discarded. The cutting table consists of a porous plastic belt over a steel table. A vacuum is pulled through the belt and table to keep the material stationary during the cutting operation. A chisel cutter, operating at up to 20,000 RPM, cuts out each ply but retracts before cutting into the porous belt. The cutter has automatic blade change, blade check and blade cleaning.

At the completion of the cutting process,the porous belt conveys the cut ply nest to the pick-up area, where each individual ply is removed by the ply plucker and transferred to a conveyor. The ply plucker uses small vacuum ports placed .75" apart, extending the width of the cutting table, to lift the cut ply off the porous belt. Only those vacuum heads directly over the desired ply are activated. Once the ply is picked up, the ply plucker transfers the ply to a loading conveyor, which in turn loads the ply into a storage magazine. Each storage magazine contains 50 individual conveyors, with a capacity of up to 200 individual plies per magazine.

Once the storage magazine contains enough plies to make one or more parts, the magazines are either shuttled to a buffer area or moved directly to the laminating area.

At the laminating area, plies are unloaded from a storage magazine onto another conveyor one ply at a time in a programmed sequence. This conveyor transfers the ply to the laminating table. At this point, the ply laminator picks up the ply from the conveyor, again using vacuum heads, and moves the ply over the laydown table, adjusting in the X direction for proper positioning. The laydown table rotates and moves in the Y direction to obtain the final position for ply laydown. During ply laydown, the laminator debulks the ply stack to compact the stack and remove air which may be trapped between plies. Quality control is maintained throughout the laminating process by video cameras mounted above and below the laminator gantry. The cameras use image processing to inspect each ply for the correct ply, ply positioning, and FOD.

Once the required number of plies for a part have been laminated, the ply stack is manually transferred to the proper tool, bagged and sent to the autoclave for curing.

The two APLS lines will be integrated by a cell controller. The entire system will be controlled at the factory level by the Integrated Composites Center (ICC) network, which is being developed under an Air Force program.

APLS will achieve an average ply lamination cycle time of 15 seconds per ply, or over 400 ply details per hour for both lines. It is capable of handling woven or unidirectional broadgoods, including BMI or fiberglass. The minimum ply detail size APLS will be capable of laminating is 1" x 3", with the maximum being 48" x 144". Part size is restricted to a maximum of 13' diameter, which is the size of the laminating table.

The benefits of APLS are numerous. It automates composite parts production past automated ply cutting to include ply removal, ply sorting, and ply laminating. It helps reduce lead times and provides much better in-process controls. Better part quality will result along with reduced rework and scrap.

The APLS should be completed and integrated into MCAIR's St. Louis facility by the end of 1988. An industry demonstration of this system is scheduled for the beginning of 1989. However, plans are under way to conduct an interim program review during the summer of 1988.

For Additional Information:
To discuss this effort further, contact:
Mr. Rich Celin
Naval Air Engineering
Center
Lakehurst, NJ 08733
(201) 323-2173

Research In Advanced Real-Time Computer Vision

Martin Marietta and NBS, in a joint research program, have developed advanced computer vision algorithms using the Pipelined Image Processing Engine (PIPE) - - a specialized, real-time image processing computer developed at NBS. The algorithms are for use in the stereo analysis of scenes and analysis of motion.

Stereo analysis of scenes is a technique used to obtain the range to points in the scene from a two-camera system. The key problem in stereo computation is to find corresponding points in the pair of stereo images. A point in one image will correspond to a point in the other image if they are the projections of the same point in the three-dimensional scene. Once corresponding points in the images have been determined, it is straightforward to derive the 3-D positions of the scene points since the camera positions and orientations relative to one another are known.

Researchers implemented a stereo matching algorithm developed at Boston University on PIPE. It is a very general stereo algorithm that attempts to find range to many points in the scene, rather than just a few points. This results in a range map, and can be used to recover range to complex-shaped objects in arbitrary natural, as well as man-made scenes.

The algorithm, which first extracts edge points in the two images and then matches them, has been tested in real-time on several scenes. It runs in approximately one second on PIPE. This compares with algorithms running on other computers at many minutes or even hours. Once a range map has been obtained, surfaces can be fit to the range data to obtain a CAD-like description of the objects in the scene.

Motion analysis algorithms involve comparing sequences of successive images. PIPE is very well suited for this task since its architecture allows for easy, real-time comparison of successive images that are obtained from the camera at a rate of sixty per second.

An algorithm that detects motion and provides velocity of motion in the image plane (i.e., the manifestation on the image plane of object motion in the world) was developed at the University of Maryland and implemented on PIPE under the joint research program. The algorithm was designed for arbitrary natural scenes and updates image velocities several times per second.

Recovery of image motion is important for several reasons. It can be used for image segmentation (e.g., extracting moving edges or moving regions) or to recover the 3-D structure and motion of objects in the scene. NBS has begun research in recovering 3-D shape from image motion by applying motion extraction techniques to images obtained from a camera mounted on a robot (either a mobile robot or a manipulator). The camera motion can be determined from sensors on the robots. Then, under the assumption that objects in the scene remain stationary, the image motion can be used to recover 3-D positions of points in the scene. The 3-D information extracted in this manner can be used for tasks such as collision avoidance,

locating the position of an object to be manipulated, or displaying the scene from other viewpoints for a human operator.

PIPE is a registered trademark of Aspex Incorporated, New York, New York which built the prototype device under contract to NBS.

For Additional Information:
To discuss the workstations equipment further, contact:
Dr. Martin Herman
AMRF Project
Building 220—Room B-124
National Bureau of Standards
Gaithersburg, MD 20899
(301) 975-3441

U.S. Army Fact Sheet

Automated Paper Molding Based Manufacturing System for 60mm M204 Increment Container Halves

The technology developed under this multiple year funded MMT was to provide a complete technical data package for the development and fabrication of an automated manufacturing system for increment containers. These felted explosive propellant charge increment containers were designed for the 60mm (M204) and 81mm (M205) mortars.

The potential processes available for manufacturing the propellant increment containers were the slurry process and the paper process. The slurry process was proved out under another effort and this report covers the paper process. The development work completed by Engineering Systems and Development Corporation on process equipment designed to fabricate container halves is documented in this report.

The report described details of the development work completed by the designer including a prototype manufacturing system which automated the NC blanking, part preforming, final molding, and part finishing operations. System demonstration testing documented design

Presently, the automated process cannot produce at the designed level, however, the technology is available, the reason for failure documented, and the package is available for private industry.

FOR ADDITIONAL INFORMATION: Tom Jameson, AMXIB-PG, Production Engineering Division, U.S. Army Industrial Base Engineering Activity, Rock Island, IL 61299-7260; (309) 782-6586.

US Army Fact Sheet

Automated Production of Stick Propellant

The equipment developed under this project provides a production system capable of accommodating 5 continuous strands of solvent triple-base propellant. The system was designed for manufacturing 1/4 inch diameter sticks with a length range of 6 to 29 inches. This system required development of demand cutters, a conveying system, automatic stick traying equipment, and associated supervisory control. The prototype equipment consists of a 5 channel strand distributor at the press interface 5 servometer cutters which are controlled to compensate for variations in strand velocity, a five-lane pneumatic deck conveyor and a 5 tier stick collection unit. The unique feature of this project was the development of the collection equipment. The collection equipment consists of an empty tray magazine, stack collector and dispenser, and a tray indexing mechanism. The system is capable of producing 75,000 lbs/mo of solvent stick propellant with significantly reduced operator exposure.

FOR ADDITIONAL INFORMATION: Mr. Thomas Jameson, AMXIB-PG, Production Engineering Division, U.S. Army Engineering Activity, Rock Island, IL 61299-7260; (309) 782-5235.

U.S. Army Fact Sheet

Low Contraction (LC) Chromium Plating

High contraction chromium coating is currently used to resist erosion in gun bores. Inherent properties make the coating susceptible to shearing and flaking. Plating with low contraction chromium provides a significant increase in wear resistance due to its superior characteristics, however, its acceptance as a new process creates several production application problems. Higher and more critical range of temperatures along with high current densities could not be handled utilizing present equipment and materials. The objectives of this effort were to develop design criteria for modification of existing plating facilities to resolve these problems and to establish the needed operating parameters.

A production type facility has been completed for the LC chromium plating of long, large caliber gun tubes. The process consists of "flow thru" chrome solution with the gun tube acting as the fluid reservoir as well as the plating surface. Computer controls were installed to monitor and control the entire process. The facility capacity is limited to full length, large caliber gun tubes.

The LC chromium plating process will improve tube erosion resistance by 30 percent and will reduce plating time by a factor of 2 or 3.

FOR ADDITIONAL INFORMATION: Mr. Robert S. Hellem, AMXIB-PG, Production Engineering Division, U.S. Army Industrial Base Engineering Activity, Rock Island, IL 61299-7260; (309) 782-5235.

NASA Tech Brief
National Aeronautics and Space Administration
Marshall Space Flight Center, Alabama

Argon Welding Inside a Workpiece

Canopies convert a large, hollow workpiece into an inert-gas welding chamber.

A large manifold serves as its own welding chamber for the attachment of liner parts in an argon atmosphere. Every crevice, opening, and passageway is provided with an argon-rich environment. Weld defects and oxidation are thereby dramatically reduced; welding time is also reduced considerably.

The manifold is part of the Space Shuttle main engine. The liner creates a space for coolant to flow around the manifold. The liner is constructed by welding together panels and tubes of assorted shapes inside the manifold shell (see Figure 1). Ample quantities of gaseous argon must be directed against all sides of a piece as it is welded. This is difficult to do in the confined space between the shell and the liner piece.

An argon atmosphere is assured by the installation of flexible gloved canopies on the manifold openings used by the welding operator for access to the work. All unused openings are sealed, and argon is supplied through the manifold coolant inlets (see Figure 2).

The flowing gas, which escapes through small holes in the gloved canopies, purges air from the interior of the manifold so that oxidation cannot degrade the weld quality. Maintained at a gauge pressure of 1 to 2 inches of water (250 to 500 N/m^2), the argon puffs out the clear plastic-film canopies. With hands placed in the gloves, the operator manipulates the welding gun, which is placed inside the manifold before the canopies are attached. This welding technique should be useful in the fabrication of heat exchangers, pump bodies, and other complicated, enclosed assemblies containing flow passages.

This work was done by Gene E. Morgan of Rockwell International Corp. for **Marshall Space Flight Center**. *No further documentation is available.*
MFS-29167

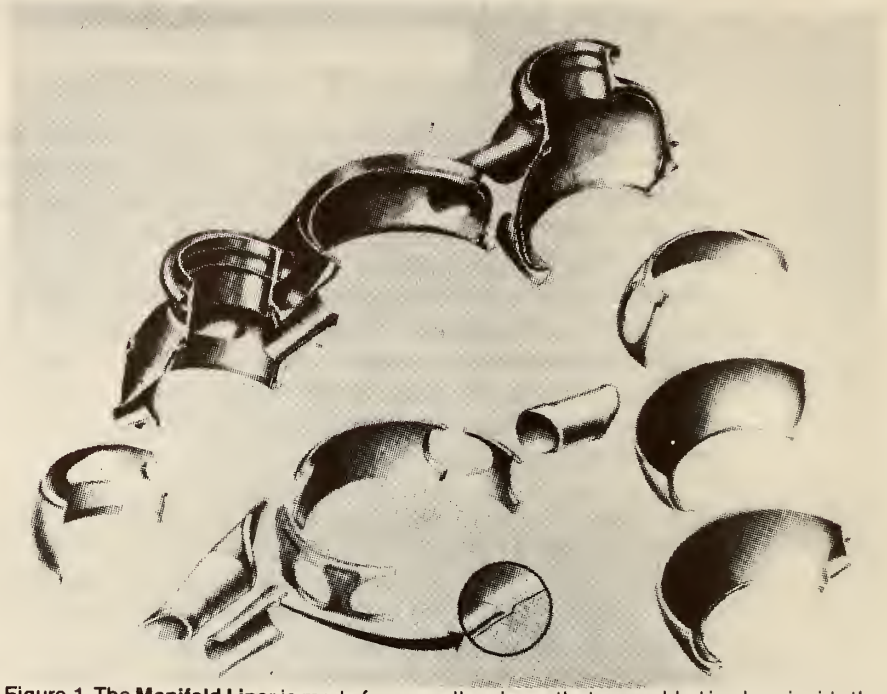

Figure 1. The **Manifold Liner** is made from smaller pieces that are welded in place inside the manifold.

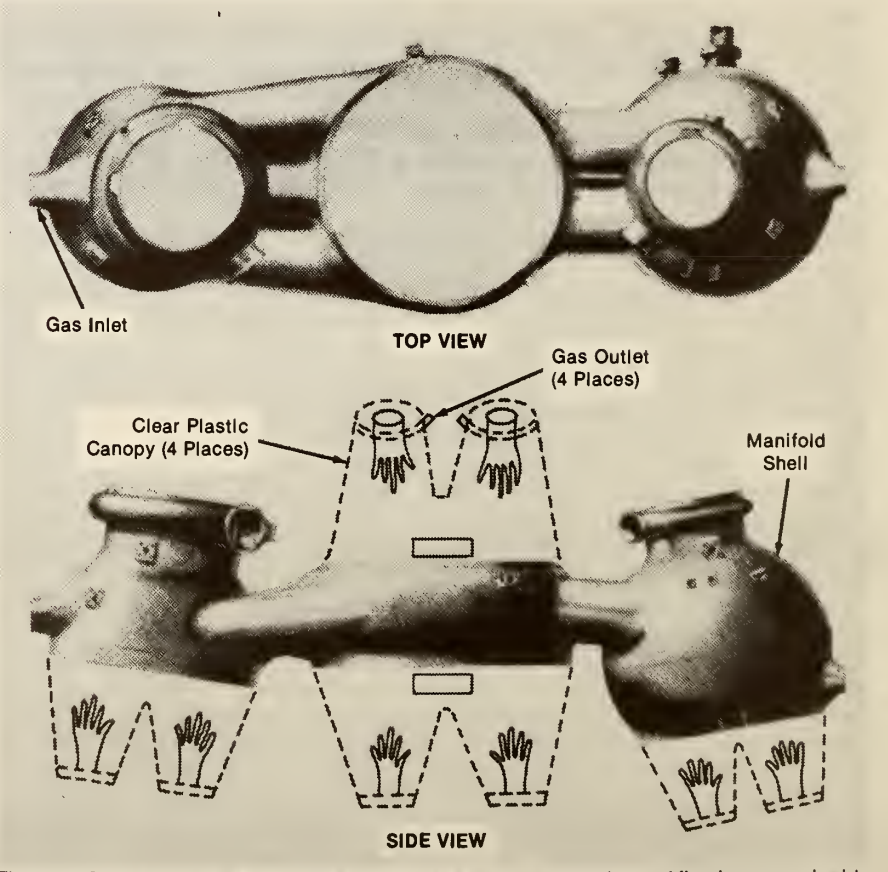

Figure 2. **Gloved Canopies** over large openings retain an atmosphere of flowing argon inside the manifold. Other openings are sealed during welding, except for the argon inlet.

FOR ADDITIONAL INFORMATION: *Contact: Director, Technology Transfer Division, P.O. Box 8757, BWI Airport, MD 21240; (301) 621-0100 Ext. 241*
REFER TO THE NUMBER LISTED AT THE END OF THIS ARTICLE

NASA Tech Brief
National Aeronautics and Space Administration
Marshall Space Flight Center, Alabama

Licensing Opportunity

Test Apparatus for Oversize Ball-Bearing Models

A see-through machine enables direct observation and indirect measurements at moderate speeds.

Enlarged scale models of ball bearings show the flow of lubricant and heat around the bearings. The scale models, used in a moderate-speed rotary test machine, obviate difficult direct measurements on real, small, high-speed bearings.

A combination of visual observation, infrared measurement, and thermocouple mapping shows the flow and heating patterns on the inner and outer races, the cage, and the balls. The rotary test machine (see figure) has transparent walls and working fluid.

In the machine, the inner and outer races are heated by electrical resistance or induction. The rolling and static elements of the bearing are monitored for speed, load, flow, and heating. The data are taken by high-speed cameras, by infrared thermography, by thermocouples fixed on the outer race, and by supplemental thermocouples attached to the inner race and connected to external circuits via a slipring. The data are scaled by nondimensional techniques to the size, flow, and speed of a real bearing.

The large-scale bearing enables the visualization of such complex heating and flow patterns as those that occur in forced-convection nucleate and film-boiling situations. Such patterns cannot be developed by analytical methods in cryogenic subcritical-pressure coolant flows of oxygen, hydrogen, and methane, for example.

This work was done by William R. Wagner of Rockwell International Corp. for **Marshall Space Flight Center.** *No further documentation is available.*

Inquiries concerning rights for the commercial use of this invention should be addressed to the Patent Counsel, Marshall Space Flight Center Refer to MFS-29284 /TN

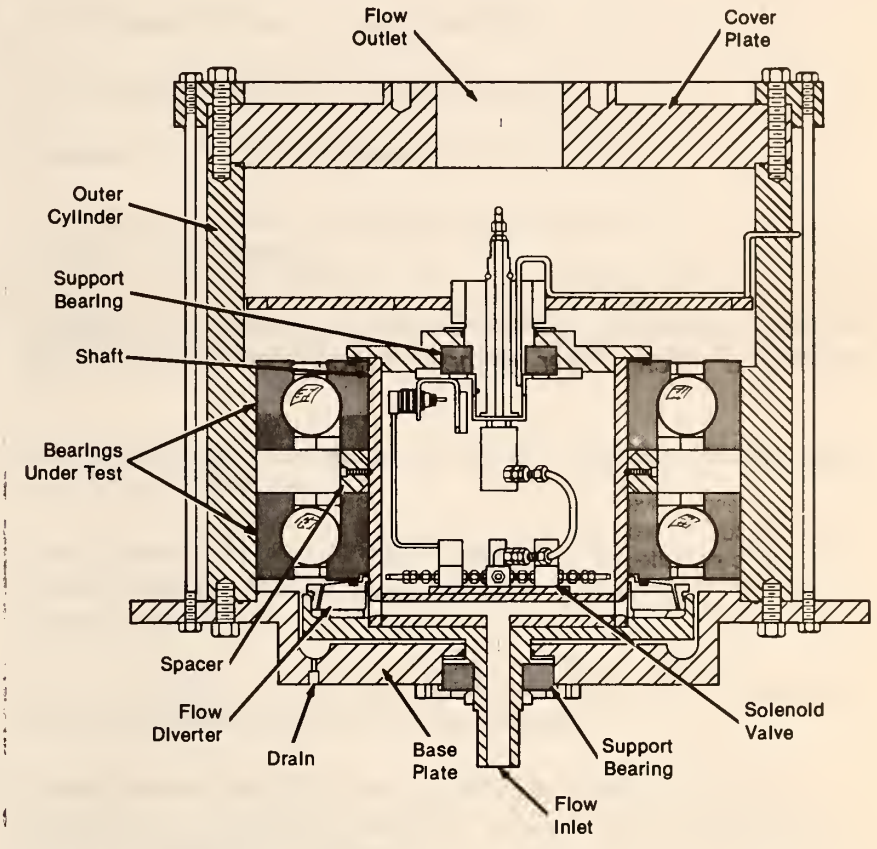

A Model of a Ball Bearing, six times larger than the real bearing, is rotated in a test machine. The transparency of the walls and the simulated lubricant reveal flow patterns and allow visible-light and infrared photographs to be made.

George C. Marshall Space Flight Center

Technology Utilization Officer: Ismail Akbay
Code AT01
Marshall Space Flight Center,
AL 35812
(205) 544-2223

Patent Counsel: Leon D. Wofford, Jr.
Mail Code CC01
Marshall Space Flight Center,
AL 35812
(205) 544-0024

FOR ADDITIONAL INFORMATION: *Contact: Director, Technology Transfer Division, P.O. Box 8757, BWI Airport, MD 21240; (301) 621-0100 Ext. 241*
REFER TO THE NUMBER LISTED AT THE END OF THIS ARTICLE

Materials

976 An Overview of Technology on Bituminous Surfacing Materials for Low-Volume Roads

977 Dyeing Flame-Retardant Fabrics (Licensing Opportunity)

978 Beta Processing Versus Crack Growth Rate

979 Laser Cladding of Magnesium with Zirconium

980 Studies of the Fracture Behavior of Ti-10V-2Fe-3A1

981 Weldability of 2219-T851 and 2519-T87 Aluminum Armor Alloys for Use in Army Vehicle Systems

982 Electrochromic Variable-Emissivity Surfaces — Temperature could be controlled by altering infrared radiative properties. (Licensing Opportunity)

983 Extending Fatigue Lives of Selected Alloys — Rejuvenating treatments have been demonstrated.

984 High-Emissivity Coatings for High-Temperature Surfaces — Plasma-sprayed coatings increase cooling by thermal radiation. (Licensing Opportunity)

985 PMR Composites of Increased Toughness — Toughness is increased without sacrificing processability or hot strength.

986 Readily Processable Polyimide — A polymer exhibits resistance to hydraulic fluid, excellent processability, and extremely high adhesive strength. (Licensing Opportunity)

Testing & Instrumentation

987 Reliability of Inspection by SLAM — Scanning laser acoustic microscopy finds flaws in ceramic specimen.

988 An Accurate Laboratory Test System Using Commercial Equipment for Eddy-Current Measurements

Other Items of Interest

998 Thermoplastic Removes Hydrogen without Producing Water

952 Corrosion in Amorphous-Silicon Solar Cells and Modules — Moisture severely affects amorphous-silicon units, bur encapsulation helps.

954 Spin Coating of Decon Agent Containers

999 Standard to Measure Carbon in Natural Materials

U.S. Department
of Transportation
**Federal Highway
Administration**

An Overview of Technology on Bituminous Surfacing Materials for Low-Volume Roads

Because agency officials responsible for the management of low-volume roads work with limited budgets, guidelines for selecting the most practical design, maintenance, and rehabilitation alternatives must be established. Bituminous surfacings provide a good, often low-cost surfacing for low-volume roads. These surfacings may consist of hot-mix asphalt concrete, cold bituminous plant mixes, mixed in-place cold mixes, surface treatments or chip seals, slurry seals, and, in some cases, recycled mixes. Recycling should be considered as a cost-effective alternative for rehabilitating distressed pavements. A report contains sufficient information on the above topics to assist engineers and administrators in the decision process of designing, constructing and maintaining low-volume roads. The text is thoroughly referenced to identify sources of additional detailed information.

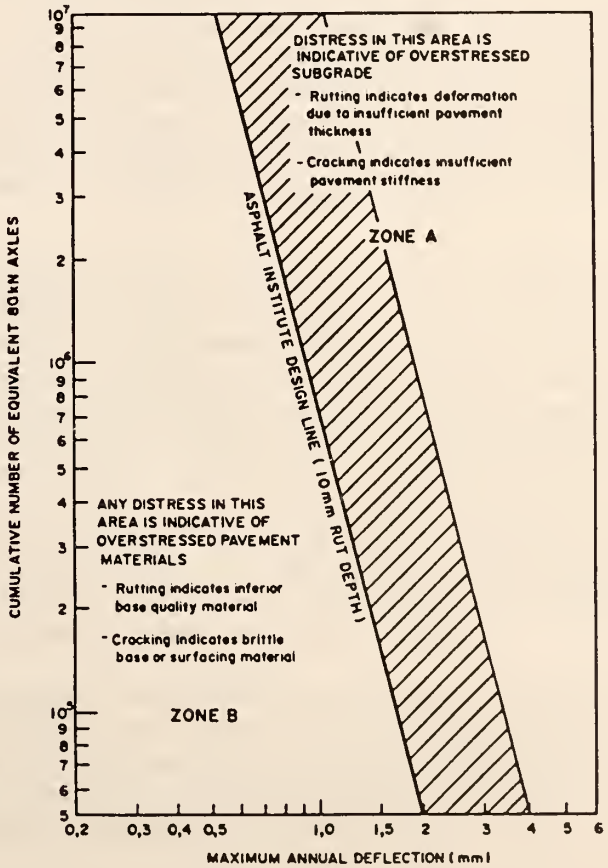
DISTRESS IN THIS AREA IS INDICATIVE OF OVERSTRESSED SUBGRADE
- Rutting indicates deformation due to insufficient pavement thickness
- Cracking indicates insufficient pavement stiffness
ZONE A
ASPHALT INSTITUTE DESIGN LINE (10mm RUT DEPTH)
ANY DISTRESS IN THIS AREA IS INDICATIVE OF OVERSTRESSED PAVEMENT MATERIALS
- Rutting indicates inferior base quality material
- Cracking indicates brittle base or surfacing material
ZONE B
CUMULATIVE NUMBER OF EQUIVALENT 80kN AXLES
MAXIMUM ANNUAL DEFLECTION (mm)
0,2 0,3 0,4 0,5 1,0 1,5 2 3 4 5 6

Deflection-traffic relation used for assessment of structural adequacy of pavement and base and surfacing quality.

SUMMARY

This chapter has concentrated on pavement condition and performance evaluation. Performance was defined in two ways. Functional performance was defined as the history of roughness or of Present Serviceability Rating or Index of a pavement over time, subject, of course, to traffic and environmental influences. Structural performance was defined in terms of physical distress manifestations, such as rutting and cracking . Structural performance also was defined to embody the concept of structural strength.

Procedures for evaluating structural and functional performance were presented, including the use of car ride meters to determine roughness, condition surveys to define the extent and magnitude of distress, and deflection to measure structural strength, which has been related to both functional and structural performance.

The special cases of aggregate-surfaced and thin bituminous-surfaced low-volume roads were addressed.

FOR ADDITIONAL INFORMATION: A copy of this report is available from NTIS, Springfield, VA 22161; (703) 487-4600.
NTIS order number: PB88-169834/NAC
Price code: A12

United States Department of Agriculture

Licensing Opportunities

Research Technology
Agricultural Research Service

Dyeing Flame-Retardant Fabrics

There are ways of processing cellulosic fabrics such as cotton and rayon, plus certain cellulosic blends, so they will be flame retardant. These processes affix the hydroxymethyl phosphonium-nitrogen polymer to the cellulosic fabric substrate.

The commercial process has two undesirable aspects. First, it requires the use of gaseous ammonia in the finish, thus requiring special equipment and processing to control this noxious gas. Second, because these fabrics will no longer retain colors or take up dye as well as untreated cotton fabrics, it is possible to offer the consumer only a limited selection of colors. For the consumer, it amounts to a trade off: the added safety that flame retardancy brings in exchange for limits on color selection and durability.

But producers and consumers may yet have a better world. ARS scientists have applied for a patent for a process that replaces the gaseous ammonia in the finish with urea. This new finish can be run on standard textile equipment. Second, this finish changes the character of the phosphorous-nitrogen polymer so that it interacts with dye to a lesser extent than finishes based on ammonia.

Advantage has been taken of the positive, or cationic electronic character conferred by the polymer system to devise substantially different procedures for dyeing flame-retardant fabrics. These procedures, based on bonding between the cationic charge of the polymer and the anionic charge of the dye, extend the range of colors and types of dyes that can be used on these flame-retardant fabrics. In addition, they provide a means of renewing the colors of such fabrics.

For further information, contact Robert J. Harper, Jr., and John V. Beninate, USDA-ARS Southern Regional Research Center, PO Box 19687, New Orleans, LA 70179. Patent Application No. 07/075,169, "Process for Dyeing Flame-Retardant Fabrics."

FOR ADDITIONAL INFORMATION: Inquiries concerning rights for commercial use of this invention should be addressed to: Office of Federal Patent Licensing, Center for the Utilization of Federal Technology, Room 304, NTIS, Springfield, VA 22161; (703) 487-4738. Refer to Patent Application 7-075,169/TN.

U.S. Air Force
Technology Note

Beta Processing Versus Crack Growth Rate

The results of a 3-year-study of the effects of the microstructure produced by beta processing on the crack-growth rate behavior of Ti-6Al-4V alloy are described in a report issued by Rockwell International. Studies were conducted using both plate and forged material. Processing conditions were designed to produce significant differences in the Widmanstatten (acicular) alpha plus beta microstructure. In all, six different microstructural conditions were examined, three produced in plate material and three produced in forged material. Tensile strength of the six conditions varied from 132 ksi to 112 ksi. Crack growth rate data were determined using compact tension specimens tested in laboratory air to 30 Hz. Tests were conducted at two R values, 0.1 and 0.7.

Microstructural features of the test materials were determined by quantitative methods. Among the factors examined were volume fraction of beta phase, number of beta phase discontinuities, alpha plate size, and alpha colony size. The chemical composition of the alpha and beta phases were also determined. None of the microstructural features produced a consistent effect on crack growth rate. However, lineal regression analysis provided useful information on the combined effects of the various features and confirmed that the large scatter observed in published information on the crack growth rates for beta processed Ti-6AL-4V could be attributed to microstructural differences. Crack propagation resistance was improved by decreasing the volume fraction of the beta phase, the continuity of the beta phase, the alpha plate width, or the alpha colony size. The volume fraction of beta phase was the most influential microstructural feature.

FOR ADDITIONAL INFORMATION: A copy of this report is available from NTIS, Springfield, VA 22161; (703) 487-4600.

NTIS order number: ADA140832/NAC

Price code: A04

Laser Cladding of Magnesium With Zirconium

Studies of the corrosion resistance of laser-clad magnesium are described in a report from the University of Illinois describing work conducted under an Air Force Office of Scientific Research contract.

Two and one-half-inch-thick magnesium plate was clad with high purity zirconium by placing a layer of 20 um diameter zirconium powder on the plate surface, compacting the powder to hold it in place on the plate during processing, and then melting the powder using a laser beam. Melting was done at 800 to 1000 watts. The resulting clad layer consisted of two phases, a zirconium outer layer and an inner layer, about 200 um thick, consisting of a mixture of zirconium and magnesium. Corrosion behavior was evaluated by potential measurements in a 3.5 percent NaCl solution. The corrosion potential of the clad material was -0.647 volts as compared to a value of -1.455 for the magnesium substrate. The results of potentiodynamic measurements made on the two materials are shown in Figure 1.

FOR ADDITIONAL INFORMATION: A copy of this report is available from NTIS, Springfield, VA 22161; (703) 487-4600.
NTIS order number: AD-A179606
Price code: A03

Studies of the Fracture Behavior of Ti-10V-2Fe-3A1

An investigation of the effects of microstructure and deformation rate on the fracture toughness of the Ti-10V-2Fe-3Al titanium alloy, supported by the Air Force Office of Scientific Research, is underway at SRI International. The preparation of material for use in this study and preliminary analysis of the proposed test techniques are described in the first annual report on this investigation.

It is planned to measure crack initiation and propagation behavior under dynamic loading using a one-point bend impact test developed in an early program. Preliminary studies indicate that an optical displacement transducer can be used to measure fracture behavior in that test. Methods for analyzing the fracture surface topography have also been developed for use in the investigation.

FOR ADDITIONAL INFORMATION: A copy of this report is available from NTIS, Springfield, VA 22161; (703) 487-4600.

NTIS order number: AD-A179264
Price code: A02

U.S. Army Fact Sheet

Weldability of 2219-T851 and 2519-T87 Aluminum Armor Alloys for Use in Army Vehicle Systems

Aluminum alloys have been the dominant structural material in light combat vehicles for the past 25 years. Only two alloys account for nearly all aluminum plate in this application: the strain-hardened 5083-H131 alloy (MIL-A-46027) and the heat-treated higher strength 7039-T64 alloy (MIL-A-46063). The 7039-T64 alloy has, however, been plagued by susceptibility to stress corrosion cracking (SCC) in the through thickness, short-transverse direction. Introduction of the 2519-T87 aluminum alloy with tensile and ballistic properties equivalent to the 7039-T64 alloy provides a high strength alternative alloy with SCC resistance for possible vehicular structure applications. The 2219-T851 alloy (MIL-A-46118) offers a SCC resistant aluminum alloy, but the tensile properties of this armor plate do not promise the ballistic resistance of either the 7039-T64 or 2519-T87. The 2XXX series alloys obtain their high strength by a solution heat treatment and quench followed by strain hardening and artificial aging. If either are to be used on Army combat vehicles, they must demonstrate adequate weldability. The purpose of this preliminary study was to evaluate the weldability of these two alloys, as measured by the weldment's tensile strength, fatigue endurance limit, resistance to SCC and ballistic performance. Primary emphasis was placed on 2519-T87 because of its promise to provide improved ballistic protection and, because it is a new alloy, it was felt that a larger data base needed to be established for future Army needs.

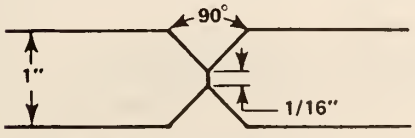

a. Joint Configuration

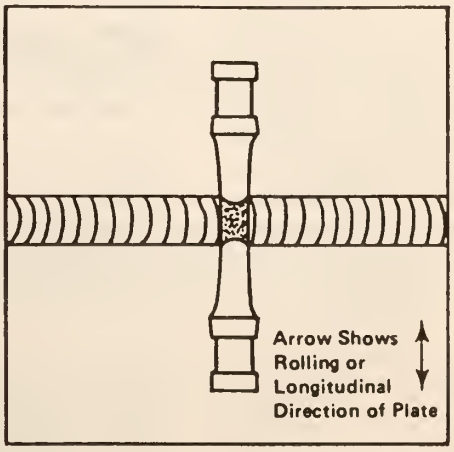

b. Test Specimen Location in Weldment

Figure 1. Double-Vee Joint for Mechanical Property Test Weldments and Test Specimen Location in Weldment

The cruciform test, which exposes the weld zone to the highest restraint and residual stresses of the four tests selected, is especially useful in evaluating the underbead SCC tendency in the HAZ. Of the ten 2519-T87 cruciforms tested, only one weldment (which was not standard) developed a crack in the HAZ.

The bent-beam test measures SCC tendency in the weld, fusion line, and HAZ due to residual stress and the stress due to the elastic strain of bending. No failures occurred after 500 hours in five bent-beam 2519-T87 specimens loaded to approximately 75 percent of the base metal yield strength.

The sandwich test subjects the middle plate to tensile stresses along the short transverse axis, which generally is most susceptible to SCC. The 7039-T64 alloy cracked after only 100 hours of testing, whereas the seven 2519-T87 specimens showed no SCC failures after 500 hours of testing.

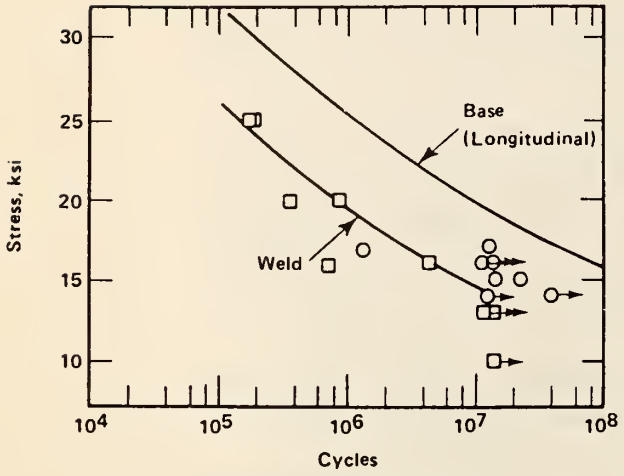

Figure 2. Rotating Beam Fatigue Data for 2519-T87 Alloy Welds

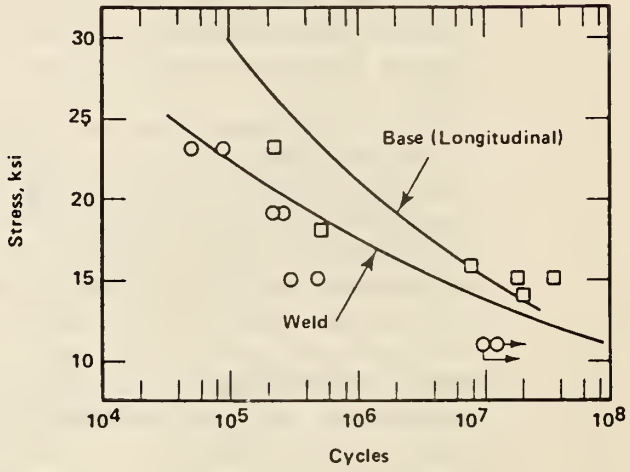

Figure 3. Axial Fatigue Data for 2519-T87 Alloy Welds

Additional work is planned to investigate the effects of joint design, welding procedures and minor weld discontinuities on ballistic impact behavior. Weldability to dissimilar aluminum alloys also is an important characteristic.

FOR ADDITIONAL INFORMATION: A copy of this report is available from NTIS, Springfield, VA 22161; (703) 487-4600.

NTIS order number: AD-A184296

Price code: A03

NASA Tech Brief
National Aeronautics and Space Administration
Marshall Space Flight Center, Alabama

Licensing Opportunity

Electrochromic Variable-Emissivity Surfaces

Temperature could be controlled by altering infrared radiative properties.

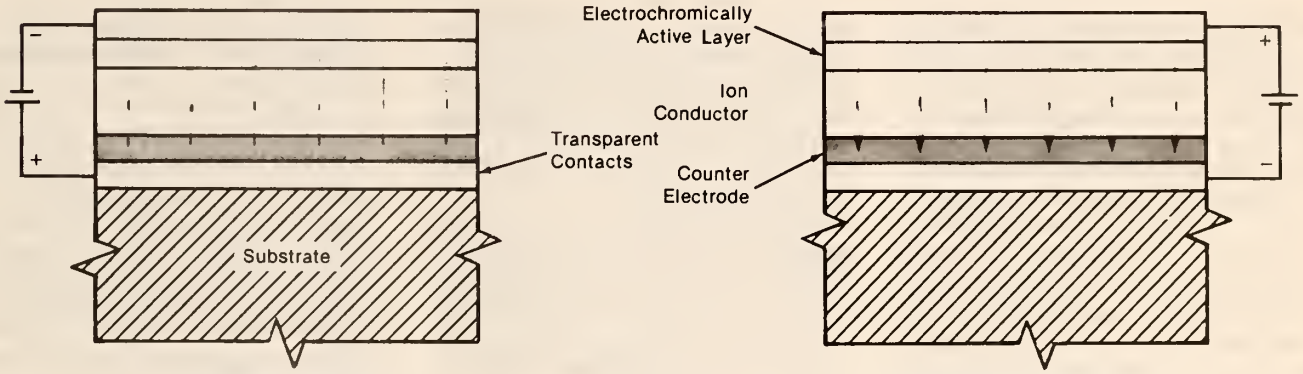

The **Infrared Emissivity** of the electrochromically active layer would be changed by applying a voltage to insert or remove Li atoms electrochemically. The change would be reversible and continuously variable between the specified limits of the layered structure.

Experimental radiative-thermal-control coats have been made by vacuum deposition of thin films that include electrochromic layers. The absorptivity, emissivity, and reflectance of a suitably coated surface at various wavelengths can be changed reversibly by the application of a suitable voltage between two of its layers. When fully developed, such variable-emissivity surfaces could be useful for the controlled radiative (for example solar) heating and radiative cooling of equipment or of inhabited rooms.

The electrochromic materials of interest are the insertion compounds, in which small atoms can be inserted or from which small atoms can be extracted reversibly. One such compound is tungsten oxide, which interacts with lithium in the reversible electrochemical reaction

$$WO_3 + xLi^+ + xe^- \underset{\text{extraction}}{\overset{\text{insertion}}{\rightleftharpoons}} Li_xWO_3$$

The insertion of Li causes a change in optical properties due to the donation of an electron from Li to the WO_3 host material. A host material without long-range crystalline order (for example, amorphous WO_3) becomes more absorptive, while a crystalline material tends to become more reflective. The wavelength dependence of the enhanced reflectivity or absorptivity (and, therefore, emissivity) depends on the nature and thickness of the host material.

A typical coat might include an electrochromically active layer of Li_xWO_3, a transparent ion-conducting (but otherwise solid and electrically insulating) layer of $LiAlF_4$, and an electrochromically passive counterelectrode of TiO_2 or Nb_2O_5. The voltage would be applied to the active and counter layers through amorphous In_2O_3 contact layers, which are nearly transparent to infrared radiation.

Thus far, three versions have been tested:

1. A structure of polyethylene terephthalate/Al/*a*-Li_xWO_3/liquid electrolyte/*a*-Nb_2O_5/In_2O_3, which is switched between a state of high solar absorptivity with high infrared emissivity and a state of moderate solar absorptivity with low infrared emissivity;
2. A structure of glass/In_2O_3/*c*-Li_xWO_3/liquid electrolyte/*a*-Nb_2O_5/In_2O_3, which can be switched between a state of low solar absorptivity with low infrared emissivity and a state of low solar emissivity with high infrared emissivity; and
3. A structure of infrared-transmissive As_2S_3/In_2O_3/*c*-Li_xWO_3/liquid electrolyte/*a*-Nb_2O_5/In_2O_3, which can be switched between thermally reflecting and thermally transmitting (blackbody) states.

The experiments show that a device can be adjusted continuously to a state between its two extreme states. The energy density required for a complete transition between extreme states is less than 0.2 Wh/m^2 (720 J/m^2). No holding voltage is required because a device remains in its optical state until voltage is applied to change it.

This work was done by R. David Rauh and Stuart F. Cogan of EIC Laboratories, Inc., for **Marshall Space Flight Center**.

Inquiries concerning rights for the commercial use of this invention should be addressed to the Patent Counsel. Marshall Space Flight Center Refer to MFS-26032/TN

George C. Marshall Space Flight Center
Technology Utilization Officer: Ismail Akbay
Code AT01
Marshall Space Flight Center,
AL 35812
(205) 544-2223

Patent Counsel: Leon D. Wofford, Jr.
Mail Code CC01
Marshall Space Flight Center,
AL 35812
(205) 544-0024

FOR ADDITIONAL INFORMATION: *Contact: Director, Technology Transfer Division, P.O. Box 8757, BWI Airport, MD 21240; (301) 621-0100 Ext. 241*
REFER TO THE NUMBER LISTED AT THE END OF THIS ARTICLE

NASA Tech Brief
National Aeronautics and Space Administration
Marshall Space Flight Center, Alabama

Extending Fatigue Lives of Selected Alloys

Rejuvenating treatments have been demonstrated.

Experiments with three alloys have shown that some combinations of heat treatment, hot isostatic pressing, and/or surface treatment can extend the cycle lives of fatigue-damaged or fatigue-precracked specimens. Successful rejuvenation tests were conducted on MAR-M246(Hf)(DS) — a directionally solidified, high-strength, nickel-based superalloy — and on the nickel-based alloy Inconel* 718. The results of tests of the titanium-based alloy Ti/5Al/2.5Sn ELI are inconclusive.

For each alloy, tests were first done to determine the "baseline" high-cycle-fatigue lives and high-cycle-fatigue failure modes over a range of test conditions. Next, controlled fatigue damage was introduced into specimens, either by fatigue testing to a specified number of cycles or by growing a fatigue crack from a starting notch. Following this, the damaged specimens were subjected to candidate rejuvenating treatments, then tested to failure. The effectiveness of each such treatment was judged by comparing the fatigue data of the damaged and treated specimens to the "baseline" fatigue data taken at the same test conditions.

The high-cycle-fatigue life of fatigue-damaged MAR-M246(Hf)(DS) was significantly extended by a solution reheat treatment at 1,221 °C for 2 h followed by aging at 871 °C for 16 h. Transmission electron microscopy provided evidence that the heat treatment reduced the density of dislocations caused by fatigue cycling.

Inconel* 718 containing a single, large fatigue precrack was partly rejuvenated by electron-beam welding to seal the crack at the surface, hot isostatic pressing at a temperature of 982 °C and pressure of 200 MPa for 3 h to heal the crack, and solution and aging reheat treatment identical to the standard heat treatment during manufacture.

Annealing at 816 or 927 °C may extend the fatigue life of fatigue-damaged Ti/5Al/2.5Sn ELI: transmission electron microscopy shows that this treatment reduces the dislocation density. However, the rejuvenation results are clouded by large variations in the tests-specimen properties.

*Inconel is a registered trademark of the Inco family of companies.

This work was done by D. E. Matejczyk of Rockwell International Corp. for **Marshall Space Flight Center**.
MFS-27131 /TN

FOR ADDITIONAL INFORMATION: *Contact: Director, Technology Transfer Division, P.O. Box 8757, BWI Airport, MD 21240; (301) 621-0100 Ext. 241*
REFER TO THE NUMBER LISTED AT THE END OF THIS ARTICLE

NASA Tech Brief
National Aeronautics and Space Administration
NASA's Jet Propulsion Laboratory, Pasadena, California

Licensing Opportunity

High-Emissivity Coatings for High-Temperature Surfaces

Plasma-sprayed coatings increase cooling by thermal radiation.

High-emissivity coatings on high-temperature refractory surfaces greatly increase their rates of heat radiation. In radiatively cooled engines and heat pipes, such coatings can prolong life and allow operation at higher powers.

A coating of zirconium diboride on tungsten or molybdenum increases the emissivity of a surface to more than 0.6 at 2,000 °C — more than twice that of the uncoated material. The coating is applied by plasma-arc spraying after the surface has been thoroughly cleaned and roughened to ensure adhesion.

On the electrode of an experimental high-power radiation-cooled electric thrustor, the coating causes the operating temperature in a typical case to decrease by 100 to 200 °C, preventing overheating and the resultant damage. The coating may also have potential applications in automotive engines: it could allow critical engine parts to operate cooler than they normally would, by enhancing radiative heat transfer.

This work was done by William D. Deininger and David Q. King of Caltech for **NASA's Jet Propulsion Laboratory**.

This invention is owned by NASA, and a patent application has been filed. Inquiries concerning nonexclusive or exclusive license for its commercial development should be addressed to the Patent Counsel, NASA Resident Office-JPL
Refer to NPO-17122. /TN

Jet Propulsion Lab.
NASA Resident Office
Technology Utilization Officer: Gordon S Chapman
Mail Stop 180-801
4800 Oak Grove Drive
Pasadena, CA 91109
(818) 354-4849
Patent Counsel: Paul F. McCaul
Mail Code 180-801
4800 Oak Grove Drive
Pasadena, CA 91109
(818) 354-2734
Technology Utilization Mgr for JPL: Norman L. Chalfin
Mail Stop 156-211
4800 Oak Grove Drive
Pasadena, CA 91109
(818) 354-2240

FOR ADDITIONAL INFORMATION: *Contact: Director, Technology Transfer Division, P.O. Box 8757, BWI Airport, MD 21240; (301) 621-0100 Ext. 241*
REFER TO THE NUMBER LISTED AT THE END OF THIS ARTICLE

NASA Tech Brief
National Aeronautics and Space Administration
Lewis Research Center, Cleveland, Ohio

PMR Composites of Increased Toughness

Toughness is increased without sacrificing processability or hot strength.

Addition-curing polyimide resin (PMR) polyimides are now gaining wide acceptance as matrix resins in composites destined for high-temperature applications in engines. Considerable cost and weight can be saved by the use of fiber-reinforced polyimide composites in place of the metals currently used in the moderately-high-temperature zones [up to 550 °F (288 °C)] of jet engines.

The technology for the application of these advanced composite materials to jet engines is developing rapidly. A graphite/PMR polyimide air-bypass duct has recently been developed to replace the titanium duct currently used on the F-404 engine that powers the Navy's F-18 fighter. Other components currently under consideration for composite applications include engine-inlet guide vanes, first- and second-stage stators, and anti-icing leading-edge wing panels.

A major concern in all of these applications is the resistance of the material to damage by impacts at low velocities. Such impacts can cause hidden internal damage in composite structures. While initially the damage may not degrade the structural integrity of the component, load reversals from vibrations induced in the structure under flight conditions can cause the damage to grow until the structure fails. This type of damage, which can result from dropped tools, runway debris, and the like, can occur in both the airframe structures and in the engine itself.

PMR polyimides, which exhibit excellent resistance to oxidation at high temperatures, are inherently brittle matrix resins. With the broadening interest in the use of composites to improve the performances of engines, there is an obvious need for a tougher PMR polyimide material more tolerant to damage.

Some newly identified PMR resin compositions provide significant improvements in composite-shear-strain and low-velocity-impact properties. The resin composition that provided the best overall balance of composite toughness and retention of mechanical properties at 600 °F (316 °C) with processability was obtained by substituting 20 mole percent of the diamine used in PMR-15 resins with a diamine containing twice the number of flexible phenyl connecting groups.

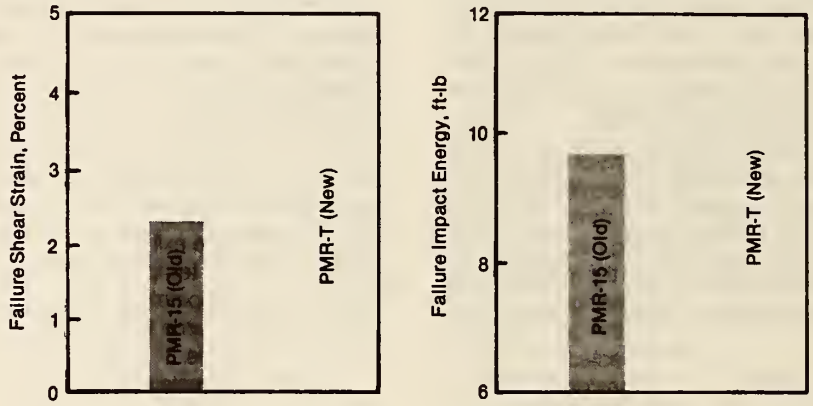

The Toughnesses of Old and New Composites were measured under impact.

The figures compare the properties of Celion 6000 graphite-fiber-reinforced composites, prepared from state-of-the-art PMR-15 resin, with those of the new PMR-T resin. The shear strain to failure and energy absorbed during low-velocity impact shown for the PMR-T composites are 85 and 25 percent higher, respectively, than the values shown for the PMR-15 composites. While the glass-transition temperature of the composites was approximately 50 °F (28 °C) lower than that of the PMR-15 composites, only a minimal difference in flexural strength of the two materials at 600 °F (316 °C) [135 ksi (93 MPa) for the PMR-15 composite and 128 ksi (88 MPa) for the PMR-T composite] was observed after exposure to air at a temperature of 600 °F (316 °C) for 1,500 h. The increased ductility offered by PMR-T resins provides PMR composite materials with better resistance to impacts at low velocities, without sacrifice of processability or long-term mechanical properties at 600 °F (316 °C).

This work was done by Raymond D. Vannucci and Kenneth J. Bowles of **Lewis Research Center**. *Further information may be found in NASA TM-87081 [N85-32148/NSP], "Graphite/PMR Polyimide Composites With Improved Toughness."*

Copies may be purchased [prepayment required] from the National Technical Information Service, Springfield, Virginia 22161, Telephone No. (703) 487-4650. Rush orders may be placed for an extra fee by calling (800) 336-4700. [A02]
LEW-14574 /TN

FOR ADDITIONAL INFORMATION: *Contact: Director, Technology Transfer Division, P.O. Box 8757, BWI Airport, MD 21240; (301) 621-0100 Ext. 241*
REFER TO THE NUMBER LISTED AT THE END OF THIS ARTICLE

NASA Tech Brief
National Aeronautics and Space Administration
Langley Research Center, Hampton, Virginia

Licensing Opportunity

Readily Processable Polyimide

A polymer exhibits resistance to hydraulic fluid, excellent processability, and extremely high adhesive strength.

As part of an effort to develop tough, solvent-resistant thermoplastics for potential use as structural resins on aerospace vehicles, a new processable polyimide was evaluated. The synthesis involved the reaction of a new diamine, 1,3-bis 2-(3-aminophenoxy)ethyl ether, with 3,3′,4,4′-benzophenonetetracarboxylic dianhydride to form the polyamic acid and subsequent conversion of it to the polyimide. Various physical properties of the polyimide were measured. Films, moldings, adhesive specimens, and composite specimens were prepared and evaluated. Of particular interest is the extremely high titanium-to-titanium tensile shear strength of this polyimide.

The polyimide was semicrystalline with a crystalline-melt temperature (T_m) of 242 °C and a glass-transition temperature (T_g) of 150 °C. After the T_m had been exceeded, thermal annealing for several hours at 210 °C was unsuccessful in inducing crystallinity. Thermogravimetric analysis showed 5 percent weight loss in air and in nitrogen at 373 °C and 408 °C, respectively. The melt viscosity of fully-imidized amorphous polyimide measured at 210 °C was 6×10^6 P at a frequency of 0.1 rad/s and 1×10^5 P at 100 rad/s.

Transparent yellow films cast from N-methylpyrrolidone solutions of 95 percent imidized polymer and subsequently dried at 210 °C gave tensile strength, tensile modulus, and elongation at 25 °C of 12,500 psi (86.2 MPa), 391,400 psi (2.67 GPa), and 4.0 percent, respectively; and at 93 °C of 9,500 psi (65.5 MPa), 291,000 psi (2.01 GPa), and 5.0 percent, respectively. Film specimens were bent back upon themselves and placed in this stressed condition in jet fuel, deicing fluid, and hydraulic fluid. After 24 h of immersion, no detectable sensitivity was observed. However, after only a few minutes of exposure in methylene chloride (a component of paint stripper), pronounced crazing was observed.

Transparent orange moldings were fabricated at 260 °C under 100 psi (0.69 MPa) and cut into compact tension specimens. The fracture toughness (K_{Ic}) at 25 °C was 2,670 psi-in.$^{1/2}$ (2.93×10^6 N/m$^{3/2}$), and the fracture energy (G_{Ic}) at 25 °C was 18.2 in.-lb/in.^{2} (3.19×10^3 N/m). The surface of the failed specimens was highly crazed and moderately rough due to yielding.

Standard Ti/Ti tensile shear specimens were fabricated at 260 °C under 100 psi (0.69 MPa) and tested. The average Ti/Ti tensile shear strength of 7,850 psi (54.1 MPa) at 25 °C was exceptionally high, possibly the highest value ever reported for single lap specimens. The failure mode was essentially 100 percent cohesive. Strengths at other conditions were also excellent except after immersion in boiling water for 72 h. The problem, however, was at the interface (adhesive failure) and not with the polyimide. Powdered aluminum filler reduced the strength somewhat at 25 °C and increased the strength slightly at 121 °C.

Small graphite fabric composites fabricated at 260 °C under 200 psi (1.38 MPa) have flexural strength, flexural modulus, and short-beam shear strength of 70,500, 7,300,000, and 4,100 psi (486 MPa, 50 GPa, and 28 MPa) at 25 °C, respectively. No testing was done at elevated temperature because of the low values obtained at 25 °C. The significant finding of extremely high Ti/Ti tensile shear strength for this polyimide in addition to its other properties indicates a high potential for such aerospace applications as the adhesion of Ti/Ti substrates.

This work was done by Paul M. Hergenrother of **Langley Research Center** *and Frank W. Harris and Mark W. Beltz of the University of Akron.*

Inquiries concerning rights for the commercial use of this invention should be addressed to the Patent Counsel. Langley Research Center Refer to LAR-13675 /TN

Langley Research Ctr.
Technology Utilization Officer: John Samos
Mail Stop 139A
Hampton, VA 23665
(804) 865-3281
Patent Counsel: George F. Helfrich
Mail Code 279
Hampton, VA 23665
(804) 865-3725

FOR ADDITIONAL INFORMATION: *Contact: Director, Technology Transfer Division, P.O. Box 8757, BWI Airport, MD 21240; (301) 621-0100 Ext. 241*
REFER TO THE NUMBER LISTED AT THE END OF THIS ARTICLE

NASA Tech Brief
National Aeronautics and Space Administration

Reliability of Inspection by SLAM

Scanning laser acoustic microscopy finds flaws in ceramic specimens.

A report describes an evaluation of scanning laser acoustic microscopy (SLAM) in the detection of surface voids in silicon nitride and silicon carbide. SLAM is an attractive technique for the nondestructive inspection of these ceramics because it can image surface and subsurface microflaws in real time. The detection of such flaws is important because they limit the strengths and fracture toughnesses of ceramic parts in advanced high-temperature heat engines.

In SLAM, a laser light is used to detect distortions, on an angstrom scale, produced on the surface of a specimen by ultrasonic waves transmitted through the specimen. From the distortion, SLAM creates a picture on a video monitor of such defects as voids, inclusions, and cracks.

In the evaluation, specimens of sintered Si_3N_4 and SiC were examined by SLAM at an ultrasonic frequency of 100 MHz, in both the as-fired condition and after polishing. The specimens were intentionally impressed with styrene microspheres during firing to introduce voids of known size, shape, number, and location in the surface.

The evaluation concentrated on the statistical reliability of the detection of voids by SLAM. In the polished specimens, SLAM detected surface voids as small as 100 μm in diameter with 0.90 probability at a confidence level of 0.95. However, the reliability of detection was substantially less for voids in unpolished, as-fired specimens. Moreover, inspection of the as-fired specimens took 10 times as long as the inspection of the smooth specimens. If ceramic engine parts are smoothly finished, as they are likely to be, the SLAM technique should detect surface and near-surface flaws quickly and reliably.

This work was done by Don J. Roth, Stanley J. Klima, and James D. Kiser of **Lewis Research Center** *and George Y. Baaklini of Cleveland State University. Further information may be found in NASA TM-87035 [N85-32337/NSP], "Reliability of Void Detection in Structural Ceramics Using Scanning Laser Acoustic Microscopy."*

Copies may be purchased [prepayment required] from the National Technical Information Service, Springfield, Virginia 22161, Telephone No. (703) 487-4650. Rush orders may be placed for an extra fee by calling (800) 336-4700. [A04]
LEW-14633 /TN

FOR ADDITIONAL INFORMATION: *Contact: Director, Technology Transfer Division, P.O. Box 8757, BWI Airport, MD 21240; (301) 621-0100 Ext. 241*
REFER TO THE NUMBER LISTED AT THE END OF THIS ARTICLE

Department of Energy

Technology Application

Oak Ridge National Laboratories

AN ACCURATE LABORATORY TEST SYSTEM USING COMMERCIAL EQUIPMENT FOR EDDY-CURRENT MEASUREMENTS

Key words: Eddy current; metals; nondestructive testing; computer program

Measuring eddy currents is the preferred method for nondestructive testing of metals because many different properties can be determined rapidly and accurately without contact with the specimen and without special surface preparation. Theoretical studies of eddy-current testing show that many different types of measurements are possible, but these tests are not used often because of the time, expense, and effort required to set up the equipment. Computer simulations of eddy-current tests are easy to run, but until recently, performing the actual tests has been relatively difficult.

Researchers in the Metals and Ceramics Division at ORNL have been able to measure experimental eddy currents and record and analyze the results with little more effort than is required to run a computer simulation. Their technique involves combining a commercial instrument [a Hewlett-Packard 4192A Impedance Analyzer (HPIA)] with a computer capable of running Fortran and communicating over an IEEE-488 bus (Fig. 1). All operating parameters can be controlled and varied over the bus, and test changes can be made with simple software commands. An eddy-current coil and test samples are required, and the probe must be moved from sample to sample in a prescribed manner. The data gathering, analysis, and presentation can all be done by the computer.

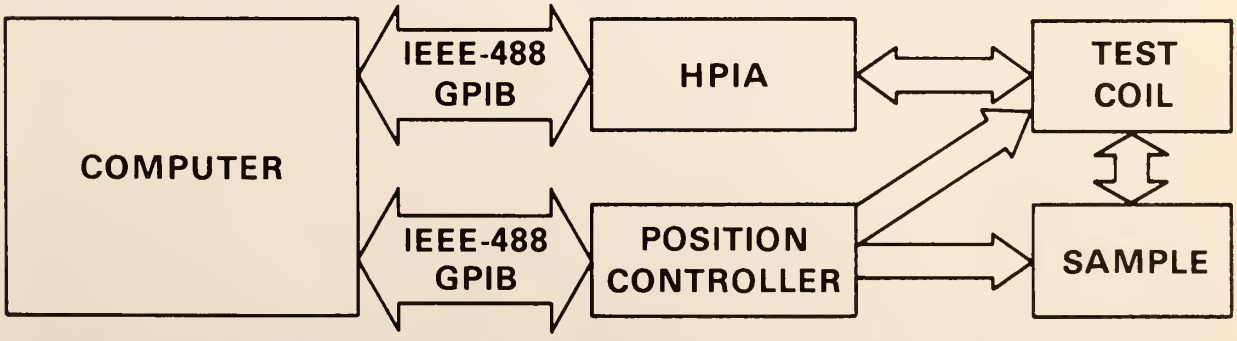

Fig. 1. Block diagram of a typical eddy-current measurement system. The IEEE-488 general-purpose interface buses (GPIBs) link the computer to the impedance analyzer and to the position controllers. The modification necessary for specific tests generally would be limited to the coils, their connections to the impedance analyzer, and the mounting of the coils and samples.

The probe's motion over the test samples can also be controlled by the computer, which can drive a mechanical positioner with stepping-motor controllers (Fig. 2), or the probe can be positioned manually. The sensitivity of the HPIA is high enough (0.01° phase shift and 0.001 dB magnitude) so that measurements can be made on all but very small defects. The stability of the analyzer is good, and noise can be reduced to a very low level by signal averaging. This system is not fast enough for many production tests, but high-speed, large-scale tests can be simulated on a computer and then verified using the HPIA before investing in the construction of an expensive production instrument.

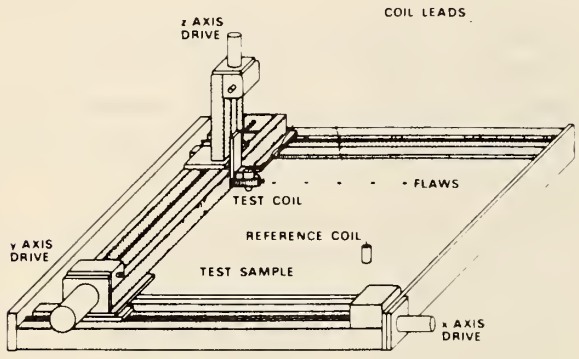

Fig. 2. An *xyz* computer-controlled eddy-current scanner.

The ORNL report, *An Eddy-Current Laboratory Test System Using Commercial Equipment* contains the computer programs and descriptions of instrumental setups for computerized eddy-current testing. Fortran computer programs have been written to have the system perform the following types of measurements: measuring and plotting frequency response or normalized impedance, through-transmission absolute-conductivity measurements, and multiple-frequency measurements of multiple-property problems. The multiple-frequency measurements are the most common and the most difficult types of eddy-current tests, but they make it possible to measure certain metallic properties even when other properties may also vary.

Additional information:

National Technical Information Service
U.S. Department of Commerce
5285 Port Royal Road
Springfield, VA 22161

C. V. Dodd, L. M. Whitaker, and W. E. Deeds, *An Eddy-Current Laboratory System Using Commercial Equipment,* ORNL-6366, Oak Ridge National Laboratory (April 1987).

Medicine & Biology

989 Dental Liquid Diets

990 New Technique to Automate Sequencing of DNA

991 Dual Purpose Soft-Tissue Equivalent and Dosimetric Phantom Material

992 Sickle Cell Anemia New Study Technique

993 Technique for Imaging Blocked Coronary Arteries

994 Pressurized Sleeve — A garment part sustains a pressure differential without unduly restricting the user.

Other Items of Interest

967 Ecological Research Needs at Hazardous Waste Disposal Sites

968 Update of Acute and Chronic Aquatic Toxicity Data for Heavy Metals and Organic Chemicals Found at Hazardous Waste Sites

Dental Liquid Diets

A new ration for military personnel who are unable to eat solid food is being developed. The Dental Liquid Ration consists of dehydrated powders that can be reconstituted with either water or milk to taste like components of a normal meal. The products are produced by dry-blending ingredients, which replaces freeze drying the entire meal. This method will decrease the cost of the product by up to 40% and will increase the production base by eliminating the need for the highly specialized freeze drying operation.

Currently, patients requiring liquid diets are often fed only sweet milkshakes, that the patients quickly tire of because of the lack of variety. Weight loss is a common problem with these patients. There are no commercially available items that are similar to these new products. Potential patient population may include maxillofacial injuries, cancer, geriatric and swallowing disorder patients. These new meals have the advantage of being easier to prepare, and require no refrigeration.

A five day menu, consisting of breakfast items, entrees, starches, vegetables, and desserts, is being developed. Six flavors of between meal milkshakes are also being developed. A one day menu will provide on average a minimum of 2500 kilocalories, and meet at least 80% of the Recommended Daily Dietary Allowance. When three milkshakes are also served per day, each day's menu will then contain 3500 kilocalories. Presently 33 new products have been developed which include items such as Apple & Cinnamon Farina, Chicken BBQ, Buttered Squash, and Strawberry Shortcake.

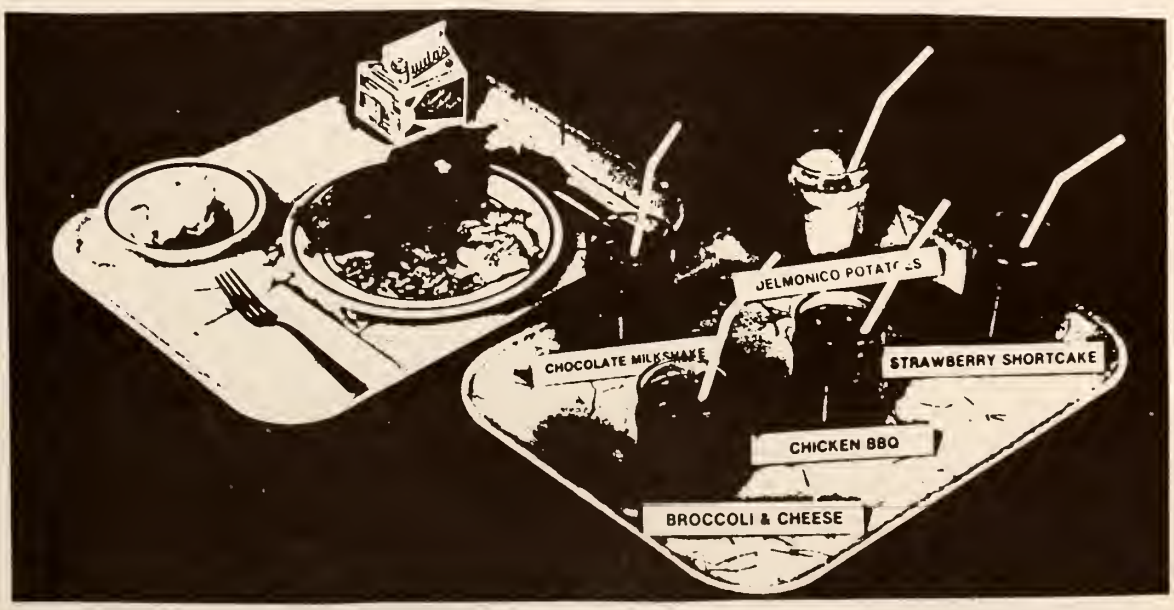

For additional information, contact:

Mrs. Susan Erickson
U.S. Army Natick RD&E Center
Natick, MA 01760-5018
TEL: 617-651-4593

or

Mr. Robert Rosenkrans
Technology Transfer Coordinator
U.S. Army Natick RD&E Center
Natick, MA 01760-5014
TEL: 617-651-5296

NBS technology update

National Bureau of Standards
U.S. Department of Commerce
Gaithersburg, MD 20899

New Technique to Automate Sequencing of DNA

Researchers from EG&G Biomolecular and NBS, in collaboration with the Center for Advanced Research in Biotechnology (CARB), have developed an improved method for automating DNA sequencing. Sequencing--determining the precise sequence of DNA bases in a gene--is one of the most important tasks in molecular biology and protein engineering. Several techniques have been developed to automate the process, but these rely on fluorescent dyes which are expensive and can interfere with the chemistry used to sequence the DNA. In addition, the dyes may introduce variations in the mobility of the DNA whose behavior is comparatively well understood. This makes it possible to design automated DNA sequencers that are smaller and less expensive than those based on fluorescent dyes.

FOR ADDITIONAL INFORMATION: To discuss these efforts further, contact Keith H. McKenney, Chemistry Bldg., Room 348, National Bureau of Standards, Gaithersburg, MD 20899; (301) 975-2582.

Brookhaven National Laboratory

Dual Purpose Soft-Tissue Equivalent and Dosimetric Phantom Material

A new human tissue equivalent phantom material has been developed. This material can provide critical dose calibration in radiation treatment where small (a few percent) excess doses can have undesirable effects.

The value of the material is that is serves dual purposes, namely as a tissue-equivalent phantom and/or dosimeter. The material provides realistic photon transport conditions, does not distort the radiation field, is moldable into complex shapes, composition can be altered to study changes in the dose distribution and disometry is possible with a variety of radiations, e.g., x-ray, electrons, neutrons, and charged particles.

This technique will be used for radiation oncology treatments for tumors.

Literature - L. Wielopolski, "Continuous Three-Dimensional Radiation Dosimetry in Tissue-Equivalent Phantoms Using Electron Paramagnetic Resonance in L-a-alanine", Med. Phys. 14 (4), July/Aug 1987, pp. 646-652.

FOR ADDITIONAL INFORMATION: Contact Dr. William Marcuse, Head, Office of Research and Technology Applications, Bldg. 475-B, Brookhaven National Laboratory, Upton, NY 11973; (516) 282-2103. Refer to BNL/AA-34/TN.

Department of Energy

Technology Application

Lawrence Berkeley Laboratory

Sickle Cell Anemia New Study Technique

A new technique that can follow, step-by-step, the sickling of red blood cells, has been developed by scientists at the Lawrence Berkeley Laboratory.

The technique, which involves sending a beam of polarized light through red blood cells suspended in environments that simulate those found in human organs and cell tissues, will allow scientists to study the specific physiological conditions that lead to a sickle cell crisis.

Sickled red blood cells lack the flexibility of normal, disc-shaped cells and are unable to squeeze through capillaries. This impairs the flow of blood delivering oxygen from the lungs to other organs and tissues in the body. Damage from the reduction in oxygen accumulates until the organs fail or tissue cells begin dying. Sickle-cell anemia is caused by a mutant form of hemoglobin known as hemoglobin S.

It is extremely important to know what the equilibrium state and the kinetics of polymerization are. These factors play a key role in the physiological processes that lead to capillary blockage and crisis.

Finding this information difficult to obtain using existing techniques, the LBL scientists developed their own method. By analyzing the scattering of the polarized light as it passes through a suspension of red blood cells, they are able to measure the rate of hemoglobin S polymerization under different stress conditions. Analysis of the data indicates that quantitative measurements can be made in real time.

The device used to make the polymerization measurements was developed by Hunt and Lofftus and is called a "polarization-modulation nephelometer." Unlike conventional nephelometers, is operates with polarized light which is sensitive to helical structures such as a hemoglobin S polymer.

For Additional Information:

Office of Research and Technology
Application
50A 4112
Lawrence Berkeley Laboratory
Berkeley, CA 94720
Telephone (415) 486-6502

Department of Energy

Technology Application

Lawrence Berkeley Laboratory

Technique for Imaging Blocked Coronary Arteries

A new technique, under development at the Lawrence Berkeley Laboratory, shows promise of leading to a non-invasive method for pinpointing blocked coronary arteries, thus identifying people at risk of heart attacks before symptoms appear.

The new technique, which employs positron emission tomography (PET) and the tracer rubidium-82, is based on studies of the heart and cardiovascular system that have been going on at LBL since 1978.

Over the past 10 years, the team has developed a technique for evaluating the flow of blood to heart muscle -- a measurement that reflects the health of the coronary arteries.

Right now, doctors have nothing that can show arterial blockage except the coronary angiogram -- a complicated and expensive procedure that involves running a catheter up an artery from the groin to the heart and pumping in dye. Angiograms require hospitalization and are not without risk to the patient. PET scans of coronary arteries, on the other hand, could conceivably be done in the physician's office as part of an individual's annual check-up -- at least for patients who fall into high-risk groups.

In PET imaging, a positron-emitting radioactive tracer is injected, inhaled, or ingested by a patient or subject, allowed to concentrate in a particular organ or type of tissue, and then is detected by means of a ring of crystals placed around the subject. The crystals detect photons created when positrons from the tracer encounter electrons and annihilate.

From this information, scientists can reconstruct an image of the radiotracer in the tissue or organ in three dimensions, and even follow the course of organic processes as they take place.

For the coronary artery studies, rubidium-82 is the tracer of choice, because of its metabolic resemblance to potassium, one of the most important of the biological trace elements. Potassium and its analogs are absorbed quickly into heart muscles -- so quickly, in fact, that within minutes after an injection the heart is seen clearly in a PET scan of the chest. And because rubidium-82 has a very short (75-second) half-life, it disappears from the heart almost as quickly as it appears. Thus, researchers can perform a scan, try out a proposed treatment or intervention (for example, administer a drug, or have the patient exercise) and then do another scan to measure its effect.

For Additional Information:

Office of Research and Technology Application
50A 4112
Lawrence Berkeley Laboratory
Berkeley, CA 94720
Telephone (415) 486-6502

NASA Tech Brief
National Aeronautics and Space Administration
Lyndon B. Johnson Space Center, Houston, Texas

Pressurized Sleeve

A garment part sustains a pressure differential without unduly restricting the user.

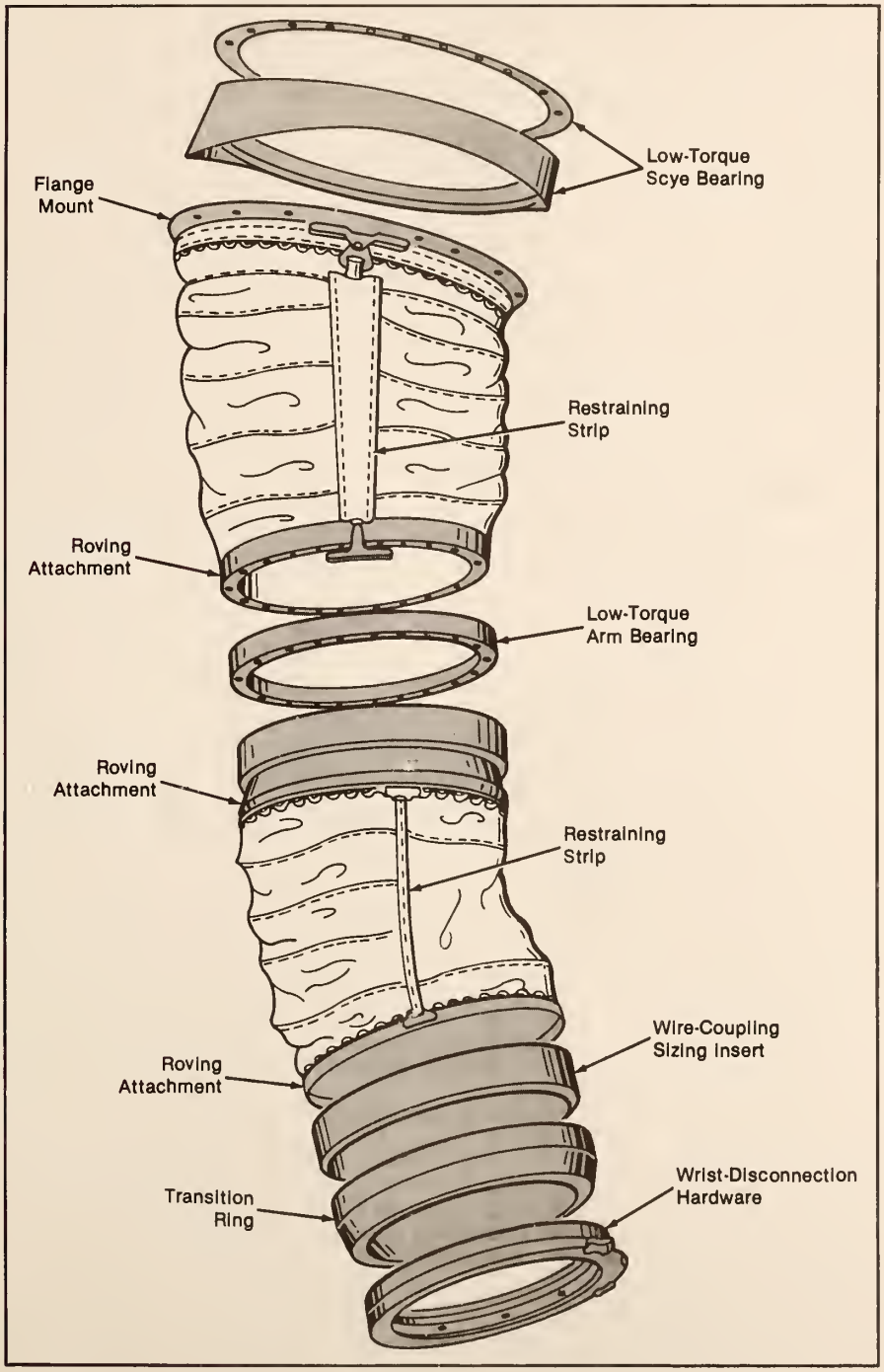

A fabric sleeve withstands a pressure difference of 8 lb/in.^{2} (55 kPa) while allowing the wearer fairly easy movement. Developed as a replacement for a space-suit sleeve rated only to 4.3 lb/in.^{2} (30 kPa), the new sleeve gives greater range of movement with lower restrictive torques. The sleeve offers the same advantages in such terrestrial applications as protective clothing and sleeves for manipulation of objects in isolation chambers.

The sleeve consists of upper and lower fabric sections fitted with shoulder, elbow, and wrist hardware (see figure). Longitudinal strips of fabric on the upper and lower sections restrain the sleeve so that it does not balloon axially under its internal pressure.

The sleeve is made of a polyester biaxial-weave fabric like that used previously in this type of space suit. The patterns of the sewn fabric sections have been modified to yield improved mobility. The restraint strips are made of a new material woven of high-strength, low-elongation polyethylene fibers. The hardware joints feature ball bearings for low torque. The center joint has a quick-connect and quick-disconnect coupling.

The sleeve was subjected to a series of tests of fabric properties, endurance of flexure cycles, torques, and ranges of movement during its development. A final group of tests by wearers gave subjective evaluations of comfort, range, and torque.

This work was done by Amy Lerner of ILC Dover, Inc., for **Johnson Space Center**. *MSC-21280 /TN*

The **Pressurized Sleeve** consists of low-torque joint hardware, sewn fabric sections, and lengthwise strips of fabric that restrain the sections.

FOR ADDITIONAL INFORMATION: *Contact: Director, Technology Transfer Division, P.O. Box 8757, BWI Airport, MD 21240; (301) 621-0100 Ext. 241*
REFER TO THE NUMBER LISTED AT THE END OF THIS ARTICLE

Natural Resources Technology & Engineering

995 Igneous Petrological Database: A Unique Global Geochemical Data Bank

NOAA Technology Brief
National Oceanic and Atmospheric Administration

Igneous Petrological Data Base: A Unique Global Geochemical Data Bank

A new release of the Igneous Petrological Data Base (IGBA) is now available. Version 3 of IGBA has a significant increase in data for the United Kingdom, Hungary, India, Portugal, Spain, and Peru. This marks an increase of 23% from Version 2, with over 12,000 specimen descriptions drawn from more than 1000 sources worldwide (see map below for locations of samples).

Version 3 of IGBA includes a bibliography of source references and a glossary which matches the abbreviations in the data base with their common language equivalents. In addition, a series of computer subroutines are provided which allow easy access and selection from the data base.

The IGBA data base was an initiative of the International Geological Correlation Program (IGCP) under the joint sponsorship of the United Nations Educational, Scientific, and Cultural Organization (UNESCO) and the International Union of Geological Sciences (IUGS). Entries into IGBA are based on published data; bibliographic sources are cited in the data base.

Locations of Survey Data

Information contained for each specimen generally includes weight-percent of e$sential oxides ($SiO_2$, TiO_2, Al_2O_3, Fe_2O_3, FeO, MnO, MgO, CaO, Na_2O, K_2O, P_2O_5, CO_2, H_2O+, and H_2O-), trace

elements, rock name, geological formation, and latitude and longitude of the sample. Each specimen description may also contain stratigraphic and physical age, mineral assemblages occurring in the specimen, and petrographic descriptors concerning mode of occurence, state of preservation, texture, structure, and type of alteration. In addition, where general information is available on specific gravity, specimen locality, field relations, modal analysis, or refractive index, it is included along with notes on analytical procedures and comments from authors, contributors, and editors.

The complete IGBA data base, including data, bibliography, reference table, and software, is available on magnetic tape or 5¼" IBM-PC compatible floppy diskette. Users should be able to perform their own sophisticated selections from IGBA with the subroutines supplied. However, custom-selected subsets of the data, based on geographic area, are also available.

Data contained in IGBA are prepared for incorporation into the data base by petrologists participating in the IGCP. For more information concerning IGCP participation, write to:

Dr. Felix Chayes
Chairman, IUGS Subcommission on
Data Bases for Petrology
Department of Mineral Sciences
Smithsonian Institution, MS 129
Washington, DC 20560 USA

Dr. Joe Frizado
Chairman, IGCP Project-239
Department of Geology
Bowling Green State University
Bowling Green, OH 43403-0218 USA

How to Order

Product Number	Cost	Description
899-A07-001	$ 90	Entire IGBA data base on magnetic tape (9-track, 1600 bpi, ASCII)
899-A25-001	$ 90	Entire IGBA data base on three 5¼" IBM-PC compatible high density diskettes
899-A07-CUS	$140	Custom select subset on magnetic tape
899-A25-CUS	$ 80	Custom select subset on one diskette. Each additional diskette is $29.

Please refer to product number when ordering.

The prices quoted here are valid through **September 30, 1988.** Prices applicable after that date may be obtained by calling (303) 497-6967.

Mention of a commercial company or product does not imply endorsement by NOAA or the Department of Commerce.

U.S. DEPARTMENT OF COMMERCE REGULATIONS REQUIRE PREPAYMENT ON ALL NON-FEDERAL ORDERS. Please make checks and money orders payable to **COMMERCE/ NOAA/NGDC.** All foreign orders must be in U.S. Dollars drawn on a U.S.A. bank. Do not send cash. Orders may be charged to an American Express card, MasterCard, or VISA card by telephone or letter; please include credit card account number, expiration date, telephone number, and your signature with order.

A ten-dollar ($10) handling fee is required on all orders; an additional ten-dollar ($10) charge is required for non-U.S.A. orders. Rush orders require an extra surcharge of fifteen dollars ($15).

Please direct telephone inquiries to **(303) 497-6967** (FTS: 320-6967; Telex: 592811 NOAA MASC BDR). Inquiries, orders, and payment should be addressed to:

National Geophysical Data Center
NOAA, Code E/GC1
325 Broadway
Boulder, CO 80303

Physical Sciences

996 JANAF Thermochemical Tables now Available Online Worldwide

997 New Technique for X-Ray Fluorescence Spectroscopy

998 Thermoplastic Removes Hydrogen without Producing Water

Testing & Instrumentation

999 Standard to Measure Carbon in Natural Materials

1000 Fast Data Acquisition for Mass Spectrometer — New equipment has the speed and capacity to process time-of-flight data. (Licensing Opportunity)

1001 Device Maintains Water at the Triple Point — A modified commercial freezer keeps water at 0.01 °C for over 10 weeks.

1002 Simultaneous Sampling of Two Spectral Sources — A fiber-optic bundle is used to sample a dye laser and a spectral lamp.

Other Items of Interest

982 Electrochromic Variable-Emissivity Surfaces — Temperature could be controlled by altering infrared radiative properties. (Licensing Opportunity)

NBS technology update

National Bureau of Standards
U.S. Department of Commerce
Gaithersburg, MD 20899

JANAF Thermochemical Tables Now Available Online Worldwide

The third edition of the (Joint-Army-Navy-Air Force) JANAF Thermochemical Tables, published by the National Bureau of Standards (NBS), has been computerized to provide scientists and engineers with rapid access to important information on the performance of materials at high temperatures.

The new JANAF file is available to subscribers of STN International (Scientific and Technical Network), an online private sector retrieval service offered worldwide. The computerized database eliminates the need to manually search through approximately 1,800 pages of thermochemical tables in two volumes.

The numerical data in the new JANAF file can be used by researchers and designers to make quick performance calculations for chemical reactors such as rocket engines, air pollution control equipment, automotive internal combustion engines, coal gasifiers and furnaces, fuel cells, liquefaction reactors and their catalyst structures, and magnetohydrodynamic generators. The information also can be used by engineers in the design of chemical plants.

Among the many advantages of the new file are the way a user can specify a thermodynamic property with a range of values, then obtain all of the chemical species which have values within the specified range. Most importantly, the program is designed to list in one table all of the values for a given property of a chemical compound when the values for that compound appear in more than one tabulation.

The computerized version of the JANAF database contains more numerical information than the printed tables. This permits users to generate equations that will reliably interpolate information between given values in different tables for specific design calculations. The properties tabulated are heat capacity, entropy, Gibbs energy function, enthalpy, enthalpy of formation, Gibbs energy of formation, and the logarithm of the equilibrium constnat for formation of each compound from the elements in their standard reference states. All values are given in SI units and are for a standard state pressure of 100,000 pascal (1 bar).

Chase emphasizes that the new computerized file, which contains critically evaluated data on the thermodynamic properties of 1,072 distinct chemical substances, including organic compounds containing one or two carbon atoms, corresponds to information in the printed version of the JANAF tables. These tables contain recommended

temperature-dependent values over a wide temperature range (0 to 6000 kelvin) with almost 1,800 single phase and multiphase tables for the crystal, liquid, and ideal gas state.

FOR ADDITIONAL INFORMATION: For information on the availability of the new JANAF file through STN, or the third edition of the JANAF Thermochemical Tables (1985), and the computer-readable database for lease on magnetic tape, contact the Office of Standard Reference Data, A323 Physics Bldg., National Bureau of Standards, Gaithersburg, MD 20899; (301) 975-2208.

NBS technology update

National Bureau of Standards
U.S. Department of Commerce
Gaithersburg, MD 20899

New Technique for X-ray Fluorescence Spectroscopy

A new technique in molecular spectroscopy under study by scientists from NBS, Brookhaven National Laboratory and Indiana University allows researchers to take "snapshots" of the electronic energy states of free molecules on a time scale so fast that the molecules can be effectively "frozen" in a particular spatial orientation. The result is an enhanced sensitivity to molecular-symmetry effects in spectroscopy not previously attained. In experiments reported in the March 14 Physical Review Letters, the team announced measurements of polarized x-ray fluorescence from methyl chloride, in which polarization of the decay fluorescence of specific electronic states in the molecule clearly depends on the symmetry of the molecular orbitals involved. These experiments demonstrate the feasibility of using this technique to obtain orientation and dynamical information for specific electronic states in molecules. The structure of active sites of large molecules, such as proteins, could be studied in this fashion in "natural" states without requiring crystallization.

FOR ADDITIONAL INFORMATION: To discuss these efforts further, contact Dr. Dennis Lindle, Physics Bldg., Room A-141, Gaithersburg, MD 20899; (301) 975-4849.

Department of Energy

Technology Application

Sandia National Laboratory

Thermoplastic Removes Hydrogen Without Producing Water

A Sandia National Laboratories scientist has developed a hydrogen getter that is based on a mixture of a polymer and a catalyst. This thermoplastic material can take up relatively large amounts of hydrogen from its environment without producing water and can be cast into free-standing structures.

Getters are used to remove undesirable impurities from gaseous environments that range from inside TV picture tubes to high-vacuum scientific instrumentation. Hydrogen can generate explosions, damage electrical and optical components, and embrittle metals.

Unlike so-called recombiners—systems that remove hydrogen through a catalytic process similar to combustion—the new material functions well without the presence of oxygen. One potential application is in gettering closed (unvented) systems. These range from high-tech electronics and specialized batteries to larger systems such as nuclear weapons, submarines, and NASA's proposed Spacelab.

Improves on other systems

Hydrogen also can be absorbed by getters such as titanium metal; however, these are suitable only for removing small quantities of the gas in high vacuum applications. Larger quantities can be eliminated by the use of mixtures that combine acetylene-containing compounds with supported platinum or palladium; these approaches, however, can he unstable (with time), and produce water, which itself can cause damage.

The new material was developed in laboratory experiments by Laura R. Gilliom of Sandia's Chemistry of Organic Materials Division. A solution of triblock copolymer (polystyrene/polybutadiene/polystyrene) is combined with an iridium-containing catalytic compound (Crabtree catalyst). After removal of the solvent, the mixture consists primarily of polymer, with catalyst loadings ranging from 10 percent to well under 1 percent, depending on the intended application.

Potential Department of Energy and Department of Defense applications are to be found in weapon systems, radioactive waste storage and transportation systems, and devices for the removal of tritium, Gilliom says. Additionally, she says, "Some systems in submarines submerged for extended periods can produce significant amounts of hydrogen in the environment. This is undesirable for a number of reasons.

The new material was tested for gettering efficacy by adding hydrogen at low pressures. Normally invested with a rubbery constituency, it stiffens as it takes on hydrogen and eventually becomes a semi-crystalline material, similar to polyethylene, as hydrogenation is completed.

The experiments, using a plug of getter material that was slightly foamed by solvent evaporation, showed an uptake of 250 cc of hydrogen per gram of getter (theoretical capacity is 275 cc/gram) at an initial rate of 50-100 cc/hr. The uptake rate is reduced when the same material is produced in pellet form.

The cost of the getter is primarily based on the cost of the catalyst and the percentage loading of catalyst within the bulk material.

FOR ADDITIONAL INFORMATION

Public Information Division,
Code 3161,
Department of Energy,
Sandia National Laboratories,
Albuquerque, NM 87185-5800
(505) 844-4207
Refer to announcement 23, No. 3

NBS technology update

National Bureau of Standards
U.S. Department of Commerce
Gaithersburg, MD 20899

Standard To Measure Carbon In Natural Materials

To meet the needs of environmentalists and other researchers in science and industry, NBS has developed a new set of materials for calibrating automated instruments to measure the carbon content in biological tissues and botanical specimens. These devices, widely used in the metals industry for the rapid analysis of carbon in steel, produce highly sensitive and precise data when they are calibrated with accurate standards. Standard Reference Material (SRM) 1216, Carbon Modified Silica, is a set of three silica matrices certified for concentration levels of carbon at 0.70, 9.06, and 17.04 percent. Each of the three materials has been measured by both prompt gamma neutron activation and combustion techniques using known, highly characterized material as controls for their certification.

FOR ADDITIONAL INFORMATION: SRM 1216 is available for $192 for the set of three materials form the Office of Standard Reference Materials, B311 Chemistry Bldg., National Bureau of Standards, Gaithersburg, MD 20899; (301) 975-6776.

NASA Tech Brief
National Aeronautics and Space Administration
Ames Research Center, Moffett Field, California

Licensing Opportunity

Fast Data Acquisition for Mass Spectrometer

New equipment has the speed and capacity to process time-of-flight data.

The data generated by a time-of-flight mass spectrometer are captured by a fast data-acquisition system. The system relies on a fast, compact waveform digitizer with 32-k memory that can be readily coupled to a personal computer. With this newly available digitizer, the system captures all the mass peaks on each 25- to 35-μs cycle of the spectrometer.

The computer enables the convenient control of the collection and management of data. It automates the data-acquisition process, including mass calibration, logging of pertinent experimental parameters, and presentation of the recorded spectral data in a variety of ways.

The system samples vapor plumes produced by laser-pulse heating of various materials. After the 1-ms pulse of vapor that follows each laser pulse, the system displays the following on video screens:

- a three-dimensional view of the time-resolved spectra from the vapor with the major mass peaks labeled by their ratios of mass to change and
- a presentation of laser intensity versus time and total ion current versus time.

Simultaneously, the system prints out pertinent experimental parameters, including the identity of the sample, date and time, laser-power-supply voltage, pressure in the vacuum chamber, and potential of the ion deflector. The operator can request prints and plots of data (see figure).

In addition, the system can be used to capture spectra in the averaging mode over much longer periods; for example, several tenths of a second or more. These longer measurements analyze vapors from continuous laser heating or calibration gases. Except for the three-dimensional format, the same displays and printouts are available.

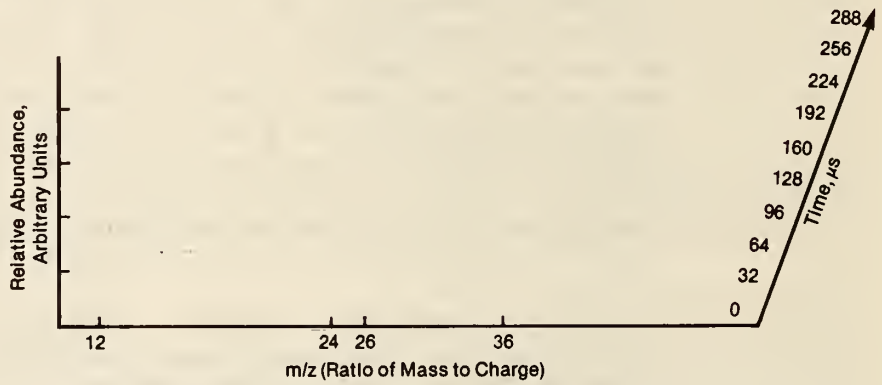

A **Pseudo-Three-Dimensional Plot** gives a time-resolved view of the mass spectra.

The time-of-flight mass spectrometer sends out a trigger pulse at the beginning of each cycle. The microchannel-plate detector of the spectrometer produces an ac component containing the spectral signal, and a dc component — the total multiplier current — that is a measure of all the masses in the vapor. The spectral signals are fed to a transient recorder (synchronized by the trigger pulses from the spectrometer) where they are stored in a signal memory and processed by a microprocessor before being transferred to the host computer.

This work was done by K. A. Lincoln of **Ames Research Center** *and R. D. Bechtel of Santa Clara University. Further information may be found in NASA TM-88374 [N8-724538/NSP], "A Fast Data Acquisition System for the Study of Transient Events by High Repetition Rate Time-of-Flight Mass Spectrometer." [A02]*

Copies may be purchased [prepayment required] from the National Technical Information Service, Springfield, Virginia 22161, Telephone No. (703) 487-4650. Rush orders may be placed for an extra fee by calling (800) 336-4700.

Inquiries concerning rights for the commercial use of this invention should be addressed to the Patent Counsel, Ames Research Center Refer to ARC-11785 /TN

Ames Research Ctr.
Technology Utilization Officer: Laurance Milov
Mail Code 223-3
Moffett Field, CA 94035
(415) 694-6471
Patent Counsel:
Darrell G. Brekke
Mail Code 200-11
Moffett Field, CA 94035
(415) 694-5104

FOR ADDITIONAL INFORMATION: *Contact: Director, Technology Transfer Division, P.O. Box 8757, BWI Airport, MD 21240; (301) 621-0100 Ext. 241*
REFER TO THE NUMBER LISTED AT THE END OF THIS ARTICLE

NASA Tech Brief
National Aeronautics and Space Administration
Langley Research Center, Hampton, Virginia

Device Maintains Water at the Triple Point

A modified commercial freezer keeps water at 0.01 °C for over 10 weeks.

A relatively inexpensive device maintains the triple point (T_p) of water for 10 weeks or longer. The T_p of water, 0.01 °C, is the most useful and important of the defining temperature points for the calibration of standard platinum resistance thermometers (SPRT's). The freezing of a T_p cell is tedious and time consuming, and because a usable cell can rarely be maintained for more than a few hours, fewer T_p measurements can be made than desired. Attempts to extend the lives of T_p cells by the use of crushed-ice baths have not been successful.

The new device (see figure) consists of four basic assemblies: a small, commercial chest freezer containing an insulated water tank; an insulated copper cell holder; an "ice switch" for cycling the freezer compressor; and an externally-mounted air pump for circulation. The tank is made of stainless steel and lined with 2-in. (5-cm) R-10 foam insulation on all interior surfaces. An access hole cut in the freezer lid allows T_p measurements without opening the lid.

The copper cell holder, mounted on standoffs, is filled with foam insulation in which holes have been cut for two cells. Copper "hats" fit over the cell tops. A ring of insulation is added to the outside of the copper box, near the bottom, to displace a portion of the ice that tends to grow in the bottom of the freezer and up the side of the cell holder.

The quantity of ice in the freezer is controlled by the "ice switch," which is constructed from a small bellows, sealed with brass at both ends, in an aluminum housing. A hole drilled in the center of the housing is lined with 2-in. (5-cm) PVC (polyvinyl chloride), and the aluminum is coated with epoxy to prevent corrosion. The bellows is filled with distilled water and bolted to the bottom of the hole. The airspace between bellows and PVC is filled with silicone oil. A spring and nylon plunger are fitted above the bellows to activate a standard 20-A miniature switch.

The bellows assembly is immersed in one corner of the freezer, with the switch well above the surface of the water. Two aluminum bars, inserted between the freezer walls and the water tank, cause ice to form in the "ice-switch" corner first. The fluid in the bellows freezes and expands, causing the plunger to open the switch, shutting off the compressor. As the fluid in the bellows melts, the plunger falls, closing the switch and turning on the compressor. Two parallel 5-kΩ, 2-W resistors, mounted across the switch and thermally bonded to the bellows housing, add heat to reduce the cycle time while the compressor is off.

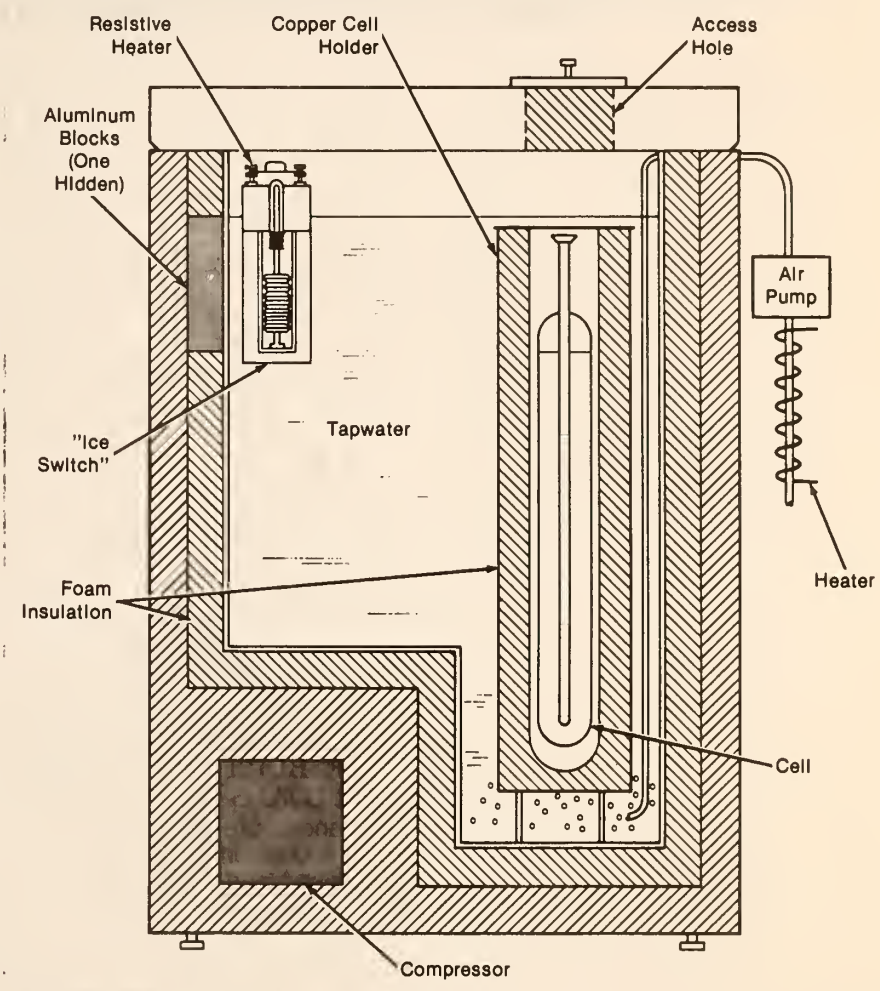

This **Modified Freezer** is used to calibrate standard platinum resistance thermometers.

The bath water is circulated by air pumped to the bottom of the tank and bubbling to the surface. The air-intake line is wrapped with heater tape to prevent ice from blocking its outlet at the bottom of the tank. A flexible wire run down through the air line may be necessary to prevent the formation of ice during long periods of operation.

The triple-point-of-water maintenance device has been in operation over a year. Daily checks of working SPRT's were used in identifying errors before they were introduced into critical test data. Experience

shows that, before cell storage is attempted, the freezer should be in operation and monitored closely for about a week to ensure a stable bath temperature that will not overfreeze the T_p. In fact, turning the freezer control to maximum was found to give better results than did a lower setting.

Typical bath temperatures swing from −10 m °C to +27 m °C over a 24-h period. The cell should be visually inspected daily before measurements are made to ensure the ice mantle is "free." If excessive ice crystals (dendrites) begin to grow from the bottom of the mantle, a 5- to 10-s immersion in ambient water keeps them at bay while minor freezer adjustments are made. Finally, 1 to 2 tablespoons of household bleach, added as needed, help prevent the bath water from discoloring and acquiring an unpleasant odor after several months of operation.

This work was done by J. W. West and C. G. Burkett of Wyle Laboratories for **Langley Research Center**. *No further documentation is available.*
LAR-13708 /TN

FOR ADDITIONAL INFORMATION: *Contact: Director, Technology Transfer Division, P.O. Box 8757, BWI Airport, MD 21240; (301) 621-0100 Ext. 241*
REFER TO THE NUMBER LISTED AT THE END OF THIS ARTICLE

Transportation & Components

1003 Acoustical Tests of a Scale-Model Helicopter Rotor — Data are obtained in simulated hovering flight in an open environment. (Licensing Opportunity)

1004 Fault-Tolerant Software for Flight Control — A redundant system performed well in flight tests. (Licensing Opportunity)

NASA Tech Brief
National Aeronautics and Space Administration
Langley Research Center, Hampton, Virginia

Simultaneous Sampling of Two Spectral Sources

A fiber-optic bundle is used to sample a dye laser and a spectral lamp.

Many applications of broadband dye lasers require that the spectral outputs be accurately known. A new technique uses a bundle of fiber optics to sample a dye laser and a spectral lamp simultaneously. By use of a real-time display with this sampling technique, the two signals are superimposed, and the effect of any spectral adjustments can be determined immediately.

Figure 1 shows some of the major components of the system. The fiber-optic bundle is split into two bundles at the input end. A portion of the beam from the dye laser is reflected to one of these bundles by an uncoated microscope slide. A spectral lamp is sampled with the other input bundle. The effect of the fiber-optic bundle is to mix the light from the two sampled sources at the output end before insertion into a detector.

For convenience, the input ends and the spectral lamp are mounted in a block. The dye-laser energy accepted by the fiber-optic bundle is attenuated by rotating the block to adjust the input angle. The output end of the fiber-optic block is fastened to the input slit of the sampling monochromator. A rapidly scanning spectrometer and oscilloscope are used to display the laser and spectral-lamp data as a function of wavelength.

Figure 2 illustrates the display obtained during the sampling of a dye laser centered at 606.5 nm. Neon reference lines at 603.00, 607.43, and 609.62 nm are also displayed, thus enabling the simultaneous determination of the dispersion and the wavelength. By the use of this system, adjustments can be made to the dye laser, and the effect can be determined immediately.

This technique is routinely used as part of the Coherent anti-Stokes Raman Scattering (CARS) system at NASA Langley Research Center. In the system, the dye laser mixes with a simultaneously-pulsed Nd:YAG laser at 532 nm to probe the vibrational levels of nitrogen. This system is used to diagnose combustion.

This work was done by Olin Jarrett, Jr., of **Langley Research Center**.
LAR-13756 /TN

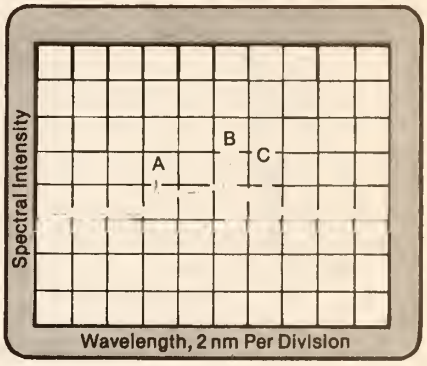

Figure 2. An **Oscilloscope Display of the Spectrum** of a broadband dye laser, centered at a wavelength of 606.5 nm, also shows neon reference lines at wavelengths A, B, and C.

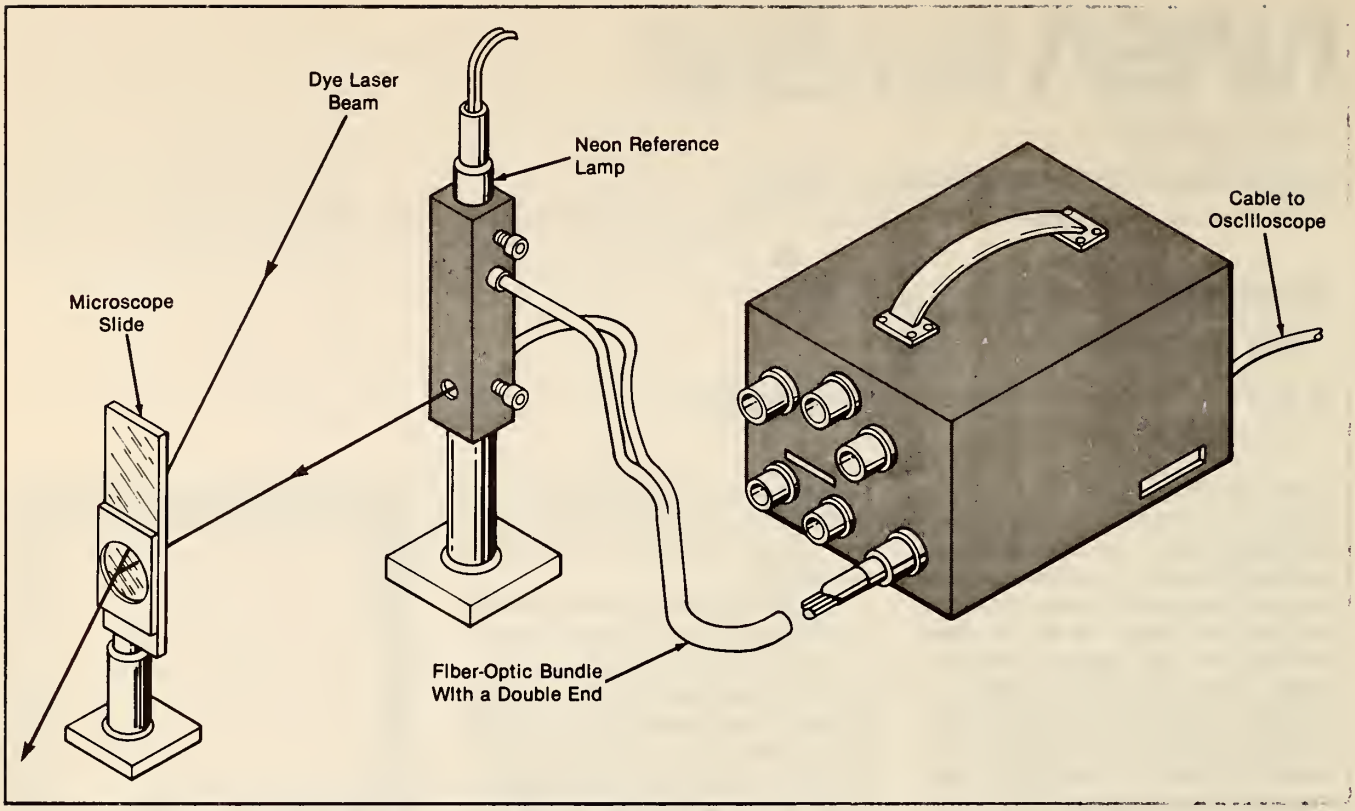

Figure 1. A **Split Fiber Optic Bundle** mixes the light from a broadband dye laser and a spectral lamp.

FOR ADDITIONAL INFORMATION: *Contact: Director, Technology Transfer Division, P.O. Box 8757, BWI Airport, MD 21240; (301) 621-0100 Ext. 241*

REFER TO THE NUMBER LISTED AT THE END OF THIS ARTICLE

NASA Tech Brief
National Aeronautics and Space Administration

Licensing Opportunity

Acoustical Tests of a Scale-Model Helicopter Rotor

Data are obtained in simulated hovering flight in an open environment.

A report discusses measurements of the sound generated in an outdoor hovering test of a 1/6-scale, four-bladed helicopter rotor. The outdoor environment is relatively well suited to the acquisition of good acoustical data because most of the undesired echoes and streaming effects of wind tunnels are not present.

The report provides information on the delineation between the acoustic near field and far field and on the effect of a simple boundary-layer-tripping device. In addition, the report covers rotor acoustics at low thrust and at high thrust.

Hovering tests yield insight into flow and noise phenomena of forward flight. The acquisition of acoustical data is much simpler in hovering flight because flow noise, shear layers, and Doppler effects are absent. In general, acoustic data obtained during hovering tests tend to be of a higher quality than those from wind-tunnel or flight tests.

The 2.13-m-diameter rotor was mounted in the standard thrust-up, wake-down configuration at a height of about 6 m above the ground, with a large unobstructed area around it. An array of microphones in a single vertical plane acquired data at a variety of distances and angles. The tip mach number and the rotor thrust coefficient were the primary test variables.

The test showed that a microphone should be positioned no closer than two rotor diameters to measure the far acoustic field of a rotor at all harmonics of the blade-passage frequency. The use of a simple device (strips of adhesive tape) to trip the boundary layer resulted in aerodynamic effects that are not completely understood: the use of tape was tried as a quick and easy alternative to the fairly-involved conventional procedure of attaching small particles of the correct size, spacing, and position to the surface near the leading edge. The results, however, were inconclusive.

The data obtained at nearly zero thrust indicate that although loading-noise effects are not completely eliminated, they can be reduced enough to enable the identification of thickness noise. This knowledge will be useful in future efforts to correlate predictions of thickness noise with measurements.

As the thrust coefficient rises from 0.09 to 0.11, the noise emitted by the rotor changes abruptly from a buzz-saw sound to a roar. This effect probably results from the interaction of the unsteady wake with the support apparatus; it does not seem to be related to rotor-stall phenomena.

This work was done by Cahit Kitaplioglu of **Ames Research Center** *and Christopher Kinney of H. S. Robinson, Inc.*

Copies of the report, "A Study of Helicopter Main Rotor Noise in Hover," may be purchased [prepayment required] from AIAA Technical Information Service Library, 555 West 57th Street, New York, New York 10019, Telephone No. (212) 247-6500.

Inquiries concerning rights for the commercial use of this invention should be addressed to the Patent Counsel, Ames Research Center Refer to ARC-11773./TN

Ames Research Ctr.
Technology Utilization Officer: Laurance Milov
Mail Code 223-3
Moffett Field, CA 94035
(415) 694-6471
Patent Counsel:
Darrell G. Brekke
Mail Code 200-11
Moffett Field, CA 94035
(415) 694-5104

FOR ADDITIONAL INFORMATION: *Contact: Director, Technology Transfer Division, P.O. Box 8757, BWI Airport, MD 21240; (301) 621-0100 Ext. 241*
REFER TO THE NUMBER LISTED AT THE END OF THIS ARTICLE

NASA Tech Brief
National Aeronautics and Space Administration

Licensing Opportunity

Fault-Tolerant Software for Flight Control

A redundant system performed well in flight tests.

A report discusses the design and testing of a redundant control system for the F-8 digital fly-by-wire airplane. The outstanding feature of the system is the fault-tolerant software [resident backup software (REBUS)] that resides in the primary digital computers. The transition to operation on backup software is smooth.

The basic F-8 airplane control system that was modified for operation with REBUS is a fail-operate, fail-safe digital fly-by-wire system with a frame-synchronized triplex digital primary system and a triplex analog-computer bypass system as backup. Commands for the control surfaces are passed through analog midvalue voting circuits, which can declare any one of the digital outputs to have failed. The analog backup is a direct electrical link between the pilot's stick and the servo-drive electronics, and its outputs are passed through the same midvalue voting circuits as those used by the primary system.

The REBUS software provides an augmented control law with three-axis, fixed-gain rate damping. Many of the self-check functions of the primary software are eliminated to reduce complexity. Overall, the REBUS software requires less than one-tenth the memory required by the primary software.

The system automatically transfers to the backup mode when there are failure declarations in two of the three primary channels. On the assumption that a generic software error may degrade the record of the state of the aircraft in the memories of the primary computers, the REBUS software is initialized to the control-surface commands at the moment of transfer: this generates no transients other than the small ones that result from the reinitialization of any active filters and changes in loop gains from state-dependent to fixed values.

To reduce complexity further, REBUS was established as an asynchronous system. Therefore, unlike the primary system, the backup system does not support the exchange of data among computers. Each computer operates on independent, dedicated sensors. Because of this inter-channel independence, one important issue in testing is the variations among channels.

The REBUS system was tested in an F-8 simulator on the ground and in an F-8 airplane in flight, using simulated software errors. The channels tracked each other closely. The transfer transients were negligible, even during high-transverse-acceleration (high-g) maneuvers. In most cases, the transfer to REBUS could not be detected in the control-surface measurements. There were no unwanted transfers. The success of the F-8 REBUS flight tests, coupled with the incorporation of similar backup-software approaches in other advanced aircraft, is evidence that the underlying control concept will find industry-wide acceptance as a viable solution to the generic software-error problem.

This work was done by Dwain A. Deets and Wilton P. Lock of **Ames Research Center** *and Vincent A. Megna of Charles Stark Draper Laboratory. Further information may be found in NASA TM-86807 [N86-19325/NSP], "Flight Test of a Resident Backup Software System." [A02]*

Copies may be purchased [prepayment required] from the National Technical Information Service, Springfield, Virginia 22161, Telephone No. (703) 487-4650. Rush orders may be placed for an extra fee by calling (800) 336-4700.

Inquiries concerning rights for the commercial use of this invention should be addressed to the Patent Counsel, Ames Research Center
Refer to ARC-11763. /TN

Ames Research Ctr.
Technology Utilization Officer: Laurance Milov
Mail Code 223-3
Moffett Field, CA 94035
(415) 694-6471
Patent Counsel:
Darrell G. Brekke
Mail Code 200-11
Moffett Field, CA 94035
(415) 694-5104

FOR ADDITIONAL INFORMATION: *Contact: Director, Technology Transfer Division, P.O. Box 8757, BWI Airport, MD 21240; (301) 621-0100 Ext. 241*
REFER TO THE NUMBER LISTED AT THE END OF THIS ARTICLE

NTIS Order Form

NTIS Telephone Numbers

To Order Reports
(703) 487-4650

For Subscription Questions
(703) 487-4630

Other Information
(703) 487-4600

Editorial Questions
(703) 487-4805

Postage:
NTIS uses First Class Delivery, or equivalent service, on all shipping. For information about one day RUSH ordering, call (703) 487-4600.

NTIS PRICE CODE SCHEDULE *

This schedule gives the current values to the price codes cited in those Tech Notes having a backup report available from NTIS.

Microfiche	
A01	$6.95
Paper copy	
A02	9.95
A03	12.50
A04 through A05	14.95
A06 through A09	19.95
A10 through A13	25.95
A14 through A17	32.95
A18 through A21	38.95
A22 through A25	44.95
A99	Call for price

Customers in Canada, United States, and Mexico use this schedule. Other addresses should write for the price listing, number PR-360-4.

Prices effective January 1, 1988

Use this form ONLY to order reports designated as available from NTIS

MAIL ORDER TO: National Technical Information Service
U.S. DEPARTMENT OF COMMERCE
5265 Port Royal Road
Springfield, VA 22161

Send me the reports I have selected on this form. I have placed order numbers in appropriate blanks and have indicated the quantity. IF ADDRESS LABEL

Last Name: .....

Title: .....

Company/Organization: .....

Address: .....

.....

City/State/Zip: .....

Telephone Number: .....

METHOD OF PAYMENT

☐ Check enclosed payable to NTIS for $ .....

☐ Charge to my NTIS Deposit Account, No: ....-.....

☐ Purchase order number: .....

Charge to: ☐ American Express ☐ VISA ☐ MasterCard

Card Number: .....

Expation date: .....

Signature: .....
(Required to validate order)

NTIS ORDER NUMBER (Use only for backup reports stated as available from NTIS)

NTIS Order Number	*Price**	*Quantity*	*Total Price*
.....	.....	.....	.....
.....	.....	.....	.....
.....	.....	.....	.....
.....	.....	.....	.....
.....	.....	.....	.....
	Shipping and handling fee		$3.00 .....
	Total		.....

- Agriculture & Food
- Computers
- Electrotechnology
- Energy
- Engineering
- Environmental Science & Technology
- Manufacturing, Machinery, & Tools
- Materials
- Medicine & Biology
- Natural Resources Technology & Engineering
- Physical Sciences
- Transportation & Components

Route To:

PENN STATE UNIVERSITY LIBRARIES
A000072010013

DEPARTMENT OF COMMERCE
nal Technical Information Service
ield, Va. 22161

AL BUSINESS
for Private Use, $300

UNITED STATES • DEPARTMENT OF COMMERCE •
Stimulating America's Progress
1913-1988

AN EQUAL OPPORTUNITY EMPLOYER

BULK RATE
POSTAGE & FEES PAID
NTIS
Permit No. G-292